NC STATE UNIVERSITY

CENTER

FOR

TRANSPORTATION

ENGINEERING

STUDIES

A COMPARATIVE STUDY OF PERFORMANCE OF DIFFERENT DESIGNS FOR FLEXIBLE PAVEMENTS

Volume I of II

by

N. Paul Khosla, Satish Sankaran,
Nakseok Kim, and Y. Richard Kim

DEPARTMENT OF CIVIL ENGINEERING

A COMPARATIVE STUDY OF PERFORMANCE OF DIFFERENT DESIGNS FOR FLEXIBLE PAVEMENTS

Volume I of II

by

N. Paul Khosla, Satish Sankaran,
Nakseok Kim, and Y. Richard Kim

A COMPARATIVE STUDY OF PERFORMANCE OF DIFFERENT DESIGNS FOR FLEXIBLE PAVEMENTS

by

N. Paul Khosla
Principal Investigator

Satish Sankaran
Graduate Research Assistant

Nakseok Kim
Graduate Research Assistant

Y. Richard Kim
Associate Professor

Research Project 23241-87-1

Final Report

in cooperation with the

North Carolina Department of Transportation

and

Federal Highway Administration
The United States Department of Transportation

CENTER FOR TRANSPORTATION ENGINEERING STUDIES
Department of Civil Engineering
North Carolina State University
Raleigh, NC 27695-7908

July 1996

Technical Report Documentation Page

1. Report No.	2. Government Accession No.	3. Recipient's Catalog No.
FHWA/NC/97-004		

4. Title and Subtitle	5. Report Date
A Comparative Study of Performance of Different Designs for Flexible Pavements	July 1996
	6. Performing Organization Code
	8. Performing Organization Report No.
7. Author(s) Dr. N. Paul Khosla, Satish Sankaran Nakseok Kim, and Dr. Y. Richard Kim	
9. Performing Organization Name and Address Center for Transportation Engineering Studies North Carolina State University Box 7908 Raleigh, NC 27695-7908	10. Work Unit No. (TRAIS)
	11. Contract or Grant No. 23241-87-1
	13. Type of Report and Period Covered Final Report 7/1/86 - 6/30/96
12. Sponsoring Agency Name and Address North Carolina Department of Transportation Raleigh, NC 27611 The Federal Highway Administration Raleigh, NC 27611	14. Sponsoring Agency Code

15. Supplementary Notes

16. Abstract

The objective of this research was to conduct a comparative study of performance of different designs for flexible pavements. This objecive was approached through extensive field and laboratory testing of test pavements. Also, a comprehensive computer-based design procedure for flexible pavements was developed based on results from the field and laboratory tests. Testing was carried out at a test facility constructed on US 421 Bypass near Siler City, North Carolina. The experimental stretch was about seven and one-half miles long and was composed of 12 pavement section types, two of each type in two directions of traffic (having different expected traffic loads), for a total of 48 sections. Of these, only 24 sections on the south-bound lane were instrumented. Response parameters were measured in the field using stress and strain gages embedded in the pavement structure, and an assembly of LVDT's were used to measure deflections at various layer interfaces. In addition, traffic volume and pavement distresses were monitored during the pavement life. Traffic measurements were made using a weigh-in-motion device.

Based on the nondestructive testing procedures, layer moduli for the various pavement layers were backcalculated. A comparison of predicted and measured responses were carried out based on measurements obtained from field instrumentation. Distress survey data, along with the measured responses, were used to compare the various designs employed in the study. In the laboratory testing, the mechanical properties of pavement layer materials were determined by subjecting specimens of the given materials to a series of dynamic load tests under environmental conditions representative of those experienced in the field. Performance prediction models for predicting fatigue cracking and rutting of the asphaltic concrete layers were developed. A study of the variability observed in the field data was performed. A reliability-based methodology to deal with the variability in pavement layer properties was developed. The application of the reliability-based methodology in pavement design computations has been demonstrated. Calibration factors for fatigue and rutting based on field and laboratory results were developed. In addition, a methodology for a calibrated mechanistic design, based on fatigue and rutting criteria, was developed. Also, based on the mechanistic principles developed, a computer program (NCFLEX) was created that could be used to analyze and design flexible pavement systems based on fatigue and rutting criteria. A comparative study of the various existing pavement design methods like AASHTO, VESYS, and the Asphalt Institute was carried out with respect to the US 421 field observed distress data.

17. Key Words	18. Distribution Statement
flexible pavements, field study, base and subgrade stabilization, fatigue, rutting, distress survey, computer based design procedure	No Restrictions 175 copies of this document were printed at a cost of $6.00

19 Security Classif. (of this report)	20. Security Classif. (of this page)	21. No. of Pages	22. Price
		200	

Form DOT F 1700.7 (8-72) Reproduction of completed page authorized

DISCLAIMER

The contents of this report reflect the views of the author who is responsible for the facts and the accuracy of the data presented herein. The contents do not necessarily reflect the official views or policies of the North Carolina Department of Transportation or the Federal Highway Administration. This report does not constitute a standard, specification, or regulation.

ACKNOWLEDGMENTS

The authors express their sincere appreciation to the authorities of the North Carolina Department of Transportation and the Federal Highway Administration for making available the funds needed for this research.

Sincere thanks go to Mr. W.K. Creech, Chairman, Technical Advisory Committee, for his interest and helpful suggestions through the course of this study. Equally, the appreciation is extended to other members of the committee, Dr. J. Corley-Lay, Mr. W. R. Brown, Dr. S. S. Wu, Mr. M. P. Strong, and Dr. M. Biswas of the North Carolina Department of Transportation and Mr. R.C. Shelton of the Federal Highway Administration for their continuous support of this study.

Sincere appreciation is also due to Dr. J. Corley-Lay and other members of the Pavement Management Unit of the North Carolina Department of Transportation for their cooperation and support during the field testing phase of this study.

Additional thanks are extended to Mr. J. H. Trogdon for his help and assistance during the field instrumentation phase of the study and Mr. B. G. Jenkins for his invaluable support and encouragement during the conduct of this study.

ABSTRACT

The objective of this research was to conduct a comparative study of performance of different designs for flexible pavements. This objecive was approached through extensive field and laboratory testing of test pavements. Also, a comprehensive computer-based design procedure for flexible pavements was developed based on results from the field and laboratory tests. Testing was carried out at a test facility constructed on US 421 Bypass near Siler City, North Carolina. The experimental stretch was about seven and one-half miles long and was composed of 12 pavement section types, two of each type in two directions of traffic (having different expected traffic loads), for a total of 48 sections. Of these, only 24 sections on the south-bound lane were instrumented. Response parameters were measured in the field using stress and strain gages embedded in the pavement structure, and an assembly of LVDT's were used to measure deflections at various layer interfaces. In addition, traffic volume and pavement distresses were monitored during the pavement life. Traffic measurements were made using a weigh-in-motion device.

Based on the nondestructive testing procedures, layer moduli for the various pavement layers were backcalculated. A comparison of predicted and measured responses were carried out based on measurements obtained from field instrumentation. Distress survey data, along with the measured responses, were used to compare the various designs employed in the study. In the laboratory testing, the mechanical properties of pavement layer materials were determined by subjecting specimens of the given materials to a series of dynamic load tests under environmental conditions representative of those experienced in the field. Performance prediction models for predicting fatigue cracking and rutting of the asphaltic concrete layers were developed. A study of the variability observed in the field data was performed. A reliability-based methodology to deal with the variability in pavement layer properties was developed. The application of the reliability-based methodology in pavement design computations has been demonstrated. Calibration factors for fatigue and rutting based on field and laboratory results were developed. In addition, a methodology

for a calibrated mechanistic design, based on fatigue and rutting criteria, was developed. Also, based on the mechanistic principles developed, a computer program (NCFLEX) was created that could be used to analyze and design flexible pavement systems based on fatigue and rutting criteria. A comparative study of the various existing pavement design methods like AASHTO, VESYS, and the Asphalt Institute was carried out with respect to the US 421 field observed distress data.

TABLE OF CONTENTS

LIST OF TABLES

LIST OF FIGURES

CHAPTER 1
INTRODUCTION

1.1 Problem Definition

The philosophy behind pavement design systems has traditionally limited itself to the calculation of the required thicknesses needed to achieve a certain "life" of the pavement. During the past decade or two, pavement design and rehabilitation methods have slowly, but surely, changed from being essentially empirical in nature to being mechanistic. The research work presented in this report is an attempt toward establishing a "mechanistic" basis for pavement design. By mechanistic, we mean an analytical-empirical method involving the calculation of pavement response linked to pavement performance. Considering the comprehensive nature of the research work adopted, partial if not conclusive, answers to the following questions are presented, namely:

(1) What kind of improvement (benefits) can we expect by moving from empirical design methods to more rationalistic mechanistic methods?

(2) How do different pavement design methods compare against one another?

(3) How do different designs (aggregate base course, full depth, cement treated base course) for flexible pavements compare against one another in their distress potential?

(4) How effective is the concept of in-use test sections in establishing mechanistic design methods for flexible pavement systems?

(5) What is the role played by environmental variables in the ultimate design?

(6) How efficient is the FWD in establishing stiffness measurements and in illustrating the structural capacity of the pavement?

(7) How accurately does a multi-layer elastic analysis predict response parameters?

(8) What are the considerations involved in deciding the various failure criteria?

A number of limitations currently exist in the available procedures for flexible pavement design. Simplified procedures and performance equations that relate to North Carolina conditions are not presently available. Comprehensive field verification is also not

currently available. Also, local agencies require specific testing procedures and performance equations that they can use with a high degree of confidence.

The presently available AASHTO (1986) Guide on Pavement Design is not mechanistic in nature and therefore do not address the above issues. In view of these limitations, there is an acute need for the development of specific procedures for material testing. Also, specific performance prediction models that can be directly used by the local agencies in the design of their flexible pavement systems are required. As mechanistic design methods in the domain of pavement engineering, still require a certain degree of empiricism, it is imperative that every agency develop their own calibration factors etc., based on local experience and tests, while still maintaining the overall mechanistic framework.

Confidence in the use of these models can be developed only by verifying their predictions against real pavement behavior. It is only with this kind of verification that we can build a high level of reliability in our mechanistic design approaches. It was with this objective in mind that the North Carolina Department of Transportation (NCDOT) embarked upon a "Long-Term Pavement Performance" (LTPP) Study." Recognizing the importance of full-scale pavement testing, such a facility was established on the US421 Bypass near Siler City, North Carolina.

1.2 Purpose of this Study

The purpose of this study was: 1) to develop specific laboratory tests that yield predictive models for rutting and fatigue cracking, and 2) to develop a computer program that can design a flexible pavement system based on user inputs and preferences that uses the models developed at NCSU.

Particular emphasis is placed on calibrating the models to observed field conditions. Emphasis is also placed on comparing the field measured and calculated pavement responses to be assured of the validity of the adopted structural analysis model.

1.3 Scope of this Study

The main thrust of this research is to develop a mechanistic design procedure, for the

design of flexible pavement systems that is easy to use by the North Carolina Department of Transportation (NCDOT). No attempt has been made to relate this to available data from other field studies to verify the veracity of the models developed. While there are several distress mechanisms associated with asphalt pavement failures, this study is limited in scope to methodologies associated with permanent deformation (rutting) and fatigue characteristics of asphalt concrete pavements. Although a wide variety of asphalts, aggregates, etc., are used by the construction industry, this study focuss on prevalent materials used by NCDOT. Any extrapolations of the findings from this research to other areas, other materials, etc., need to be carried out with a reasonable level of engineering skepticism.

1.4 Objectives

The objectives of this research study are the following:

(1) To review existing design methodologies.

(2) To evaluate the predictive capabilities of a multi-layer elastic model in assessing pavement response parameters for different kinds of flexible pavement systems.

(3) To study the factors that affect NDT measurements obtained from FWD tests, and to review the associated process of backcalculation in response to the different types of flexible systems adopted in the test plan.

(4) To evaluate the effect of different types and thicknesses of pavement layers on pavement distress and performance.

(5) To design and suggest laboratory testing procedures for the testing of various component materials in a flexible pavement system. These tests are configured to yield material parameters that can be incorporated in a mechanistic design program.

(6) To suggest specific performance prediction models using the results from laboratory and field test results.

(7) To study the variability existing in the stiffness estimates of the various material used, and to suggest a probabilistic approach to handle the problem.

(8) To build a calibrated mechanistic computer based flexible pavement design program.

(9) From experience gained, suggest future research.

1.5 Research Objectives - A Chapter-wise Look at the Contents of this Report

Based upon the general background presented in the preceding discussion, this report is divided into eleven chapters. The first chapter presents the scope, objectives, and limitations of the project.

The second chapter deals with the literature survey performed. The survey covers a variety of published material, covering a diverse range of topics such as field testing, instrumentation, material testing, and mechanistic design procedures. An argument on the necessity of moving from a performance related mixture design to a performance based mixture design is made. Chapter three discusses the instrumentation and the field testing protocol. Chapter four is devoted to the analysis of field response measurements. This chapter covers in detail such topics as measurement of backcalculated moduli, comparison of field measured and predicted responses, comparison of the different designs adopted based on response measurements and distress survey results, etc.

Chapter five provides detailed information on the various lab tests undertaken for the characterization of the various materials; namely, asphalt concrete layer (surface, binder, and base mixtures), aggregate base course materials, cement treated base course materials and subgrade soils. Chapters six and seven are devoted to the development of performance prediction models for asphaltic concrete materials for fatigue cracking and permanent deformation. Chapter eight presents the integration of the various models into a unified mechanistic design philosophy. Details regarding the computer-based approach and the actual working of the various subroutines are outlined.

Chapter nine provides a look at variability observed in field measurements. Also provided is a methodology to account for this variation under a probabilistic framework. Chapter ten provides a comparison of the mechanistic approach developed at NCSU with existing design approaches like AASHTO -1986, VESYS, and the Asphalt Institute Method. Chapter eleven is the summary of major conclusions made during the course of this study. This chapter also provides future research recommendations based on results obtained during this intensive study.

1.6 Limitations

No attempt has been made to relate research results to available data from other field studies to verify the veracity of the models developed. While there are several distress mechanisms associated with asphalt pavement failures, this study is limited in scope to methodologies associated with permanent deformation (rutting) and fatigue characteristics of asphalt concrete pavements. Although a wide variety of asphalts, aggregates, etc., are used by the construction industry, this study focusses on prevalent materials used by NCDOT. Any extrapolations of the findings from this research to other areas, other materials, etc., should be carried out with a reasonable level of engineering skepticism.

CHAPTER 2
LITERATURE REVIEW

Many present day pavement design methods are completely empirical in nature. Considering the large number of variables involved, and their various modes of interaction, doing away with this empiricism all together would be quite impossible. Nevertheless, increased usage of mechanistic design concepts in flexible pavement design, provides an increased level of reliability in our design procedures. Although the use of mechanistic design concepts in the design of cement concrete pavements has been quite prevalent, this is not the case with the design of asphaltic concrete pavements. The use of such methodologies appear to hold great promise in the areas of flexible pavement design.

Traditionally, methods for design of pavements in engineering practice fall under the following two approaches, namely

(1) The theoretical analysis approach, and

(2) The experimental field approach.

Theoretical analysis is used to evaluate pavement response parameters like stresses, strains and deflections in the layered pavement system. As such, they cannot evaluate performance characteristics, like cracking, rutting, etc., which are of primary interest to pavement engineers.

On the other hand, the experimental field approach, involving full scale field testing, although expensive, produces reliable data on the performance of the pavement and therefore is of considerable interest to the pavement engineer.

Theoretical analysis by itself fails to yield pavement performance measurements and the experimental field approach runs into problems when results need to be extrapolated for varying conditions. It is therefore obvious to the research engineer that there is a definite need to bridge the gap between theory and performance.

The ideal method for bridging this gap would be to come up with relationships, based on a broad spectrum of test conditions. These relationships would relate measured

performance with theoretical response measurements. When this is done, future pavements can be designed based solely on direct computation without involving any full scale pavement tests. Care needs to be exercised in the nature and extent of extrapolation, based on a thorough knowledge of the theories and assumptions involved in the development of the relationships. In other words, relationships developed for a particular region in the country may not necessarily be valid in other parts. Although the method of combining theory and field performance is a valid concept, and much effort has been expended on obtaining correlation factors, the lack of adequate reliable correlations spurs continued research in pavement design and analysis methods.

Critics of the full-scale field-testing concept maintain that each test section represents but one specific condition, and that extrapolation of the findings to other untested regions are dangerous. It is the authors opinion that in spite of the limitations, full-scale field-tests offer the best possible opportunity to observe pavement performance under actual conditions. Keeping this in mind, this research study utilized data from full-scale field tests to develop a mechanistic model for the design of flexible pavement structures.

2.1 Review of Flexible Pavement Design Methods

Various methods are presently available for the design of flexible pavement structures. They extend from the empirical to the mechanistic-empirical. A few of these are presented below, to give the reader an insight into the changes that have occurred in the various facets associated with the process of flexible pavement design.

(1) Catalog methods

These methods help the designer in selecting ideal pavement structures based on available designs that have been clearly cataloged. The Germans and French have used such a procedure for the design of their pavements. A summary of the French system (Ullidtz,1987) is provided below.

Figure 2.1 shows an example for the design of new roads. T_i is the traffic class and S_i is the soil class. The latter depend on the type of soil, the frost depth, and the drainage

Chaussée du type 6

COUCHE DE BASE : GRAVE-CIMENT GC (B)

COUCHE DE FONDATION : GRAVE NON TRAITEE

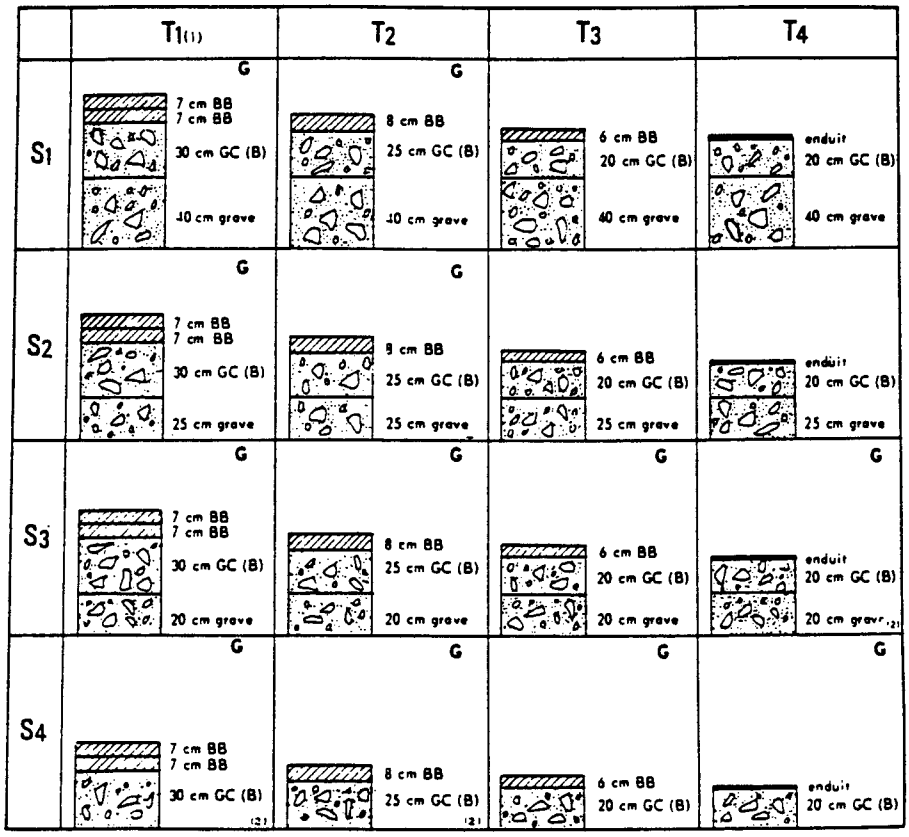

Figure 2.1 Example for the design of new roads (from the french pavement design catalog)

conditions. If a structure is not indicated by a "G" special precautions may have to be taken in the presence of frost. The catalog does not give any indication on the performance of the different structures.

(2) CBR method:

The California Bearing ratio (CBR) was one of the first empirical design methods to be developed for pavement structures (during 1928-1929). For each layer to be used in the pavement structure, the CBR is determined and the necessary thickness of the material above this layer is read from a chart or calculated from an equation. In the 1940's the US Army Corps of Engineers adopted the CBR method of design for airfield pavements.

Turnbull and Ahlvin (1957) came up with the closed form equation given below, that is presently used by the A.S. Corps of Engineers.

$$t=(0.231 \log n + 0.144)\sqrt{\frac{P}{8.1\ CBR} - \frac{A}{\pi}}$$

t = pavement thickness in inches,

n = number of passages or coverages,

P = wheel load in lbs,

CBR = California bearing ratio (CBR) of subgrade, and

A = tire contact area in square inches.

(3) British Road Note 29 and 31

Road Note 29 was first published in 1960 to provide a guide to the structural design of roads in Britain for varying climate, materials and traffic loads. Road Note 29 deals solely with the construction of new roads and not with the resurfacing and maintenance of existing roads. A typical design chart is shown in Figure 2.2. This design method, also, is not very helpful in predicting the performance of the pavement.

Road Note 31, was developed for the structural design of bitumen surfaced roads in tropical and subtropical countries (ref Road Note 31). Road Note 31 also contains an

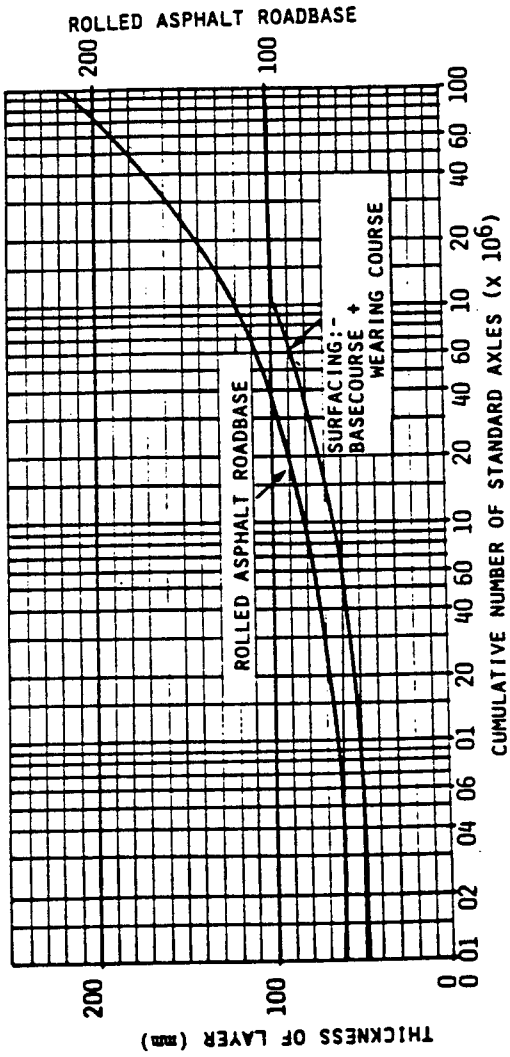

Figure 2.2 Simplified example of design diagram used in "Road Note 29."(Road Note 29, 1978)

appendix on the use of deflection beam surveys in designing road strengthening measures.

(4) AASHTO 1974,1986

The design procedure recommended by the American Association of State Highway and Transportation Officials (AASHTO) is based upon the results of extensive AASHO Road test in Ottawa, Illinois in the late 1950's and early 1960's. It was the first time a functional concept of failure was introduced beyond the traditional notions of structural failure. Detailed description of the method can be found in Chapter 10.

(5) ASPHALT INSTITUTE

From 1954-1969, eight editions of Manual Series NO. 1 (MS-1) were published by the Asphalt Institute for the thickness design of asphalt pavements. The procedures recommended in these manuals are empirical. The ninth edition is based on a mechanistic-empirical methodology, using the mechanistic multi-layer theory in conjunction with empirical failure criteria to determine pavement thickness.

(6) VESYS

The VESYS program was developed under the sponsorship of the U.S. Federal Highway administration (FHWA) by several prestigious academic institutions, consulting firms and Highway agencies. The analysis in VESYS is done under a probabilistic framework rather than a deterministic fashion, to account for inherent variability in material input parameters, traffic distributions, climatic factors, etc. The VESYS output consists of means and variances of the three primary distress modes, and of the combined PSI values. A detailed description of the VESYS method can be found in chapter 10.

(7) SHELL

The Pavement design method presented in the SHELL manual is based on elastic layer theory, measured material properties and rational performance criteria. The large number of design parameters includes traffic during the design life, subgrade properties,

temperature and paving material properties, each of which have a significant effect on pavement thicknesses. The system has been developed over a period of many years and takes into account laboratory and field measurements.

2.2 Multi-Layer Analysis Programs - A Review

In 1943, Burmister presented a method for determining stresses and displacements in a 2-layer system. Since then several computer programs have been developed that calculate pavement responses (stresses, strains and deflections) of various layered systems. Although essentially most programs adopt a linear elastic analysis, programs that use visco-elastic analysis are also available. Programs that consider non-linearity in the layer materials are also now available. Finite-element programs that include non-linear materials, inertial effects, discontinuities etc., also exist. Some popular ones are listed below.

(1) BISTRO and BISAR: These were developed by the Shell researchers and used in their SHELL design method.

(2) ELSYM5: Developed by CHEVRON

(3) WES5: This was developed by the waterways experiment station in Vicksburg, Mississippi.

(4) ALIZE III: Developed by the Laboratoire Central des Ponts et Chaussées, in France.

(5) CIRCLY: Commonwealth Scientific and Industrial Research Organization of Australia.

(6) ILLIPAVE / ILLISLAB: These were developed at the University of Illinois at Urbana Champaign for the analysis of flexible/rigid pavements. Both of these are finite element based methods.

2.3 Calibrated Mechanistic Procedure

Mechanistic design procedures are based on the assumption that a pavement can be modeled as a multi-layered elastic or visco-elastic structure on an elastic or visco-elastic foundation. Assuming that such a model can provide reliable results, one can predict pavement response parameters at various depths, within and below the pavement system. The

validity of the assumptions involved have been proved by many authors (Burmister, Mcleod). This report, based on work done on an instrumented pavement test site, also validates the use of a multi-layered linear elastic model for various flexible pavement systems. Due to variability in design inputs, the models need to be calibrated. The Calibrated mechanistic model is a more specific name for the mechanistic-empirical procedure. The purpose of "calibration" is to establish transfer functions, relating mechanically determined responses to specific forms of physical distress. Many studies based on a mechanistic approach have yielded useful design methods. Some of these studies, Report I-2, NCHRP 1990, studies by the Asphalt Institute, Kentucky Department of Transportation, Shell International etc. have resulted in specific guidelines for a mechanistic approach. The 1986 version of the AASHTO guide incorporates some of these principles in an indirect way.

2.3.1 Benefits of a Calibrated Mechanistic Method

It is a consensus among most researchers that methods using a mechanistic framework offer the best opportunity to improve pavement technology. The 1986 AASHTO guide lists the following benefits obtained from the use of a mechanistic approach:

(1) Estimates of the consequences of new loading conditions can be evaluated. For example, the damaging effects of increased loads, high tire pressures, multiple axles, etc., can be modeled using mechanistic procedures.

(2) Materials can be better utilized. For example, the use of stabilized materials in both rigid and flexible pavements can be simulated to predict future performance.

(3) Improved procedures to evaluate premature distress can be developed or conversely to analyze why some pavements exceed their design expectations. In effect, better diagnostic techniques can be developed.

(4) Aging can be included in estimates of performance. Effect of hardening of asphalt on fatigue cracking and rutting can be modeled.

(5) Seasonal effects such as thaw-weakening can be included in estimates of performance.

(6) Consequence of subbase erosion under rigid pavements can be evaluated.

(7) Methods can be developed to evaluate the long term benefits of providing improved

drainage in a roadway section.

2.4 Test Tracks

Different testing configurations to simulate real field conditions and realistic loading configurations are available. Some of the methods and equipment used are detailed below:

(1) Test tracks not open to real time traffic

(2) Heavy vehicle simulator (HVS)

(3) Accelerated Loading Facility (ALF)

(4) Test tracks that are open to traffic or tracks built into existing roadways.

Test tracks of the first kind can be extremely small so as to be accommodated within a building, or they can be of a larger size to simulate actual conditions better. Such test tracks are completely instrumented, and a given mechanical load traverses over the entire length. The loading time and the magnitude of the load are controlled, and usually made to mimic actual field loading. Test tracks can be either linear or circular. The test track at Nantes, France is an example of a circular test track facility.

The HVS is a mobile accelerated pavement testing rig that tests as-built pavements. Acceleration of testing is achieved through the backward and forward movement of a dual wheel load over a selected 8m by 1m test section. Additional acceleration is achieved by overloading the dual wheel load (up to 200 Kn versus the 40KN standard). In addition, sophisticated response measuring equipment is present to measure deformation and deflection at the road surface, and at different depths of the pavement. Crack movement, moisture content and temperature changes can also be monitored.

ALF is a mobile, accelerated loading device originally designed by the Australian Road Research Laboratory). In 1985, the Federal Highway Administration (FHWA) sponsored a research program to develop a U.S. version of the ALF device (Berry and Panuska, 1987; Byrd and Hutchinson 1985). The following is a description of the ALF as summarized by Sebally et al. (1989). The machine is 105 ft (32m) long, 13 ft (4.0 m) wide, and 19 ft (5.8 m) high, and weighs 120,000 lb (54,000 kg) fully assembled. The ALF requires little external power to operate because gravity is used to accelerate and decelerate the trolley assembly.

The test wheel travels at 12.5 mph (20km/h) over 40 ft (12.2 m) of the pavement. To simulate highway traffic, loads are applied to the pavement when the wheels are traveling in only one direction. The load is applied to the pavement through dual truck tires.

Because of problems in controlling environmental variables, pavement test sites open to regular traffic, is not a commonly adopted research setup. This nevertheless, offers the best possible real life scenario. There is therefore a compromise involved in this form of experimental design. The test track used in this study falls under this category.

2.4.1 Results from Field Testing - A Survey

It is the observed performance under actual conditions that judges the adequacy of any given design method. Three major road tests under controlled conditions were conducted by the Highway Research Board from the mid 40's to the early 1960's. Three of these road tests are mentioned below. The WASHO and the AASHO road test results are discussed in detail as both these test programs were conducted on flexible pavement structures.

(1) Maryland Road Test

The objective of the project was to determine the relative effects of four different axle loads on a particular concrete pavement. The tests were conducted on a 1.1- mile (1.76 km) section of concrete pavement constructed in 1941 on US301, approximately 9 miles (14.4 km) south of La Plata, Maryland (HRB, 1952).

(2). WASHO Road Test

The WASHO road test was conducted under the supervision of the Western Association of State Highway Officials (WASHO), in Malad, Idaho(HRB,1955). The results of the test as summarized by Huang (1994) are provided below:

(a) The amount of damage to the pavement increased in the order of 18,000 lb (80 KN) single axle, 32,000 lb (142 KN) tandem axle, 22,400 lb (100 KN) single axle, and 40,000 lb (178 KN) tandem axle.

(b) The behavior of a pavement with 4 in. (10.16 cm) HMA was far superior to that of equal total thickness with 2 in. (5.08 cm) HMA.

(c) Based on pavement distress, a tandem axle with a total load about 1.5 times that of a single axle load is equivalent to the single-axle load; whereas a tandem axle with a total load about 1.8 times a single-axle load produced equal maximum deflections.

(d) Deflection of the pavement surface under traffic was influenced by vehicle speed, temperature of the surfacing, load, and moisture content of the top layer of the basement soil. Deflection decreased as speed increased up to 15 mph (24.1 kmph), after which deflections decreased but slightly as speed increased. When the moisture content of the basement soil exceeded 22%, deflections increased with the increase in moisture contents.

(3) AASHO Road Test

The Objective of this project was to determine the significant relationship between the number of repetitions of specified axle loads of different magnitudes and arrangements and the performance of different thicknesses of flexible and rigid pavements (HRB, 1962). The test facility was constructed along the alignment of Interstate 80 near Ottawa, Illinois, about 80 miles (128 km) southwest of Chicago. The results of the test (on flexible pavements) as summarized by Huang (Huang, 1994) are provided below:

(a) The superiority of the four types of base under study fell in the following order: bituminous treated, cement-treated, crushed stone, and gravel bases.

(b) Rutting of the pavement was due principally to decrease in thickness of the component layers. About 91% of the rutting occurred in the pavement itself, with 32% in the surface, 14% in the base, and 45% in the subbase. Thus, only 9% of a surface rut could be accounted for by the rutting of the embankment.

(c) Generally cracking was more prevalent in sections having deeper ruts than in sections with shallower ruts.

2.4.2 Instrumentation

The pavement instrumentation refers to the in-situ (embedded) instrumentation in the

pavement structure to measure pavement responses, like, stresses, strains, and displacements. Different test sites around the world have implemented different kinds of gages to measure these parameters. Some of the best references on instrumentation for pavement research work are available in the OECD publications (OECD,1985). The OECD pavement test site involved a variety of instrumentation, as the research work involved many member countries. The OECD experiments involved the use of horizontal and vertical strain gages, stress gages, and deflection sensors. For measurement of temperatures, in the various layers, copper constant thermocouples were used. Frost penetration into the pavement structure was determined using a cryopedometer. Water table depths and measurement of water content was made using piezometer and tensiometer.

Huhtala et al. (1990) have provided a summary of various types of strain gages available. Testing at the Turner Fairbank Highway Research Center (TFHRC) in Mclean, Virginia, utilized H beam strain gages at the bottom of the asphalt binder. Multi-depth deflectometers have primarily been used in South Africa, where they were first developed. In the U.S.A., the Texas Transportation Institute (TTI) has successfully used them in their test sections. The multi-depth deflectometers (MDD), can be used not only to measure deflection at different depths and under varying loading conditions, but can also be used to measure permanent deformation occurring in different layers. A detailed description of the MDD can be found in Section 3.2

2.5 Critical parameters in flexible pavement design - nature, cause and manifestation.

Current analysis procedures in the design of flexible pavement structures consider the following two parameters as critical quantities affecting the performance of a flexible pavement. They are:

(1) The tensile strain at the bottom of the asphalt concrete layer.

(2) The compressive stress or strain on the top of the subgrade layer.

Tensile Strain at the Bottom of the A.C. layer

By tensile strain at the bottom of the ac layer, what is normally referred to is the longitudinal tensile strain, rather than the transversal strain. Transversal strains are, however, greater. Huhtala et al. (1990) have summarized the complex issues involved in the selection of longitudinal strains over transversal strains.

Traditional longitudinal strains are unequivocal and easy to handle, for instance the computer may calculate the maximal values automatically. The transverse strains accumulate, however, if there is not enough time to relax before the next axle. Relaxation depends on the temperature and is greater at higher temperatures. The transversal strains are greater than longitudinal and successive passes accumulate it. Questions regarding which of the two, transversal or longitudinal strain , single or accumulated continue to remain a hotly debated topic (Huhtala et al., 1990).

Although any multi-layer elastic program can be used to provide an estimate of the tensile strain, from a research standpoint, a couple of issues need to be dealt with. Primarily one can use either the normal or the principal strain. Strains measured in the laboratory may in essence be normal strains. Some feel that, as crack initiates at the principal planes, it is the principal strains that need to be used. Huang (1993) advocates the use of the horizontal principle strain(ϵ_t) , instead of the minor principle strain.

$$\epsilon_t = \frac{\epsilon_x + \epsilon_y}{2} - \sqrt{\left(\frac{\epsilon_x - \epsilon_y}{2}\right)^2 + \gamma_{xy}^2}$$

where

ϵ_x = Strain in the x direction

ϵ_y = Strain in the y direction

γ_{xy} = Shear strain on the x plane in the y direction.

2.6 Design factors

Design factors that affect the mechanistic design of flexible pavement structures fall

into four major categories,

(1) Traffic and Loading

(2) Environment

(3) Materials

(4) Failure criteria.

(1) Traffic and Loading

In a mechanistic approach, one of the primary input parameters is the nature and magnitude of the load. From these input parameters, the parameter of interest, tire contact pressure, needs to be obtained. As indicate by Figure 2.3 (Huang, 1993), the contact pressure is greater than the tire pressure for low pressure tires. This is because the walls of the tires are in compression, and the sum of vertical forces due to wall and tire pressure must be equal to the force due to contact pressure. The contact pressure is smaller than the tire pressure for high pressure tires, because the walls of the tires are in tension. As heavier axle loads have higher tire pressures, the use of tire pressures as the contact pressure is therefore on the safer side.

Different layer-analysis programs consider different approaches towards determining contact areas. Figure 2.4 below, shows some configurations used by the various agencies. All these configurations attempt to model an 18 Kip (80-KN) single axle load with a tire pressure of 80 psi (552 Kpa).

The AASHTO study introduced the concept of Equivalent Single Axle Loads (ESALs) to convert mixed traffic loads into a single equivalent load based on damage concepts. This procedure is used in almost all design methods. A brief critique of the limitations of this concept is provided in the following paragraphs.

It has been argued by researchers that the primary source of error in mechanistic-empirical models is the variability inherent in statistical-empirical constructs, such as the Equivalent Single Axle Load (ESAL) concept, and the Miner's fatigue hypothesis. It has further been surmised (Ioannides,1992), that although these may be relatively good as posteriori descriptors of pavement performance, they are found to be quite poor apriori

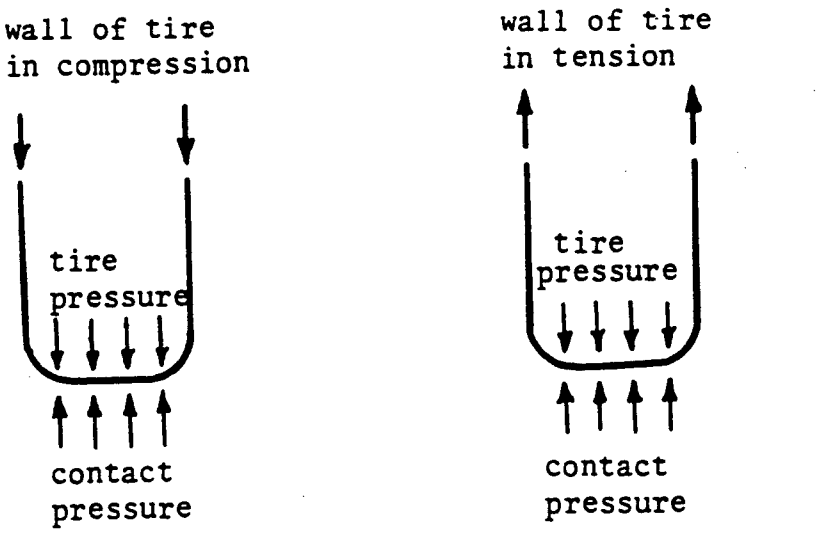

Figure 2.3 Relationship between contact pressure and tire pressure (Huang, 1993).

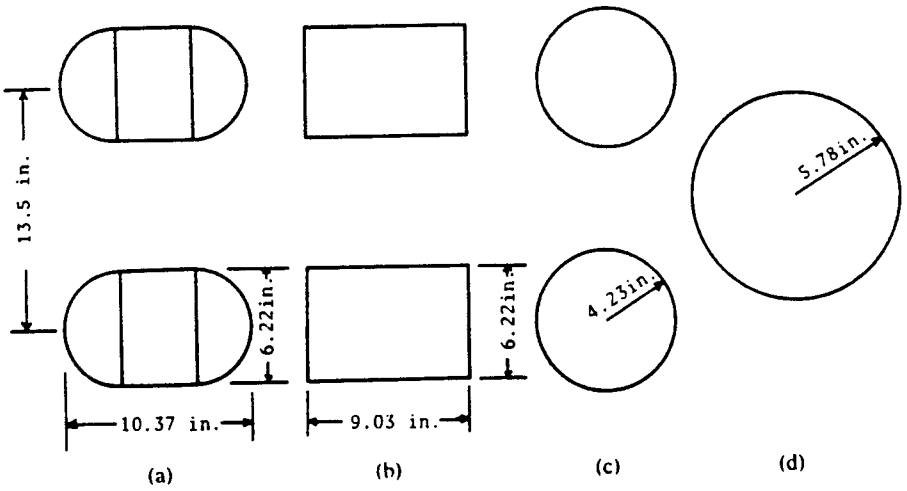

Figure 2.4 Dimension of tire contact area (Huang, 1993).

predictors thereof. It therefore only seems natural that it may be better to employ the actual load spectra in the analysis.

Until the beginning of the AASHO road test, early researchers used to plot distress versus time data. With the adoption of the statistical/empirical ESAL concept by the AASHO committee on design (AASHTO), the abscissa of the serviceability trend was changed from time to the number of ESALs. In so doing, damage from factors unrelated to applied loads was again disregarded. Consequently, although the ESAL concept may provide an overall description of the effect of past mixed traffic, it's effectiveness in predicting future pavement performance is doubtful.

(2) Environment

The environmental factors that influence pavement design are mainly temperature and moisture.

(a) Temperature: The major effect of temperature is on the asphalt modulus. The elastic and visco-elastic properties of HMA are significantly affected by changes in temperature. During the winter, when the temperature is low, the HMA becomes rigid and reduces the strain in the pavement. However, stiffer HMA has lower fatigue life. Temperatures also affect the depth of frost penetration in subgrade.

(b) Moisture: Moisture affects the stiffness of the aggregate base courses and subgrades. Adequate drainage is important in the design and construction of good quality, long lasting pavements.

(3) Materials

Material characterization is very important for any mechanistic design process. These yield important material parameters like moduli, poissons ratio etc., that are integral to any kind of analytical process. Relevant material properties are discussed in greater detail in Chapter 5. Specific tests may need to be conducted to yield properties, necessary for application in failure models and for predicting specific distresses.

(4) Failure Criteria

In any mechanistic-empirical model for pavement design, a number of failure criteria need to be established. Failure criteria, normally used in the design of flexible pavement systems are;

(a) Fatigue cracking: Failure criteria based on fatigue cracking, relates the allowable number of load repetitions to the tensile strain, based on laboratory fatigue tests on HMA specimens.

(b) Permanent deformation: Rutting in flexible pavements is indicated by permanent deformation or ruts along the wheel tracks.

(c) Thermal cracking: This type of distress includes both low temperature cracking and thermal fatigue cracking.

Low Temperature Cracking: Usually occurs in regions with very cold climates (temperatures below -10 deg F). Most comprehensive study on this subject was done by Christison et.al. (1972)

Thermal Fatigue Cracking: Occurs in milder regions, if excessively hard asphalt is used or if the asphalt becomes hardened due to aging.

CHAPTER 3
INSTRUMENTATION AND FIELD TESTING

3.1 Test Section Description

In the fall of 1989 and spring and summer of 1990, twelve pavement section types, two of each type in two directions of traffic (having different expected traffic loads), for a total of forty-eight sections, were constructed on US 421 Bypass near Siler City, North Carolina (Khosla et al.,1992). Typical pavement sections and the actual design thickness are included in Figure 3.1 and Table 3.1, respectively.

3.2 Instrumentation

Dynatest Consulting Incorporated furnished the soil pressure transducers and the asphalt strain gauges. These instruments were manufactured by Dynatest Corporation in Denmark. Their design is based on more than twenty years of research in gauge design and installation, performed at the Technical University of Denmark. Dynatest Corporation also furnished the recording equipment for measuring the response of the transducers.

The moisture cells ("200-X") were manufactured by Watermark. These cells measure, in effect, the soil suction that can be later converted into moisture content using calibration curves. The resistance display unit for the moisture cells was also manufactured by Watermark.

The thermocouple wire was the standard type "T," cut to length according to the needs of the site. The temperature display unit was a "JKT Digi-Sense" type. The installation of the gauges other than the MDDs was carried out by Dynatest personnel, with assistance from North Carolina State University. The MDDs were installed by technicians from the Texas Transportation Institution.

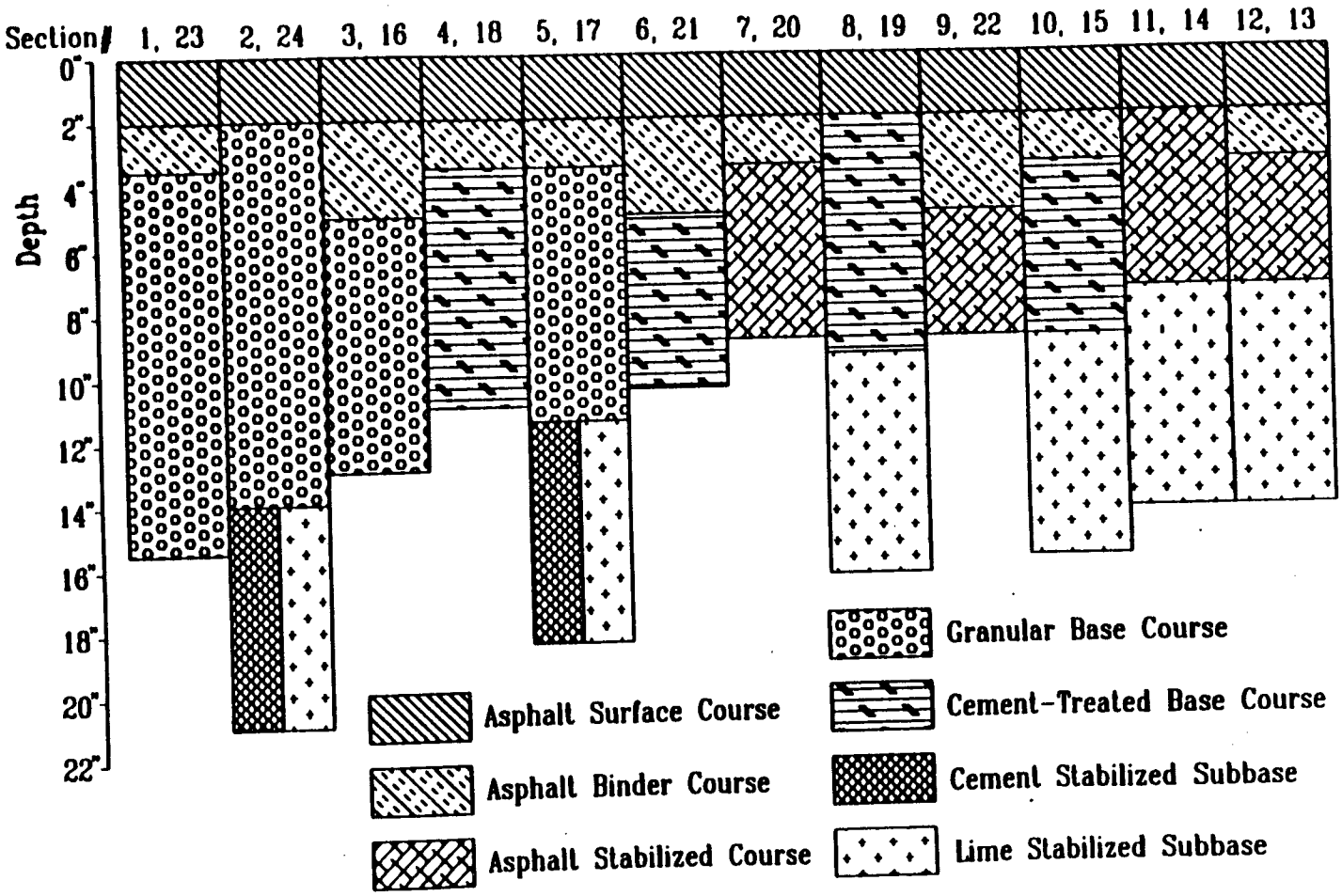

Figure 3.1 Test section layout.

Table 3.1 Test section descriptions.

Section No.	HDS	HDB	HB	ABC	CTB	Stabilized Subgrade
1, 23	2"	1.5"		12"		No
2	2"			12"		Cement
24	2"			12"		Lime
3, 16	2"	3"		8"		No
4, 18	2"	1.5"			7.5"	No
5	2"	1.5"		8"		Cement
17	2"	1.5		8"		Lime
6, 21	2"	3"			5.5"	No
7, 20	2"	1.5"	5.5"			No
8, 19	2"				7.5"	Lime
9, 22	2"	3"	4"			No
10, 15	2"	1.5"			5.5"	Lime
11, 14	2"		5.5"			Lime
12, 13	2"	1.5"	4"			Lime

Note: HDS = Asphalt surface course
HDB = Asphalt binder course
HB = Asphalt-stabilized base course
ABC = Aggregate base course
CTB = Cement-treated base course

Multidepth Deflectometers (MDD)

This device measures the transient deflection between a particular location in the pavement and an anchor located about 8 feet below the surface. It is an LVDT (Linear Variable Differential Transformers) based instrument. The measuring unit is an LVDT mounted within a module that can expand laterally to clamp onto the sides of the hole. As many as six modules may be placed in any hole. The minimum distance that modules can be placed apart is limited by the length of the module, which is approximately 6 inches (150 mm). The anchor for the LVDT cores is placed approximately 8 feet (2.44 m) below the pavement surface. Figure 3.2 shows the c/s of an MDD unit. Figure 3.3 shows the position of LVDT's in various MDD sections.

SOPT Pressure Cell

The design for the SOPT (Soil Pressure Transducer) cell was developed by the Technical University of Denmark. They are of a hydraulic type with an oil filled cavity. The cells are made of pure titanium, and their geometry has been improved by tapering the edges at 45 degrees. The induced liquid pressure is measured with a full strain-gauge bridge. These pressure cells are commercially available, and according to the manufacturer, have a service life of $3x10^6$ cycles. The soil pressure cells are designed for use in both cohesive and granular materials. These transducers are normally used to measure vertical stress at the top of the subgrade, which is often used as a critical parameter in pavement design. The SOPT cells are temperature compensated for use within the range of -5 degrees to 300 degrees Fahrenheit. The SOPT cells chosen for this project were the ones designed for fine grained soils.

PAST Strain Gauges

Deformations inside bituminous layers under the action of a given load are usually measured with strain gages. These deformation sensors contain a thin wire or film under electric current. The electrical resistance R of the wire varies by

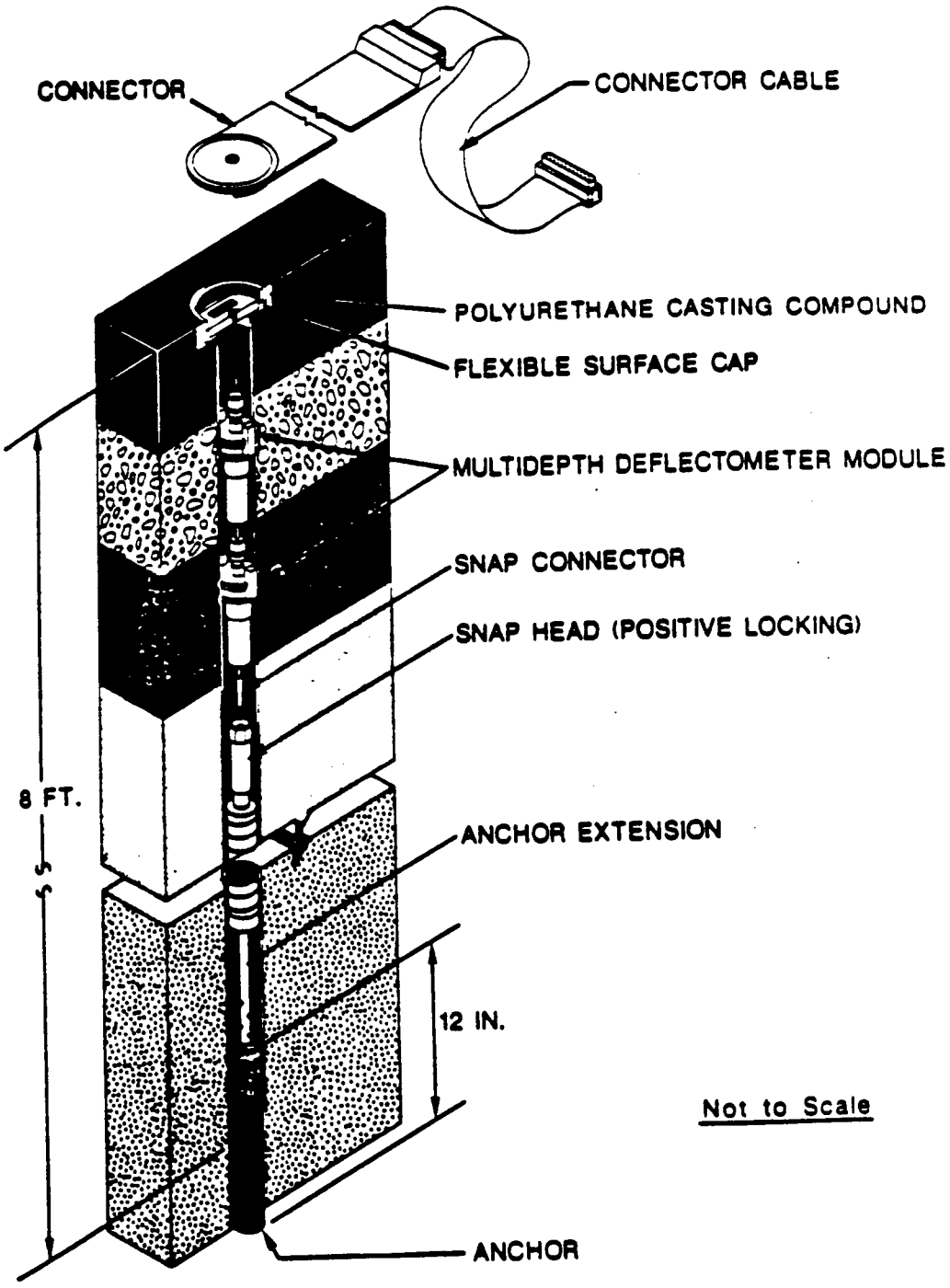

Figure 3.2 Schematic drawing of typical MDD setup after installation.

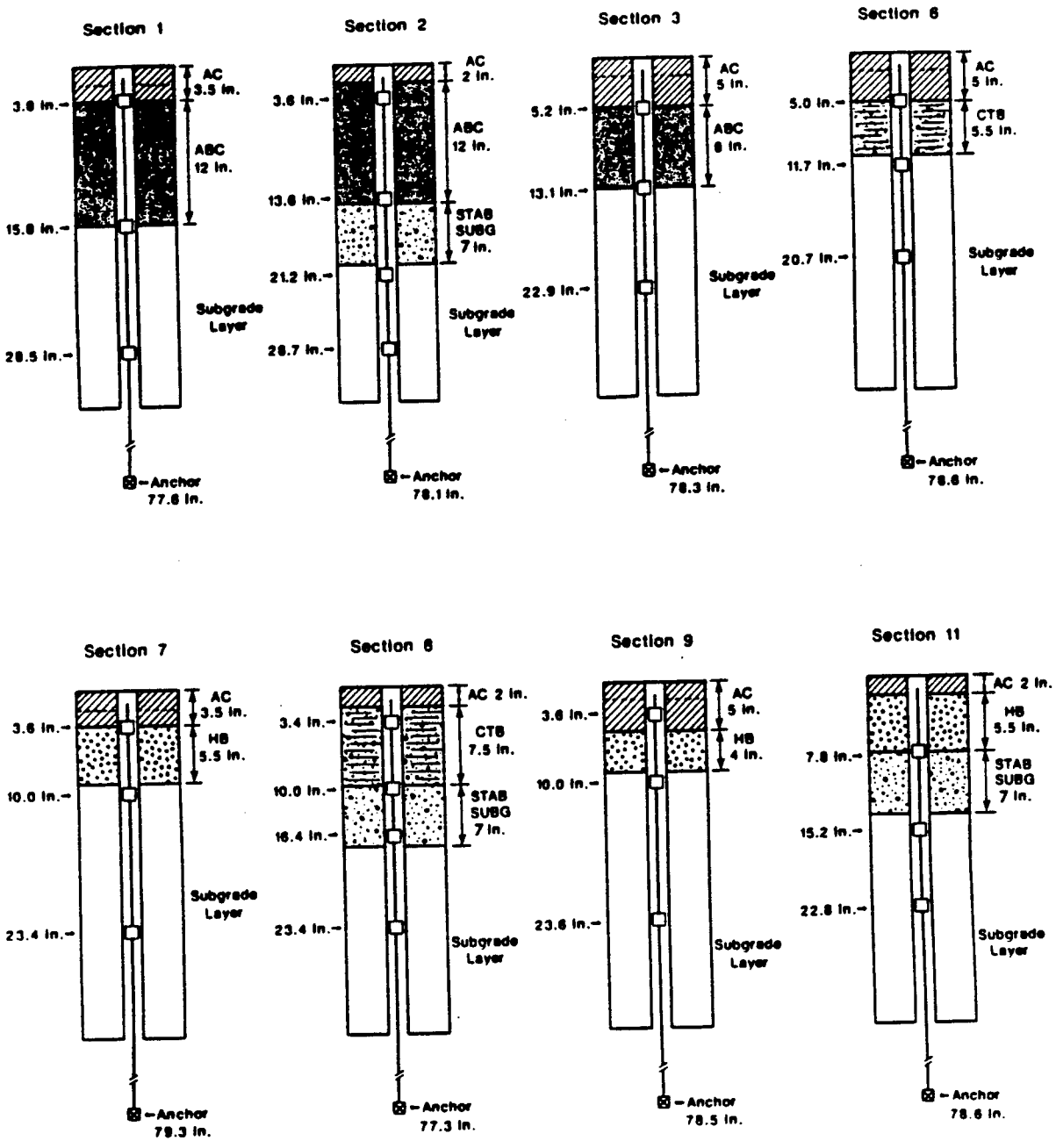

Figure 3.3 MDD locations in test sections.

R / R_o upon a mechanical elongation $\epsilon = \Delta L / L_o$. Thus we can write: $\Delta R / R_o = k \epsilon$. The gage factor (k) is characteristic of the gage.

A PAST (Pavement Strain Transducer) unit is an "H" type precision strain gage, constructed using materials with relatively low stiffness, while having high flexibility and strength. The gages are protected against mechanical and chemical deterioration by means of a multilayer coating, allowing them to perform effectively up to as many as 100×10^6 loading cycles or 36 months (whichever comes first). The temperature range of the PAST series of gages is some -20 degrees to 300 degrees Fahrenheit.

The average modulus of the PAST cell body is approximately 20 psi (138 KPa). This ensures a negligible influence on the surrounding AC materials, resulting in accurate temperature dependent measurements under virtually all field conditions. The strain gage in the PAST transducer is completely embedded in a strip of glass fiber reinforced epoxy. Each end of the epoxy strip is securely fastened to a stainless steel anchor to ensure proper mechanical coupling to the AC material after installation. The PAST transducer has a resistance of 120 ohms, a gage factor of 2.0, and it is temperature compensated with its specified temperature range. It can be incorporated into a full bridge setup with up to 12V excitation voltage. Figure 3.4 shows the typical location and orientation of the gages. Instrumentation details for individual sections are provided in APPENDIX A.

3.3 Installation of Gages

Due to some miscommunication between the contractor and the Dynatest personnel, two of the twenty-four sections already had a full thickness of base placed by the time Dynatest and NCSU personnel were notified to install the first set of gages.

One of these two "lost" sections was recovered by digging through noncompacted base and placing the soil pressure, temperature, and moisture transducers and then replacing the same volume of base material to the same uncompacted density. The moisture cell and a thermocouple lie immediately adjacent to the soil pressure cell.

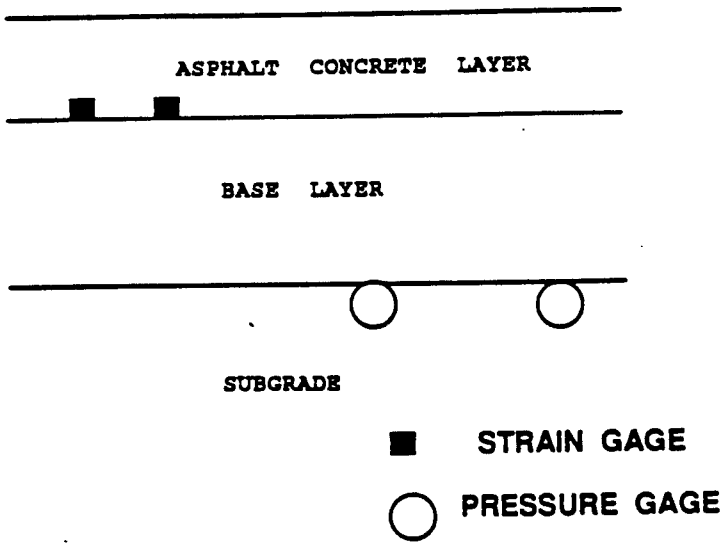

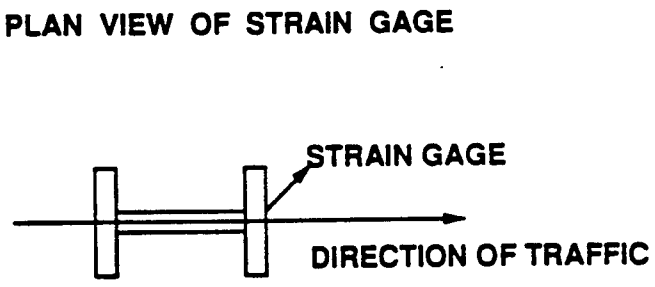

Figure 3.4 Location and orientation of strain and pressure gages.

The remaining SOPT gages were installed as planned, i.e., before the subgrade was covered and compacted by subsequent layers. Thus, all but one of the twenty-four sections were equipped with two (and in.one case three) SOPT units, along with the requisite moisture and temperature sensors.

When it came to the construction of the asphalt layers, essentially the same problem occurred. The contractor believed that the PAST transducers were to be installed above the asphalt base materials, instead of below. Thus, three of the twenty-four test sections had to be milled through and the gages placed. The installation of gages in the remaining twenty-one sections was carried out as planned. The fresh asphalt mix was subsequently placed above the gages and compacted.

All SOPT transducers were installed in the subgrade soil just beneath the base course. For sections having stabilized subgrade, the SOPT transducers were installed just beneath the stabilized layer. The following is a step-by-step procedure of SOPT transducer installation.

(1) Excavate a small area approximately 1 inch (2.54 cm) in depth for each gage.
(2) Sieve a small amount of minus 200 material in the bottom of excavated area for the gage to rest and then compact.
(3) Place the gage in the excavated area and sieve an additional amount of minus 200 material on top of the gage to protect it from damage from large aggregate.
(4) Add original subgrade material to fill gage location to grade and carefully compact.
(5) Locate gage elevation with respect to an appropriate benchmark and record.

All PAST transducers were installed beneath the lowest asphalt layer. Deformation is measured using a strain gage attached to the bituminous material. In reality the difficulty is in making the strain gage an integral part of the pavement. To lay the gages before compaction would involve exposing the gages to high temperatures and mechanical stresses. To install it in the finished pavement has its own share of complications involving separation

etc. There were no reports of any gages having failed immediately after installation. This is heartening considering the failure rate of gages could be as high as 30-50%. The following is a general description of the PAST transducer installation procedure.

(1) Apply a thin layer of bitumen prime within the area where the transducer is to be placed.

(2) Place a thin layer (approximately ½ inch (1.27 cm)) of sand asphalt mix on prime. Press the anchor bars of the transducer into the sand asphalt mix until contact between the strain gage bar and the sand asphalt mix is established. Allow sufficient time for the mix to cure.

(3) All cables should be protected with 1 to 1.5 inches (2.54 - 3.81 cm) of unbound fine material.

(4) Using hot asphalt mix from the paver, remove the aggregate greater than ½ inch (1.27 cm) and place a 3/4 inch (1.91 cm) layer on the transducer as cover material.

(5) Compact the material by applying a static pressure on the mix.

(6) Place asphalt mix to design thickness with a paver and compact using either a vibratory, pneumatic or steel wheel roller.

In June 1990, the Texas Transportation Institute instrumented eight of the twenty-four experimental test sites with the Multidepth Deflectometers (MDDs). The LVDTs used were hermetically sealed AC type with a range of either ± 125 or ± 0.25 inch. To install the MDD required that a 1.3 inch (3.30 cm) diameter hole be drilled to a depth of 8.4 feet (2.56 m). Once drilling was complete, the anchor, linings, top cap, MDD modules and center cores were installed. A saw cut 3/4in. (1.91 cm) deep and 3/8 in. (.95 cm) wide was then cut to accommodate the sensor cables. The cable ends were connected to a junction box, placed inside the existing buried concrete box. The cables and the top cap assembly were made waterproof by a loop sealant material supplied by 3M.

3.4 Description of Testing Equipment

Falling Weight Deflectometer

Deflection measurements have long been used to evaluate the structural capacity of in-situ pavements. The falling weight deflectometer (FWD) is one such device that can be used to obtain deflection measurements. The falling weight deflectometer, delivers a transient force impulse to the pavement surface. The impulse force can be varied by changing the drop weights and by increasing or decreasing the drop heights. The load is transmitted to the pavement through a loading plate, 11.8 in. (300 mm) in diameter. The load pulse is a half sine wave with a duration of 25 to 30 ms. The magnitude of the load is measured by a load cell. Deflections are measured by seven velocity transducers mounted on a bar that can be lowered automatically to the pavement surface with the loading plate. The Dynatest FWD is also equipped with a microprocessor-based control console that can fit on the passenger side of the front seat of a standard automobile.

18-Kip and 24-Kip trucks

Standard DOT dump trucks were utilized for this purpose. Special weights were added to the Back axles to satisfy the weight requirements.

3.5 Field Testing

The following two types of field tests were conducted on the instrumented sections.

- Moving Wheel Load Tests
- Falling Weight Deflectometer (FWD) Tests

For this research work all analyses were limited to tests using the FWD, with data from moving wheel load tests used for reinforcing some conclusions wherever necessary.

In addition to these two types of tests, the traffic level was monitored along the highway using weigh-in-motion equipment. This state-of-the-art equipment measures the weight of each vehicle and counts the number of axles and classifies each vehicle into one of

the twenty-four different categories. This data was stored in an on-site computer connected by Modem to the NCDOT Raleigh office. The data was downloaded periodically and summary reports developed. Frequent pavement ratings were made, and longitudinal profiles were monitored along with rut depth measurements.

The field testing was done about four times a year. Testing was carried out during the following months: September 1990, December 1990, February 1991, March 1991, May 1991, August 1991, October 1991, March 1992, June 1991, October 1992, February 1993, June 1993 and August 1993. During the testing period of June 1992, the truck tests were not conducted. Instead specific test sections were chosen, and FWD testing was conducted more than once at different temperatures. The testing team comprised personnel from both the NCDOT and North Carolina State University. Each of the testing periods lasted about five working days. Adequate early information about anticipated weather conditions was obtained before the beginning of each day of the trip to reduce delays that could result in inconvenience to the road users.

Moving wheel load tests were conducted at various load levels and at different vehicle speeds approximately four times per year. Tests were conducted using vehicles with 18-kip (80 KN) and 24-kip (107 KN) axle loads at speeds of 10, 35, and 55 miles per hour (16, 56, and 85 kmph). For each test section, measurements for stresses, strains, and deflections were recorded along with temperature and moisture readings. These tests were repeated for the various seasonal conditions encountered locally in North Carolina.

FWD tests were conducted using Dynatest Model 8000 FWD. These drops were made both on the gages, and also at specific intervals along the test sections. While the FWD gave a reliable method of observing deflection basins and thus providing a good estimate of layer moduli, the truck runs were expected to provide peak values of the stresses and strains.

A typical version of the field-testing sequence consisted of:

(1) Measurement of temperature and moisture levels in various layers.

(2) Collection of the following information for each of the truck passes, namely:

(a) Stresses and strains

(b) MDD measurements (in sections having MDD's)

(c) Plotter printouts for the entire strain and stress history of the truck passes and FWD drops.

The trucks were flagged off to a start and directed so that their dual wheels passed over the gages. Any lateral placement of the wheels (vehicle wander) from the gages was also measured.

(3) FWD drops were conducted on the embedded gages and on the MDD's. Three drops were conducted on each gage as a minimum. For each drop, the respective peak values along with the entire history for strains or pressures were recorded.

CHAPTER 4

ANALYSIS OF FIELD RESPONSE MEASUREMENTS

This chapter deals with the analysis of pavement response measurements like stresses, strains and deflections. Also, data from visual survey distress measurements are provided to compare the performance of the pavement test sections. Falling Weight Deflectometers have been utilized for the backcalculation of pavement layer moduli. The data from FWD testing has been primarily used for most of the analysis in this chapter. Also, data from the 18 Kip field tests have been used wherever necessary to supplement the information. Additional data regarding other loading conditions are provided in an Appendix available with this report.

In this report, all data obtained from the field (stress, strain, deflection, and distress measurements) are referred to as "field measured" results. Backcalculated values of pavement layer moduli are treated as "field measured" results. This is to distinguish them from laboratory determined moduli. All other responses obtained using elastic layer programs are treated as predicted values.

4.1 Measurement of Backcalculated Moduli

Most of the currently available techniques for backcalculation of pavement layer moduli use computer programs based on the multi-layered elastic theory. These programs attempt to match the deflection basin measurements to the deflections predicted by the multi-layered elastic theory, given the layer thicknesses, Poisson's ratios, magnitude and area of the applied load. These backcalculation programs can follow either of the following two solution methods: (a) iterative numerical integration of elastic layer equations or (b) application of efficient searching techniques to search a data base of deflection basins generated for ranges of layer thickness and modulus.

MODULUS 4.0 is a data base backcalculation program. It can be applied to a two, three, or four-layer system with or without a rigid bedrock layer. A linear elastic program is used to generate a data base of deflection bowls by assuming different modulus ratios (Scullion et al., 1990). The deflection basin data base is produced by a factorial of elastic layer

program (CHEVRON) runs. For a four-layer system, the elastic layer program is automatically run at least 27 times (3 surface x 3 base x 3 subbase modulus ratios). Once the data base is generated for a particular pavement, the linear elastic program is not called again, no matter how many bowls are to be analyzed. Instead a pattern search routine is used to fit measured and calculated bowls.

Moduli values for all of the 24 sections were backcalculated by the MODULUS program using the data from the FWD tests performed between December 1990 through August 1993, a total of twelve trips. FWD drops were made on the gages and along the entire length of the pavement sections at test locations, 100 ft. apart. Since the backcalculated moduli values vary along the length of the section, only those FWD drops made on the gages, were considered for backcalculating the layer moduli in this report. Generally three drops were made on each gage giving sufficient number of deflection bowls for reliable analysis. During the backcalculation process, depth to bedrock was not considered an input parameter, but instead was estimated using a default routine built into the program. Two different sets of sensor spacings were adopted during this research. The outermost sensors were placed at either at 48 inches (1.22 m)or at 36 inches (0.91 m). The difference in sensor spacings could play a role in the calculation of depth to bedrock. The calculation routine, uses the outer sensors (Sensor Nos. 5, 6, and 7) to extrapolate to a zero deflection point for calculating the depth to bedrock.

Backcalculated moduli of 24 sections for the various trips are presented in Tables 4.1 to 4.10. Some data fields are left blank due to non availability of data. In processing the FWD surface deflection data to determine the moduli values, the following assumptions were made:

(1) The moduli of all thin surfacing less than four inches thick were fixed at a constant value. These moduli were determined by the MODULUS program based on the type of coarse aggregates used in the surface course and the asphalt concrete temperature at the time of FWD testing. For all the trips, asphalt concrete surface temperature was measured using a hand-held temperature measuring unit. The unit has a probe

Table 4.1 Layer Moduli backcalculated using FWD data collected on US421 test sections (December 1990).

SECT #	A.C.LAYER MODULI (ksi)	BASE MODULI (ksi)	SUBBASE MODULI (ksi)	SUBGRADE MODULI (ksi)	DEPTH TO BED ROCK (inches)
1	1007	21.1		8.5	80
2	1045	42.1	137.7	13.8	62
3	535	17.5		8.8	63
4	1681	1494		22	300
5	1681	20.1	544.8	20.1	252
6	3788	162		22.9	300
7	620			12.8	145
8	1529	368	74.3	15.6	76
9	700			12.2	273
10	1785	1893	113.2	19.1	300
11	851		57.2	18.7	207
12B	944		20.7	18.9	129
12A	758		23.6	14.3	93
13B	319		17.3	10.8	98
13A	817		26.5	17.6	156
14	658		37.6	12.5	130
15	548	1405	68.9	23	300
16	947	47.6		15.9	46
17	835	44.6	61.9	18.3	48
18	835	504		19.4	300
19	362	1018	59.9	17	235
20	680			17.2	105
21	1111	144		21.3	96
22	1237			18.2	300
23	362	22.9		7.2	70
24					

Table 4.2 Layer Moduli backcalculated using FWD data collected on US421 test sections (February 1991).

SECT #	A.C.LAYER MODULI (ksi)	BASE MODULI (ksi)	SUBBASE MODULI (ksi)	SUBGRADE MODULI (ksi)	DEPTH TO BED ROCK (inches)
1	508	23.1		7.3	71
2	350	38.9	110.6	11	54
3	586	19.8		7.7	55
4	508	3000		22.4	300
5	774	25.7	208.4	20.7	198
6	5073	251		21.4	300
7	1017			13.6	300
8					
9	1294			12.3	300
10	971	2832	107.8	19.7	300
11					
12B	1248		21.3	17.4	154
12A	1610		20.2	19.7	170
13B	443		13.5	10.5	119
13A	1120		22.6	17.3	220
14	928		42	14	238
15	1432	790	68.7	22.9	300
16	1819	41.4		13.1	51
17	1339	17.3	269.4	17.3	48
18	1294	410		22.5	300
19	376	1397	57.6	18.1	300
20	715			16.7	113
21	1309	155		21	103
22	1451			16.2	300
23	1123	10		6.8	84
24	1339	39.2	50	7.2	95

Table 4.3 Layer Moduli backcalculated using FWD data collected on US421 test sections (March 1991).

SECT #	A.C.LAYER MODULI (ksi)	BASE MODULI (ksi)	SUBBASE MODULI (ksi)	SUBGRADE MODULI (ksi)	DEPTH TO BED ROCK (inches)
1	592	16.4		6.3	69
2	592	38.1	128.1	12.8	57
3	231	8.6		6.6	46
4	314	2294		20.6	300
5	548	27.1	229	21	240
6	2102	567.2		19.4	300
7	711			11.6	251
8	615	313.7	102.1	23.7	96
9	450			8	167
10	489	2983	93.1	18	300
11	375		168	15.1	123
12B	797		18.5	15.2	147
12A	1139		18.8	18.8	192
13B	164		8.2	8.2	74
13A	122		6.2	6.2	57
14	468		27.3	9.1	95
15	508	621	65.3	21.8	300
16	752	46.2		14.2	45
17					
18	690	356		22.4	300
19	690	664	64.2	14.6	300
20	422			12.6	72
21	372	294		18.7	81
22	454			12.5	164
23	256	15.4		4.5	60
24	283	33	100	7.9	123

Table 4.4 Layer Moduli backcalculated using FWD data collected on US421 test sections (May 1991).

SECT #	A.C.LAYER MODULI (ksi)	BASE MODULI (ksi)	SUBBASE MODULI (ksi)	SUBGRADE MODULI (ksi)	DEPTH TO BED ROCK (inches)
1	219	15		4	58
2	168	53	213.6	21.4	88
3	125	5.6		4.7	38
4	248	2082		20	300
5					
6	340	887		13.1	176
7	235			5.6	72
8	453	267	96.6	21	94
9	352				117
10	165	2344	112.4	16.9	300
11	199		29.3	9.8	69
12B					
12A					
13B					
13A	397	11.3		11.2	97
14	221		21.4	7.1	76
15	314	763	61.5	20.5	300
16	340	40.3		9.3	35
17	181	36.8	76.5	20.5	47
18	158	417		14.8	300
19	233	1215	82.8	14.1	300
20	307			10.6	66
21	144	241		15.9	68
22	315			8.4	91
23	241	16.6		5.3	64
24					

Table 4.5 Layer Moduli backcalculated using FWD data collected on US421 test sections (August 1991).

SECT #	A.C.LAYER MODULI (ksi)	BASE MODULI (ksi)	SUBBASE MODULI (ksi)	SUBGRADE MODULI (ksi)	DEPTH TO BED ROCK (inches)
1	248	16.2		4.7	58
2	420	55.3	328.8	32.8	244
3	217	10.9		6.4	51
4	191	1796		20.2	300
5	256	32.8	254.3	25.4	300
6	307	1967		9.3	74
7	212			4.4	55
8	161	364	187	20.4	85
9	86			2.7	46
10	233	2041	73.6	16.6	300
11	75		23.5	7.8	59
12B	105		18	7.2	51
12A	158		12.7	9.2	60
13B	88		6.3	6.3	56
13A	213		10.6	9.6	72
14	249		22	7.3	74
15	350	839	56.4	18.2	175
16	163	43.6		12	34
17	142	33.9	56.3	18.8	46
18	144	341		9.8	137
19	144	1277	52.9	13.1	258
20	347			12.2	73
21	381	237		14.6	68
22	162			6.9	71
23	186	15.4		5.2	55
24	191	45.7	50	13.7	220

Table 4.6 Layer Moduli backcalculated using FWD data collected on US421 test sections (October 1991).

SECT #	A.C.LAYER MODULI (ksi)	BASE MODULI (ksi)	SUBBASE MODULI (ksi)	SUBGRADE MODULI (ksi)	DEPTH TO BED ROCK (inches)
1	569	13.5		6.7	59
2	745	56.2	216.8	21.7	112
3	468	17.1		8.5	67
4	835	1512		20.8	244
5	470	28.8	249.1	23.5	256
6					
7	510			6.6	68
8	868	189.3	71	10.7	16
9	310			5.3	68
10	350	1765.4	68.2	17.2	300
11	389		32.9	10.7	78
12B	672		19.3	12.7	80
12A	847		16.4	16.3	104
13B	216		8.5	8.5	82
13A	869		13.3	13.2	106
14	792		32.2	10.7	114
15	1084	772.4	55.6	18.5	300
16	756	59		18.8	48
17	508	42.9	56.3	18.6	46
18	420	221.3		12.9	124
19					
20	932			15.7	97
21	843	241		17.4	83
22	1382			13.7	176
23	453	11		7.1	60
24	453	48.4	50	12.2	147

Table 4.7 Layer Moduli backcalculated using FWD data collected on US421 test sections (March 1992).

SECT #	A.C.LAYER MODULI (ksi)	BASE MODULI (ksi)	SUBBASE MODULI (ksi)	SUBGRADE MODULI (ksi)	DEPTH TO BED ROCK (inches)
1	376	13.4		5.3	60
2	337	35.1	122.3	12.2	56
3	188	13.8		6	50
4	293	2805.1		21.1	300
5	248	29.3	217.5	20.5	184
6					
7	629			5.5	66
8					
9	361			5.7	81
10	453	2337	130	16.5	300
11	632		47.5	15.6	130
12B	311		23.6	8.8	67
12A	497		18.5	12.4	82
13B	199		8.5	8.5	79
13A	771		16.4	12.7	100
14	888		31.6	10.1	110
15					
16	774	57.6		15.4	47
17	639	30.4	86.9	16.5	46
18	868	350.6		22.6	204
19					
20	1195			15.7	117
21	1826	254.1		18.1	106
22	812			11.7	141
23	470	10		4.1	56
24	508	35.7	50	8.2	109

Table 4.8 Layer Moduli backcalculated using FWD data collected on US421 test sections (October 1992).

SECT #	A.C.LAYER MODULI (ksi)	BASE MODULI (ksi)	SUBBASE MODULI (ksi)	SUBGRADE MODULI (ksi)	DEPTH TO BED ROCK (inches)
1	390	10.9	0	4.3	49
2	405	57.7	177.4	17.7	80
3	169	18.7		6.4	55
4	804	1948.1		20.4	300
5	241	35.3	249.6	25	300
6					
7	489			6.6	68
8	901	188.8	91.4	11.5	81
9	256			4.7	66
10	283	2058	63.4	16.8	300
11	266		36.3	11.9	87
12B	719		36.3	13.1	91
12A	925		15.9	15	93
13B	112		8.7	7.6	61
13A	583		14	11.7	100
14	386		38.7	5.9	59
15					
16	555	50.8		15.3	43
17	508	43.3	71.3	18.7	47
18	901	370.9		17.6	144
19					
20	524			12.5	75
21	573	219.6		17.3	73
22	846			9.3	102
23	639	10		3.6	47
24	935	37.5	50	10	140

Table 4.9 Layer Moduli backcalculated using FWD data collected on US421 test sections (February 1993).

SECT #	A.C.LAYER MODULI (ksi)	BASE MODULI (ksi)	SUBBASE MODULI (ksi)	SUBGRADE MODULI (ksi)	DEPTH TO BED ROCK (inches)
1	664	10.5		3.4	53
2	639	46.5	190.8	11.1	58
3	307	21.7		6.3	62
4	1164	1243.7		21	281
5	1681	20.5	251.1	20.5	298
6					
7	718			6.2	76
8					
9	603			7.7	138
10					
11	558		76.1	13.2	120
12B	1323		43.1	12.3	105
12A	1933		37.8	13.8	117
13B	225		8.7	8.7	101
13A	1263		16.9	12.1	113
14	899		28.6	9.5	109
15					
16	1382	48		13.8	49
17	1339	17.9	161.4	16.5	48
18					
19					
20	1219			15.6	107
21	910	270.5		20.4	104
22	1292			12.9	163
23	835	10		2.8	47
24	935	32.3	50	6.6	97

Table 4.10 Layer Moduli backcalculated using FWD data collected on US421 test sections (June 1993).

SECT #	A.C.LAYER MODULI (ksi)	BASE MODULI (ksi)	SUBBASE MODULI (ksi)	SUBGRADE MODULI (ksi)	DEPTH TO BED ROCK (inches)
1	161	10		1.6	45
2	325	48.7	256.6	25.7	125
3	149	7.8		5.3	44
4	283	1667		17.5	300
5	142	31.9	254.2	25.4	300
6					
7	145			3.2	50
8					
9	187			3.4	62
10	201	2460.9	111.6	15.4	300
11	179		30.3	9.1	69
12B	120		24.4	6	48
12A	212		10.4	9.4	64
13B	78		5.4	5.1	47
13A	234		8.3	8.3	69
14	238		20.5	6.2	69
15					
16	340	50.1		13.8	42
17	138	32.3	92.6	21.5	49
18	161	622.5		15.1	144
19					
20	284			10.7	67
21	326	229		16.2	72
22	456			10.1	119
23					
24	436	37.9	50	11.4	257

that reads the temperature on contact.

(2) For the sections with the asphalt concrete base, both the surface and base were counted as a single layer.

(3) Depths to bedrock were left to be calculated by the MODULUS program for all the sections.

(4) The stabilized subgrade was assumed to be seven inches thick.

The assumptions one and two were made based on available literature and the researchers' experience with the backcalculation techniques. Although actual depths to bedrock were measured during the construction of the test sections, it was determined not to use these values because the drilling locations in the sections could have been different from those where the MDDs were installed. Moreover, actual depths to bedrock were available for sections with MDDs only. The asphalt concrete moduli values from six trips, are plotted against the surface and pavement temperatures in Figures 4.1 and 4.2, respectively. Pavement temperatures is the average of the surface temperature and the temperature measured at the interface of that layer with the next layer. Thermocoples embedded in the ac layer where used to supplement temperature information wherever necessary. Two types of AC modulus are presented, one is the fixed modulus assumed by the MODULUS program and the other is the backcalculated modulus based on surface deflection basin data. Both these methods exist as two different options in the MODULUS program. For the remainder of this report, these analyses are called fixed analysis and full analysis for simplicity. Being calculated from the coarse aggregate type used in the AC surface and the temperature, the fixed AC moduli values cannot account for the change in the properties of AC layers due to traffic loading and aging. This deficiency is demonstrated in Figure 4.1 as a greater number of the backcalculated AC moduli values are positioned lower than the curve used to generate the fixed moduli values.

4.1.1 Influence of Depth to Bed Rock on Moduli Values

During the backcalculation process, depth to bedrock was not considered as an input

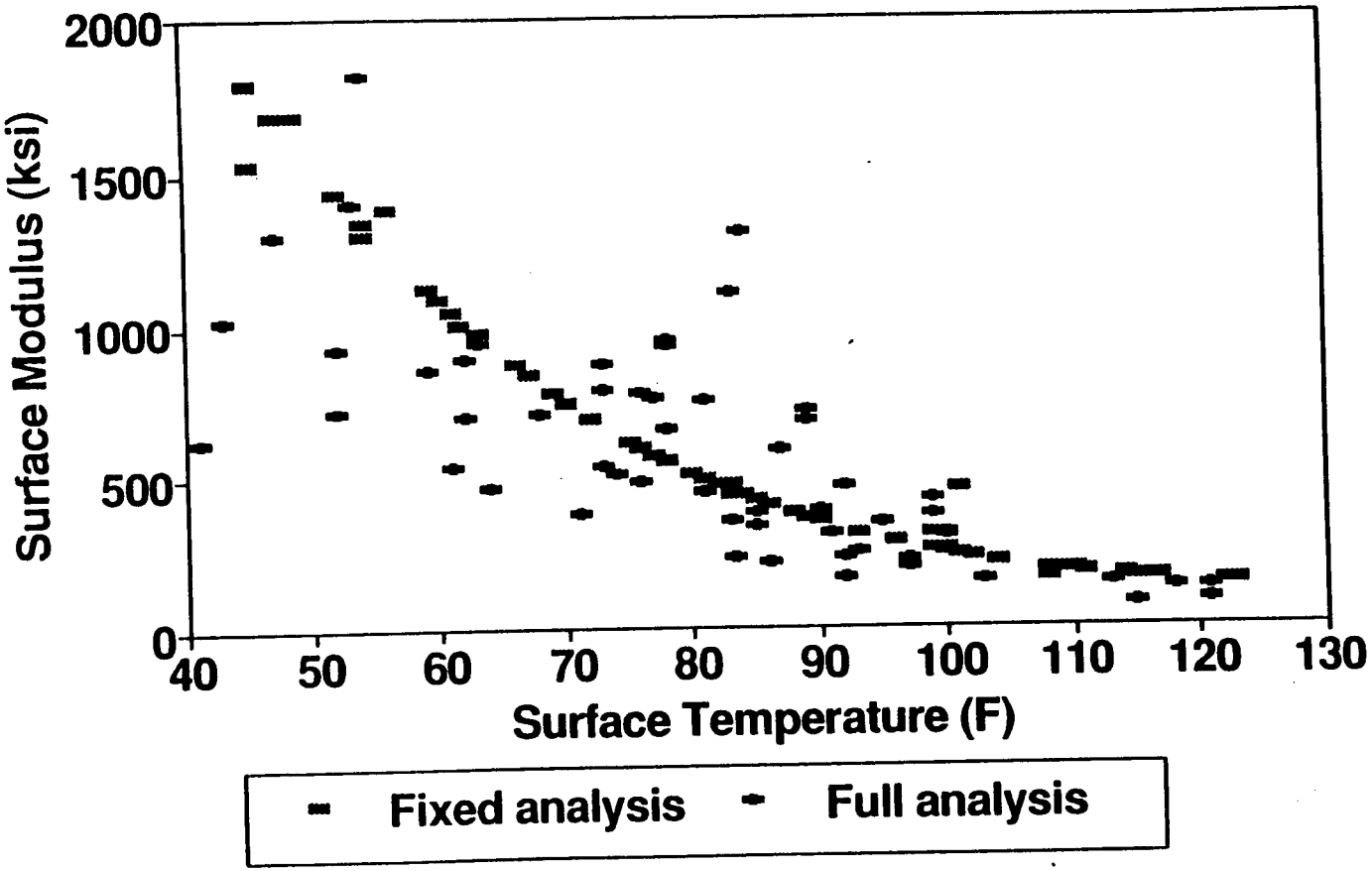

Figure 4.1 Relationship of surface moduli with surface temperature.

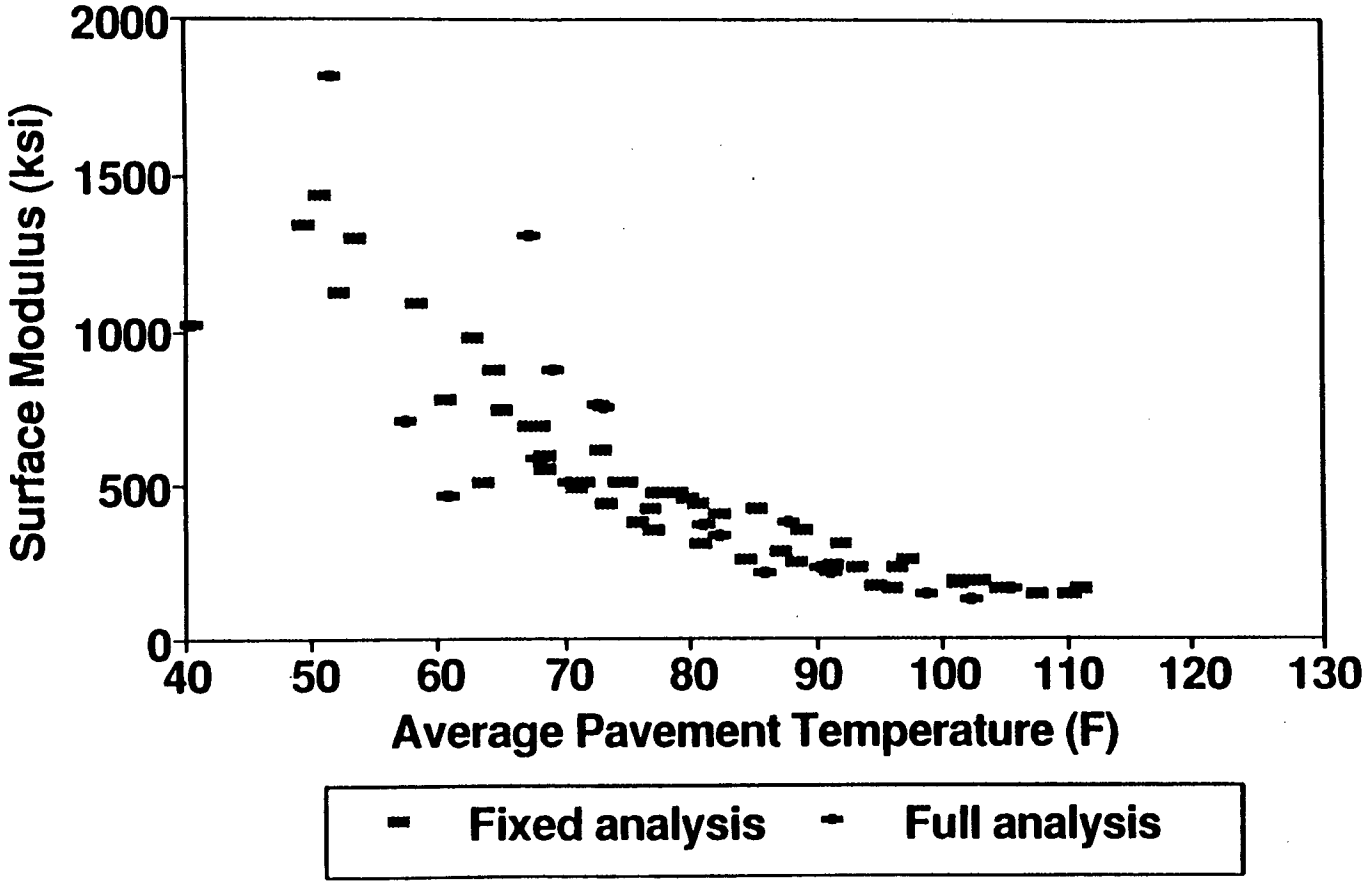

Figure

Figure 4.2 Relationship of surface moduli with pavement temperature.

parameter, but instead estimated using a default routine built into the program. Differences existed between calculated depth to bedrock values on the same location, but on different trip dates. Calculated depth to bedrocks were for most part different from those observed in the field. They varied over a wide range, making it difficult to estimate a pattern. This study was performed for the MDD test sections for which the depth to bedrock was available. Clearly, the subgrade modulus value obtained, is a function of the depth to a rigid layer implying that if the depth of the bedrock layer is unknown then the MODULUS program should be run with different values of depth to rigid layers to minimize absolute error between calculated and measured deflections. Previous research (Scullion et al., 1990) has shown that the best fit between measured and calculated bowls occurred with a rigid layer placed at approximately 300 inches (7.625 m) below the surface. As most calculated depths to bedrock are less than 300 inches (7.625 m), the subgrade moduli values need to be considered with a certain amount of engineering skepticism. For depths lesser than 60 inches (1.52 m), absolute error per sensor could exceed 25%.

It was also found that the calculated depth to bedrock in the full-depth AC sections is a strong function of the pavement temperature (see Figure 4.3(a)). The depth to bedrock for other sections is not very sensitive to the temperature change as can be seen from Figures 4.3(b) and 4.3(c).

For the MODULUS 4.0 program, currently being used, two approaches are adopted for acquiring the moduli. The first one is for thin surface courses in which there is no option for user input of depth to rigid layer. Sections 1, 23, 2,24, 4, 18, 5, 17, 8, 19, 10, 15 fall under this category. The second method adopts a default scheme for filling the value for the depth to rigid layer, which could be altered by the user. Sections 3, 16, 6, 21, 7, 20, 9, 22, 11, 14, 12, 13 fall under this category.

Correct information on depth to bedrock could help toward getting improved values of the modulus. Data from auger borings could be used to input the depth to bedrock. Even where the depth to bedrock numbers cannot be directly used, these provide a valuable tool in understanding the sensitivity of the moduli values obtained.

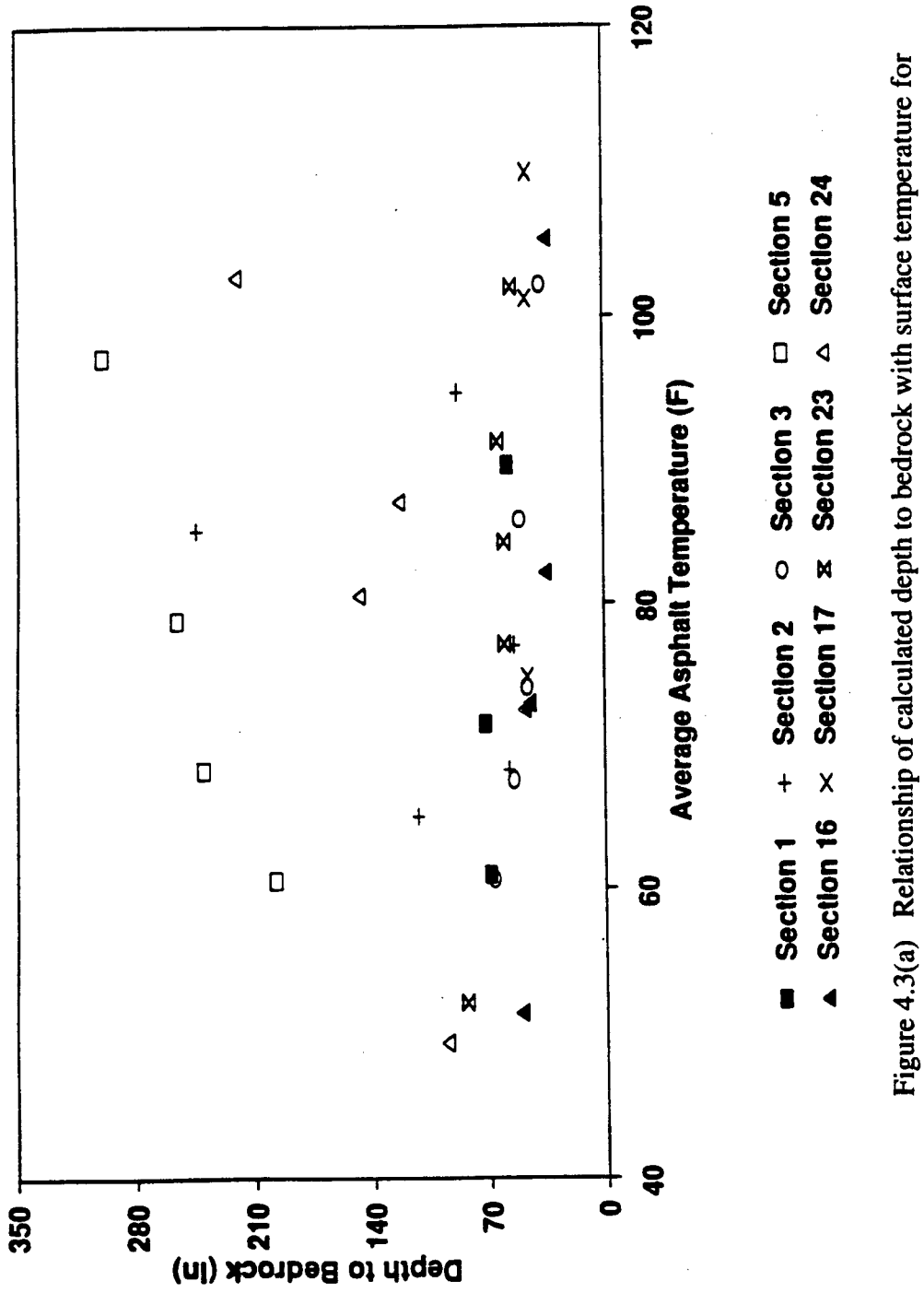

Figure 4.3(a) Relationship of calculated depth to bedrock with surface temperature for aggregate base course sections.

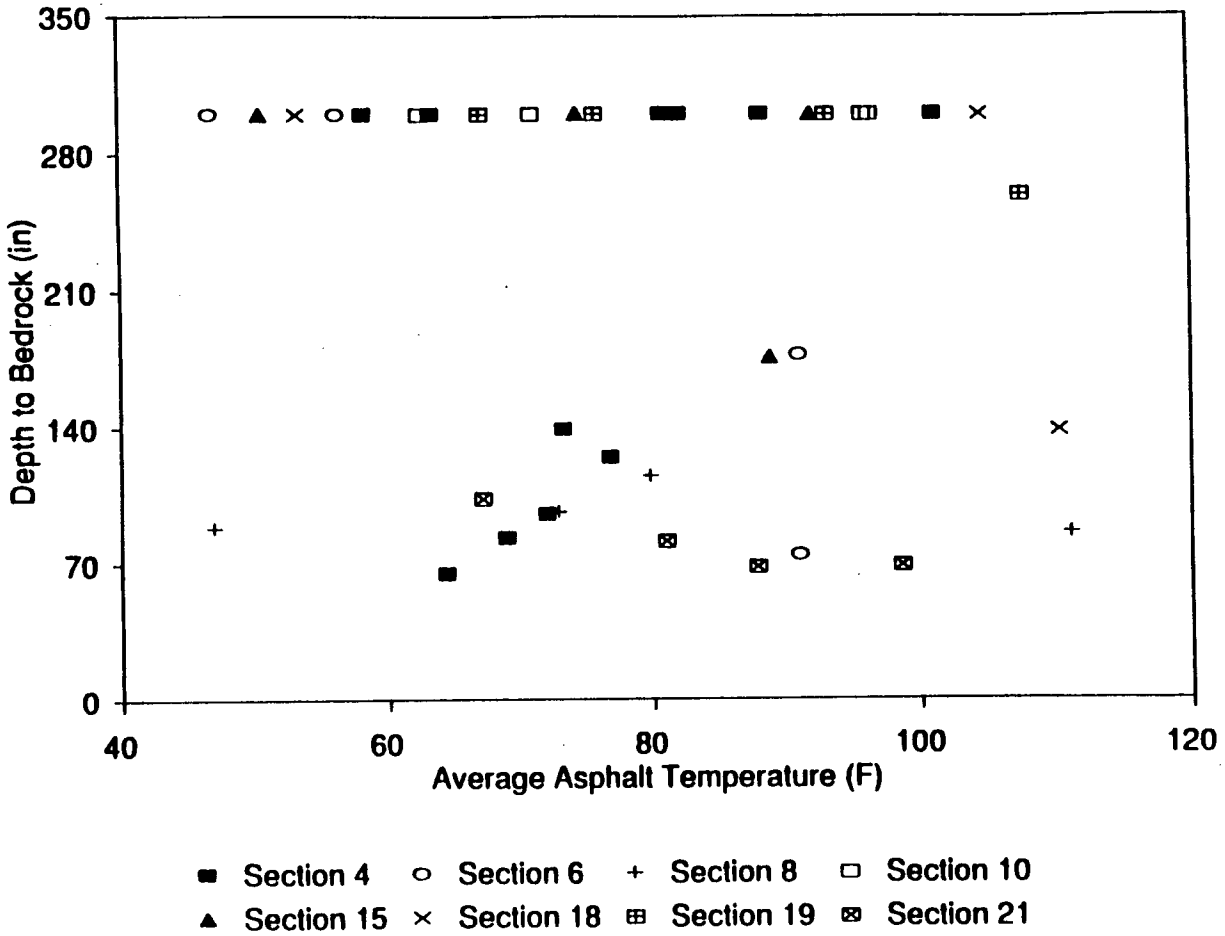

Figure 4.3(b) Relationship of calculated depth to bedrock with surface temperature for cement-treated base course sections.

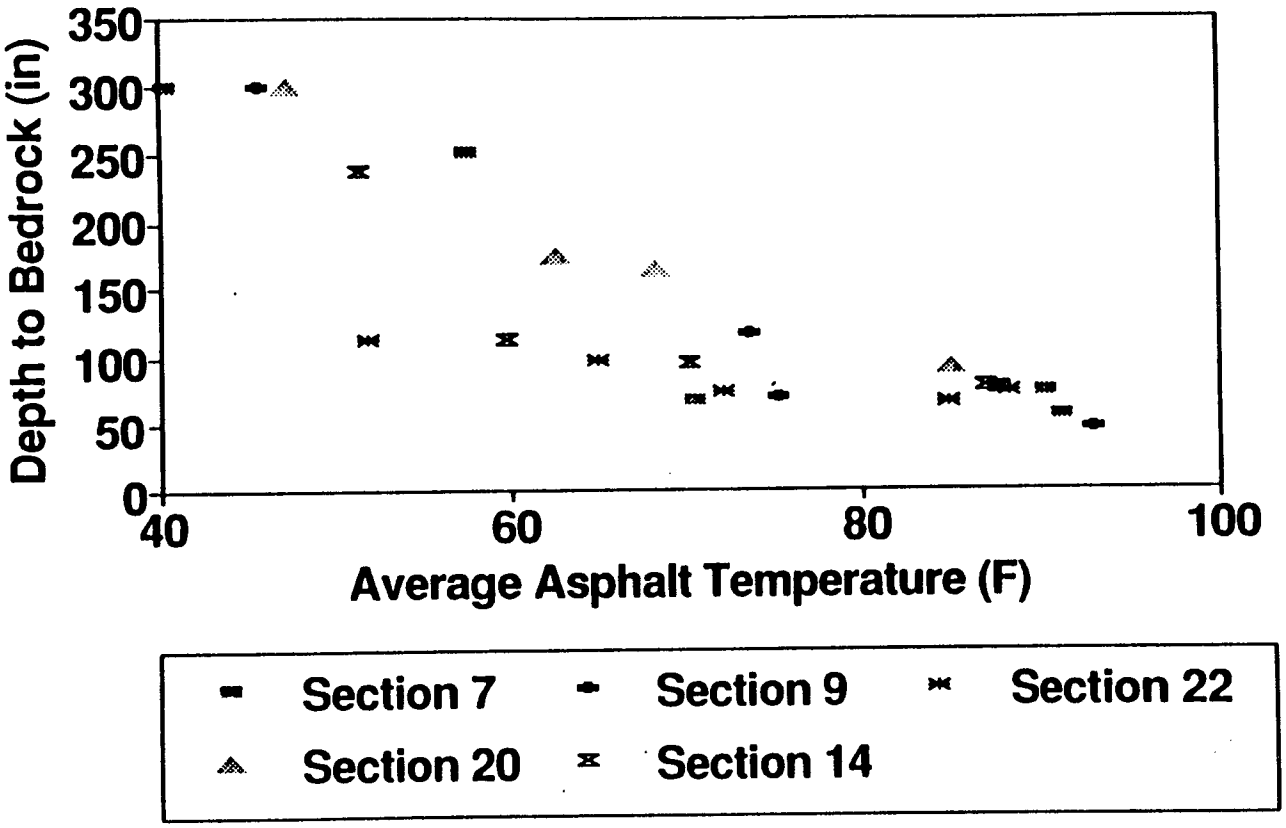

Figure 4.3(c) Relationship of calculated depth to bedrock with surface temperature for full depth AC sections.

4.1.2 Effect of Temperature on Moduli Values

The effect of temperature on the deflection measurements can be observed in the backcalculated moduli for sections tested during different periods of the year. This is to be expected considering the temperature dependency of asphalt concrete.

Pavement temperatures were a major source of variability in the analysis of the data. Consideration had to be given on how to represent pavement temperatures in the calculations. The OECD experiments suggest that adjustments for temperature be related to the type of structure (OECD,1991). However no adjustments were made for the measured temperatures in this project The surface temperature was used for the backcalculation of the moduli. The pavement temperature (temp. at various depths) was used in determining the temperature regime for conducting the various lab tests.

Pavement temperatures from thermocouples installed at different depths below the pavement surface as well as the air temperatures were measured during the daytime by the NCDOT and NCSU crew members. The pavement temperatures decreased with depth during the daytime, due to the effect of the suns rays. In this research, the relationship between air temperature and pavement temperatures at different depths were generated regardless of weather conditions and seasonal effects. The following relationship between the air temperature and pavement temperature was obtained from the analysis of temperature data.

$$PT=(923.91+0.31D)EXP[(0.016-4.26X10^{-4}D)(AT)]$$

where,

PT = pavement temperature in degree fahrenheit

D = depth (inch) beneath the pavement surface, and

AT = air temperature in degree fahrenheit

Figures 4.1 and 4.2 show backcalculated surface moduli as a function of surface temperature and average asphalt-layer temperature. Two types of AC modulus are presented, one is the fixed modulus assumed by the MODULUS program and the other is the

backcalculated modulus based on surface deflection basin data. Average asphalt-layer temperatures were obtained using measurements made at the surface and at the bottom of that layer. Thermocouples at 1 inch depth were also used when necessary to supplement temperature information. In the case of multiple asphalt layers, temperature measurements from thermocouples closest to the mid-depth were avaraged for obtaining the average temperature of the entire AC layer. The equation provided above for pavement temperature was used to obtain temperature regimes for laboratory tests.

4.1.3 Effect of Moisture on Moduli Values

Water mark sensor readings (soil suction values) were used to observe trends in subgrade moduli values with changing moisture contents. As can be seen from Figure 4.4 there is considerable scatter making it almost impossible to come to any immediate conclusion. From a theoretical standpoint this is quite a challenging task as it allows sufficient room for a variety of problems. For one thing, moisture effects need to be studied along with temperature. The subgrade moduli values are those obtained from a backcalculation routine. Lack of a trend as observed here, points toward shortcomings in the backcalculation program. As can be noticed, the subgrade moisture values are almost always less than 10 (soil suction number). Laboratory tests show that these could correspond to moisture levels of around 15% and above. That would mean that for all practical purposes the subgrade soil has usually been saturated. Further work is necessary to make any conclusive statements regarding the effect of subgrade moisture on subgrade moduli, especially the one obtained by backcalculation.

4.2 Analysis of FWD Deflection Data

This section deals with isuues dealing with the various tools available for extracting information from FWD deflection bowls, without necessarily having to conduct comprehensive backcalculation procedures.The general methodology is explained along with some specific examples. Also, the effect of surface temperature on deflection measurements is explained.

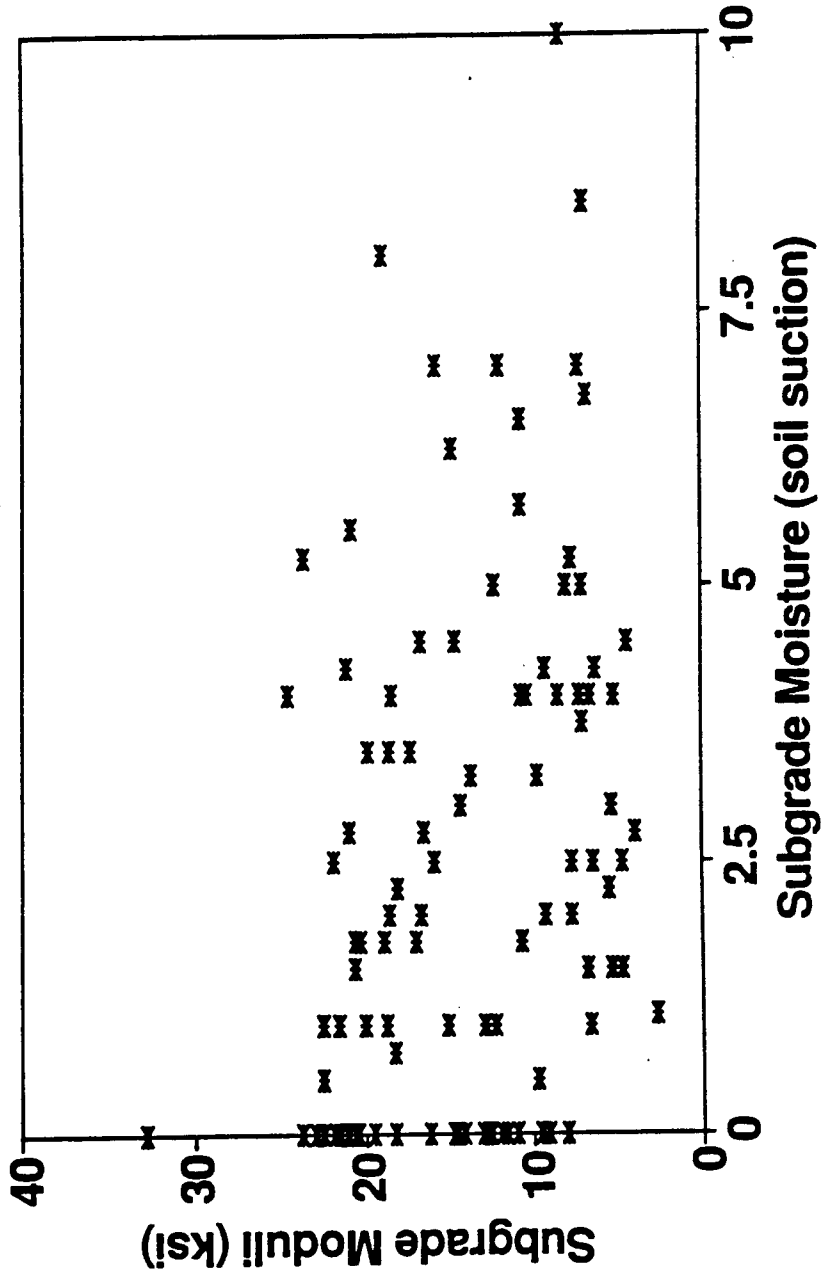

Figure 4.4 Relationship between backcalculated subgrade moduli and subgrade moisture.

4.2.1 Temperature Correction of Moduli for AC Modulus

A large number of methods for correcting peak deflections based on on ac temperature are presently available. Figure 4.5 shows actual field measurements made on Section 9 during June 1992. Readings were made at 3 different locations (milepost) on Section 9, during different periods of the day. The variation in Peak deflection is reflected in the figure. It can be seen that the the curve fitted lines for the three mileposts are almost parallel to one another, indicating that specific relationships for temperature correction of deflection can be determined for typical pavement configurations. Figure 4.6 shows similar measurements made at two different locations on Section 7. The difference in the slopes between the curve fits of Section 7 and Section 9 (both full-depth sections), indicate the need for a temperature correction factor based not only on the type of pavement (ABC, CTB, full-depth), but also on the actual structural thicness of the pavements. No temperature correction procedure was adopted as part of this research, but such an effort would be necessary if the deflection data was to be used for overlay design. This project primarily dealt with comparison of pavement performance. Also, since stiffness values were required for different seasons (temperature and moisture conditions), no normalization was carried out to remove the temperature variable. Nevertheless many methods are presently available to correct FWD measured deflection and backcalculated moduli for temperature. Seasonal and spatial variability in FWD data is discussed in detail in Chapter 9.

4.2.2 Direct Determination of Subgrade Moduli from Deflection Bowl Measurements

Figure 4.7 shows deflection basins obtained for Section 1 during different periods of the year. An exponential fit of the form $y = A\ exp^{x\ B}$ was performed on individual deflection bowls. R square values over 0.98 were consistently obtained for these fits. Figure 4.8 shows a plot between the A factor and the Subgrade moduli (backcalculated using more rigorous methods). Thus, using rigorous backcalculation procedures subgrade moduli versus A factor curves can be generated for many cases. This can then be used as a data base for determining subgrade moduli using simple curve fitting techniques can then be used on other. An

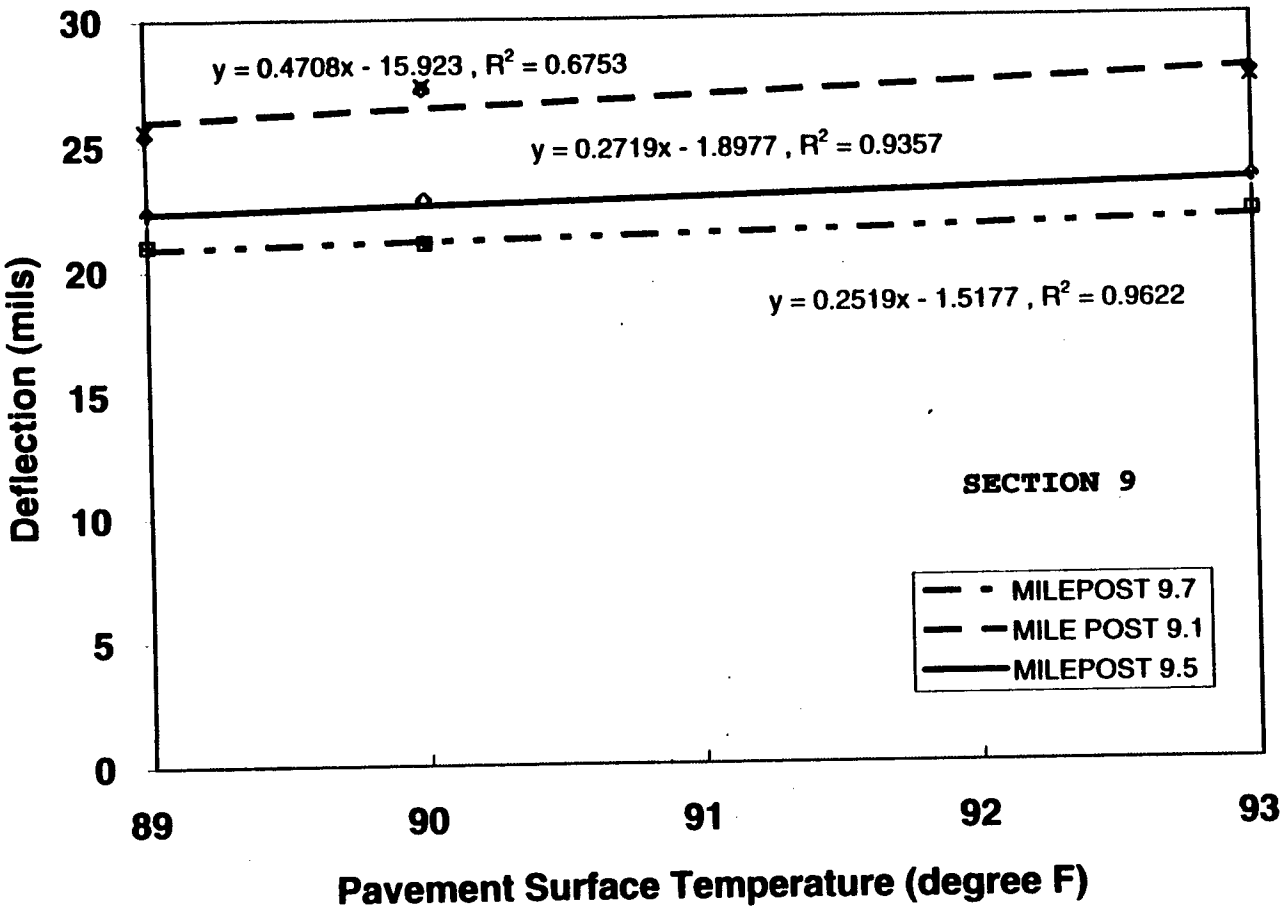

Figure 4.5 Deflection measrements made on Section 9 (June 1992).

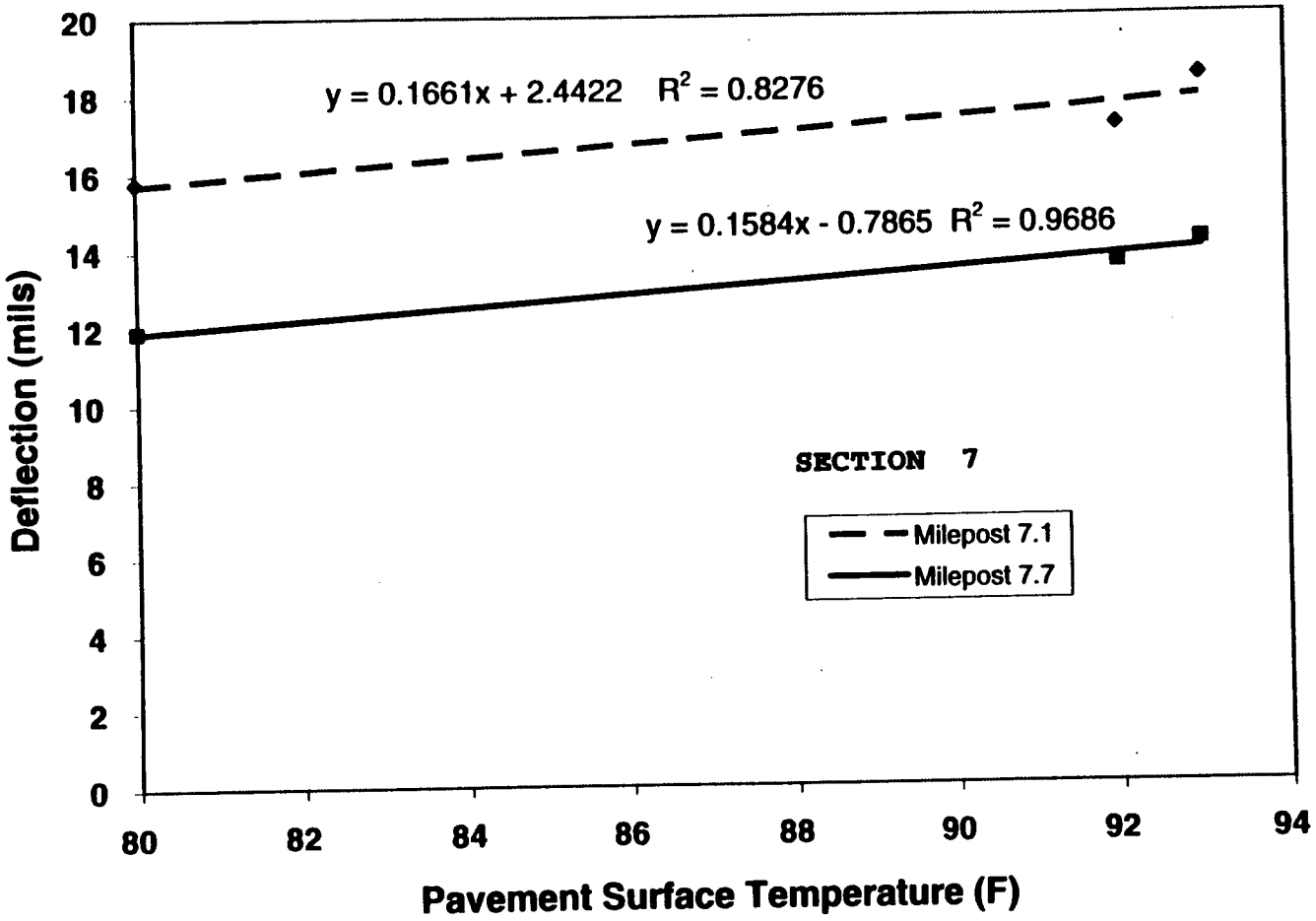

Figure 4.6 Deflection Measurements made at two Locations on Section 7.

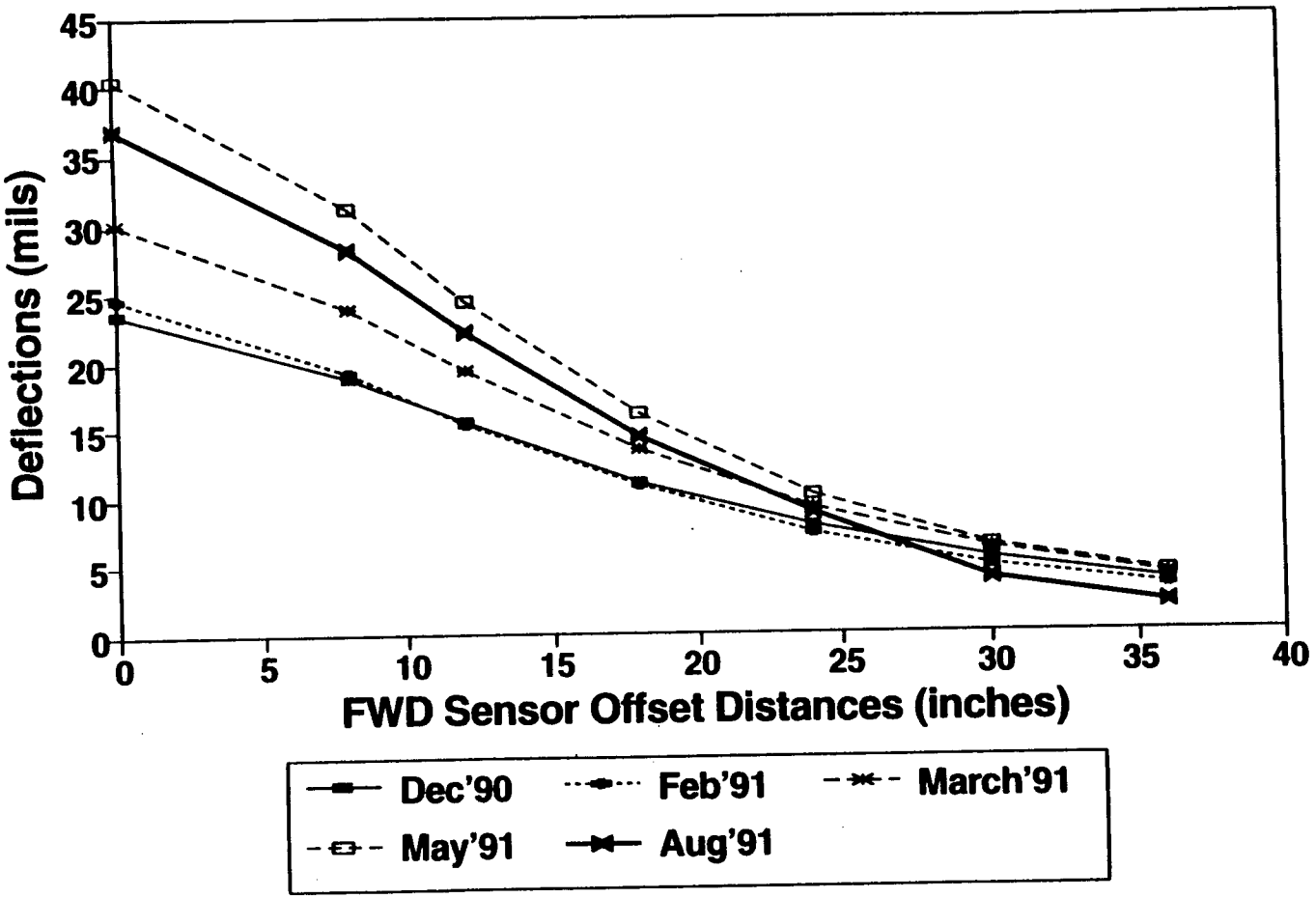

Figure 4.7 Deflection basins obtained for Section 1 during different testing periods.

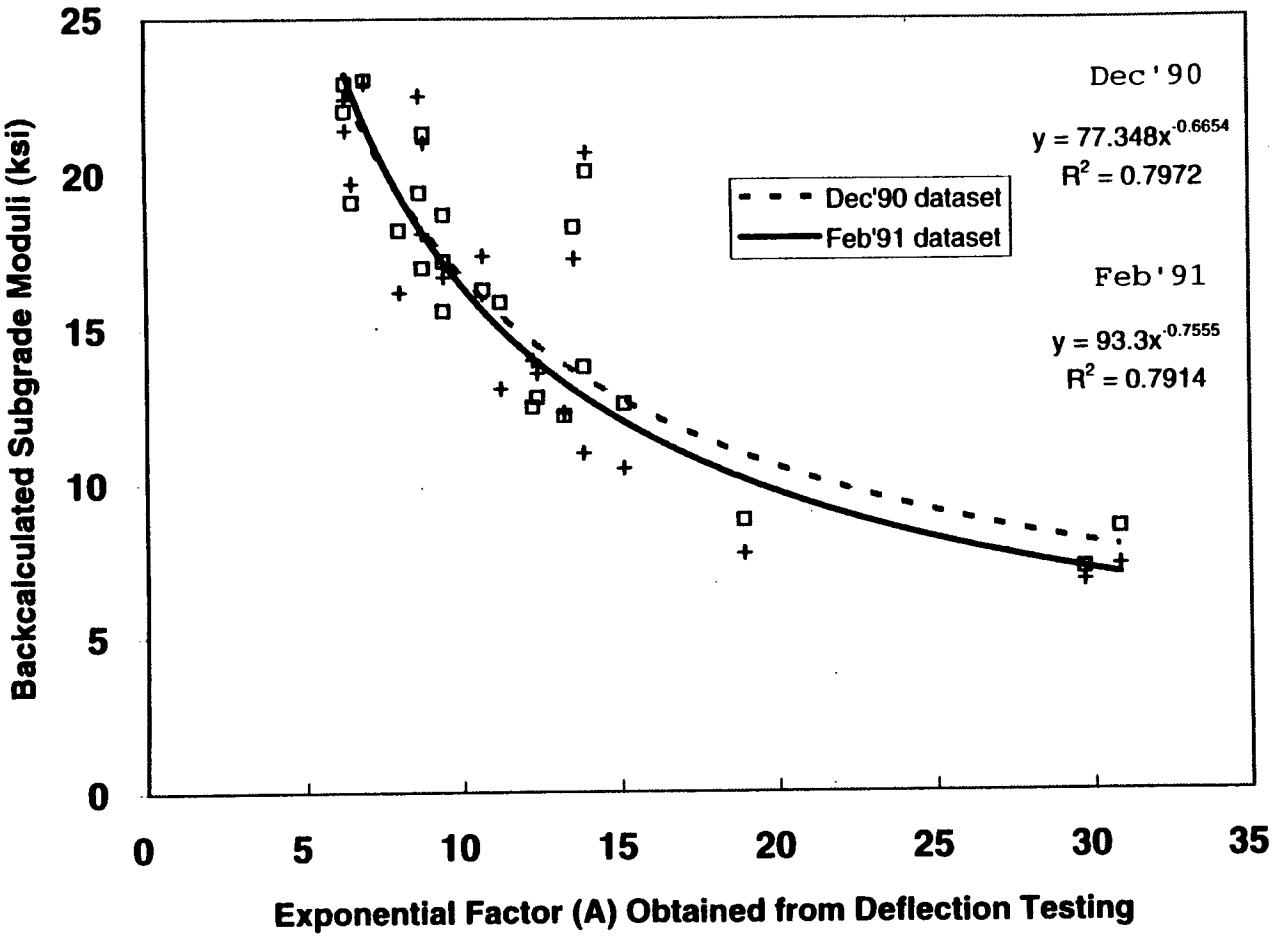

Figure 4.8 Exponential fit obtained between A factor and backcalculated subgrade moduli.

exponential fit can be performed on future deflection bowls to determine the A factor, which along with the database of curves can then be used to calculate the subgrade moduli.

4.2.3 Measurement and Interpretation of Curvature Indices from Deflection Bowl Measurements

It has long been felt that the actual curvature of the deflection bowl may be a better indicator of pavement condition, than just the peak deflections. Molenaar (Molenaar, 1994) has mentioned cases in Netherlands were computation of strains for secondary roads made based on relationships derived from curvature index. Surface curvature index (SCI) is the difference in deflection measurements between the sensor under the load (W_1) and the second sensor (W_2) . Figure 4.9 shows values for SCI, measured for all 24 sections during different periods of the year. The sections are grouped into 3 categories, based on the nature of the base type. High SCI values indicate good health of the pavement. Aggregate base course pavements have higher SCI compared to Full depth pavements. CTB pavements have the lowest SCI values. This figure also indicates difference in the SCI measurements for different periods of the year. The plot is cummulative in nature. Figures 4.10 and 4.11 show the base curvature index (BCI) and the base damage index (BDI) respectively. Base curvature index (BCI) is the difference in deflection measurements between the third sensor (W3) and the fourth sensor (W4) . The Base Damage index (BDI) is the difference in deflection measurements between the second sensor (W_2) and the third sensor (W_3) . The BDI is lowest for CTB sections showing a strong base course, and highest for ABC courses implying a weak base course. This meant that, although, some of the CTB sections exhibited large amounts of surface cracking, these cracks may be reflective in nature. It should be kept in mind that the Base Damade Indices do not truly reflect the effective performance of the pavement sections. The CTB sections were considered to have performed rather poorly due to excessive reflective cracking. These factors seem to merely point to the strength of the underlying layers rather than explain the effectiveness of the support offered.

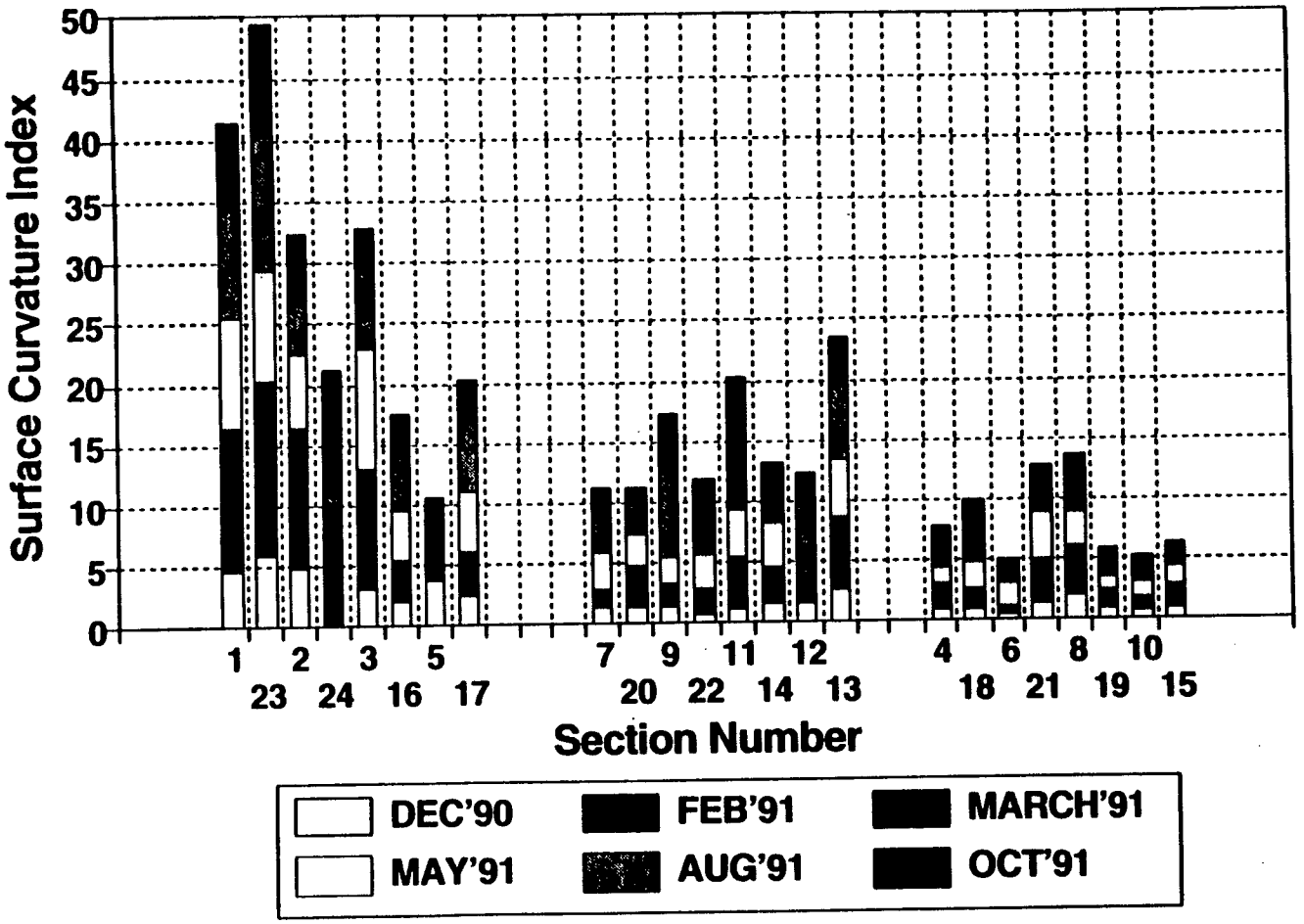

Figure 4.9 Surface Curvature Indices measured for different sections during different periods.

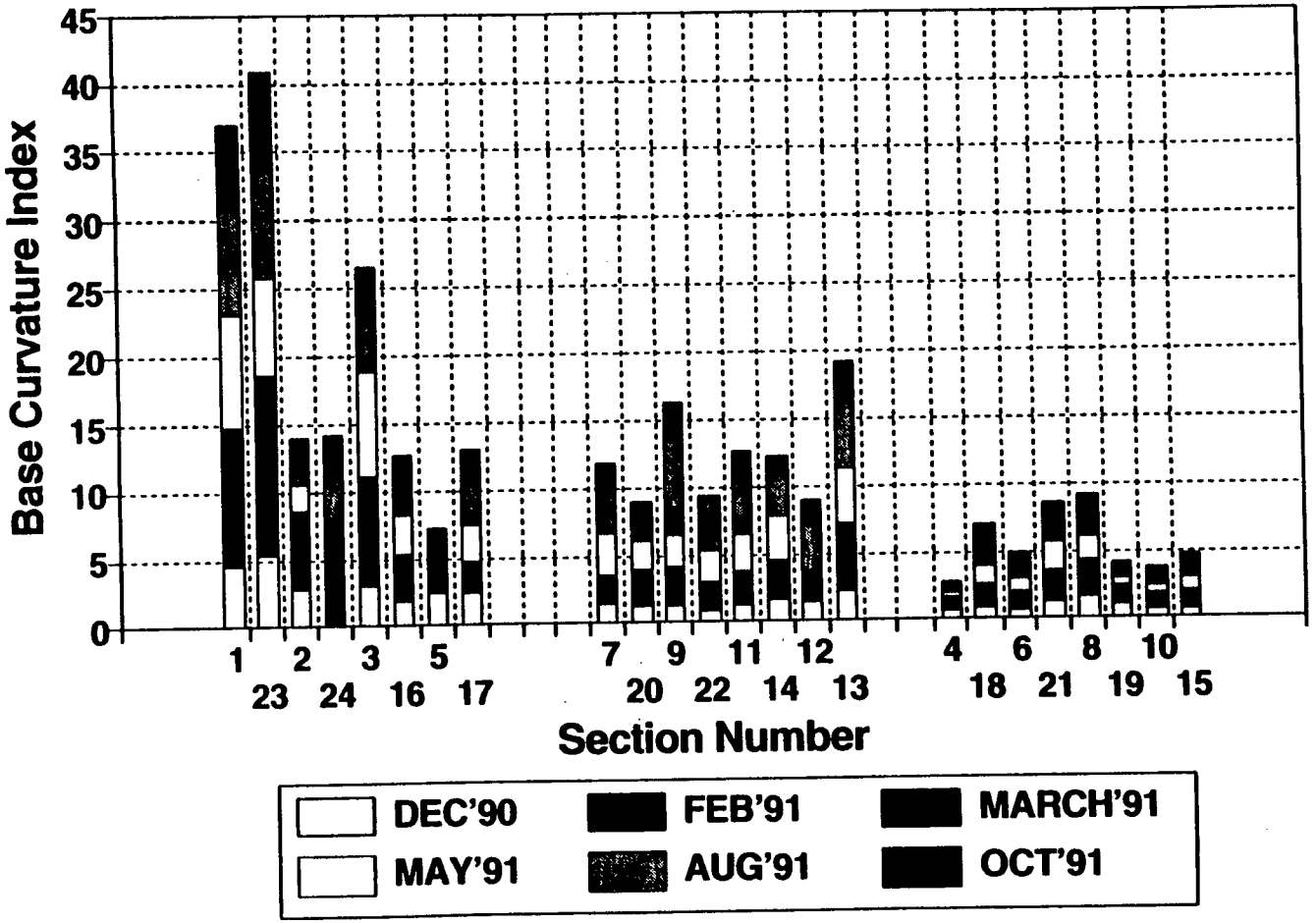

Figure 4.10 Base Curvature Indices measured for different sections during different periods.

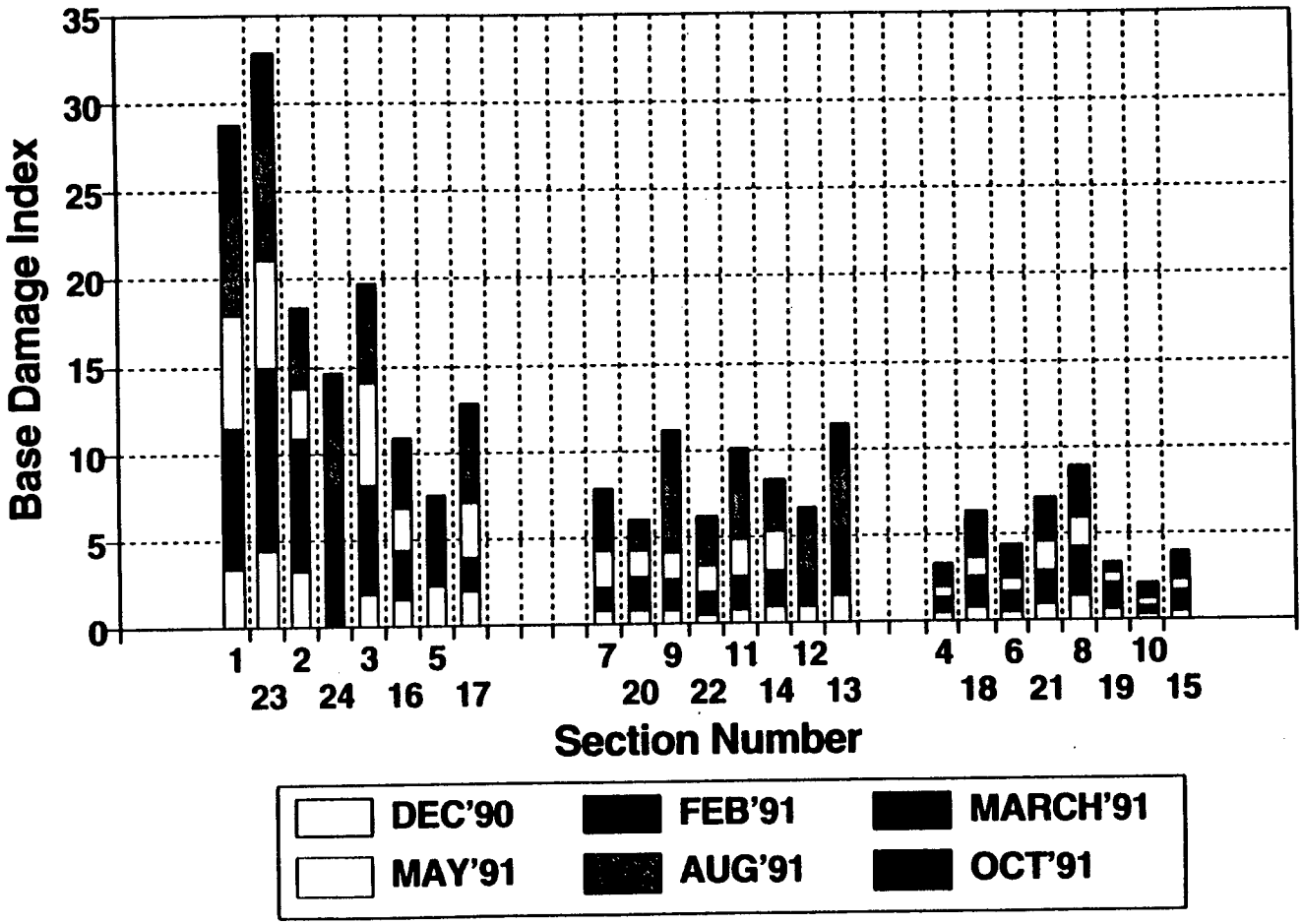

Figure 4.11 Base Damage Indices measured for different sections during different periods.

4.2.4 Relating FWD Measured Surface Deflection to Strain at the Bottom of the AC Layer

In any mechanistic procedure it is important to relate an input like wheel load, to an output or pavement response, such as stress or strain. Saal and Pell (1960) recommended the use of horizontal tensile strain at the bottom of the asphalt layer, as a parameter to minimize fatigue cracking. The following section provides a method of obtaining horizontal tensile strains using the FWD.

The FWD has provided a quick and useful way of measuring pavement surface deflections. Measurement of horizontal tensile strains at the bottom of the asphalt layer has not been that easy, requiring the use of elastic layer analysis. Many researchers have attempted directly to relate the peak surface deflections measured under a FWD loading to the tensile strain at the bottom of the asphalt layer using instrumented pavement sites. These relationships are as regression equations, and have been attempted primarily on full depth asphalt pavements. Figures 4.12(a) to 4.12(c) demonstrate the relationship between pavement strains and peak surface deflections. Regression relationships have been derived for all three design types. All data points plotted in Figures 4.12(a to c) are mean values.

As can be seen from Figures 4.12(a) the best regression relationships obtained between measured strains and maximum surface deflections were for the full depth asphalt sections. As can be seen from Figures 4.12(b) and 4.12(c) the R^2 values for sections with aggregate base course and cement treated base courses were relatively low. It can therefore be concluded that for full depth pavements the maximum surface deflection can be used reasonably to estimate the horizontal tensile strain at the bottom of the asphalt layer. For pavements with ABC and CT base courses, these methods provide comparatively poor correlation (R square of 0.53 and 0.12). It is therefore reccommended that such methods are best when used for full depth asphalt concrete sections. Alternatively, correlation studies between Surface Curvature Index (Section 4.2.3) and other indices obtained as a difference of different sensors (FWD geophones) may provide better correlation with the tensile strain at the bottom of the ac layer (Molenaar, A.A.A., 1994).

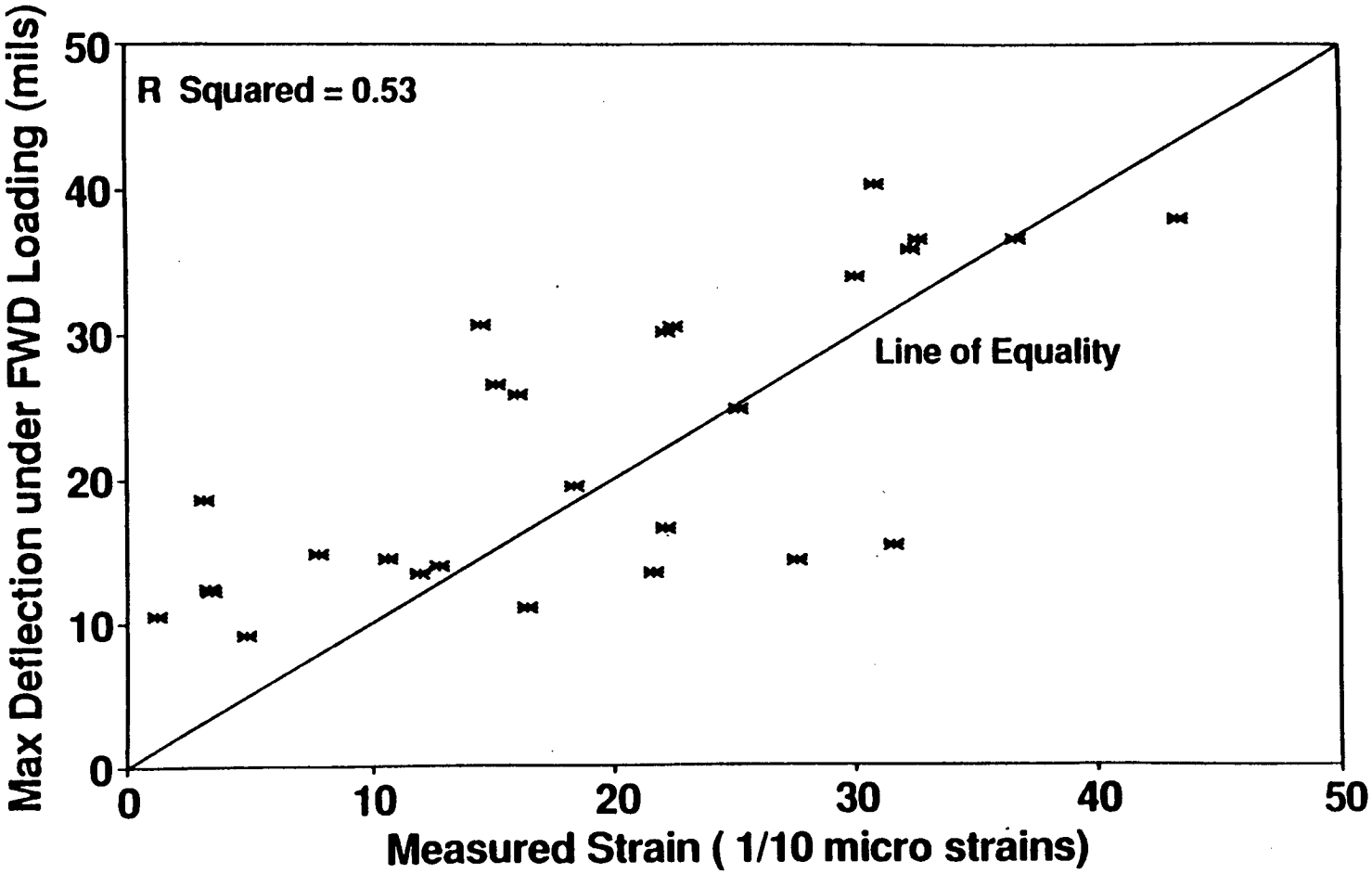

Figure 4.12(a) Relation between pavement surface deflection to pavement strain for aggregate base course sections.

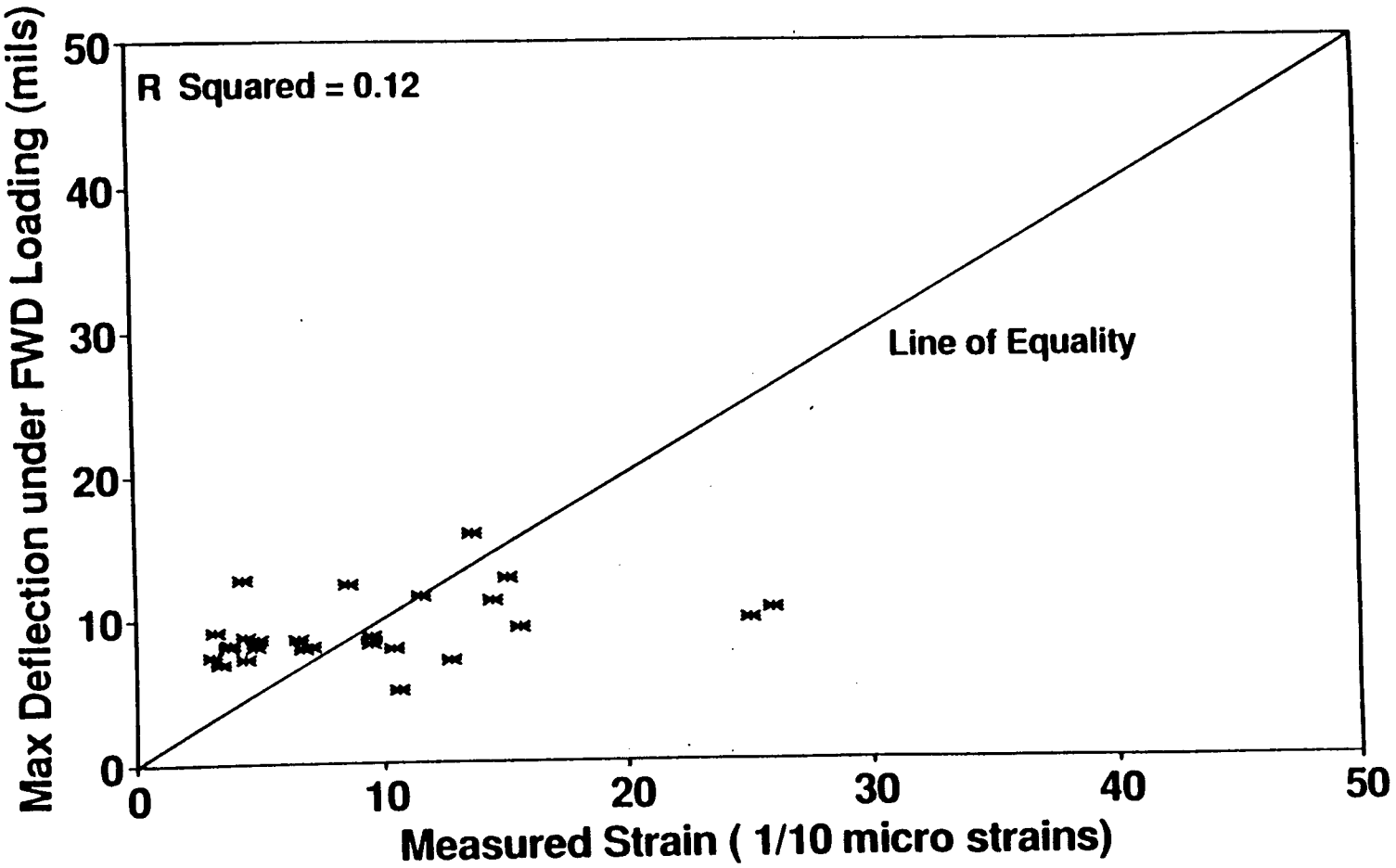

Figure 4.12(b) Relation between pavement surface deflection to pavement strain for cement-treated base course sections.

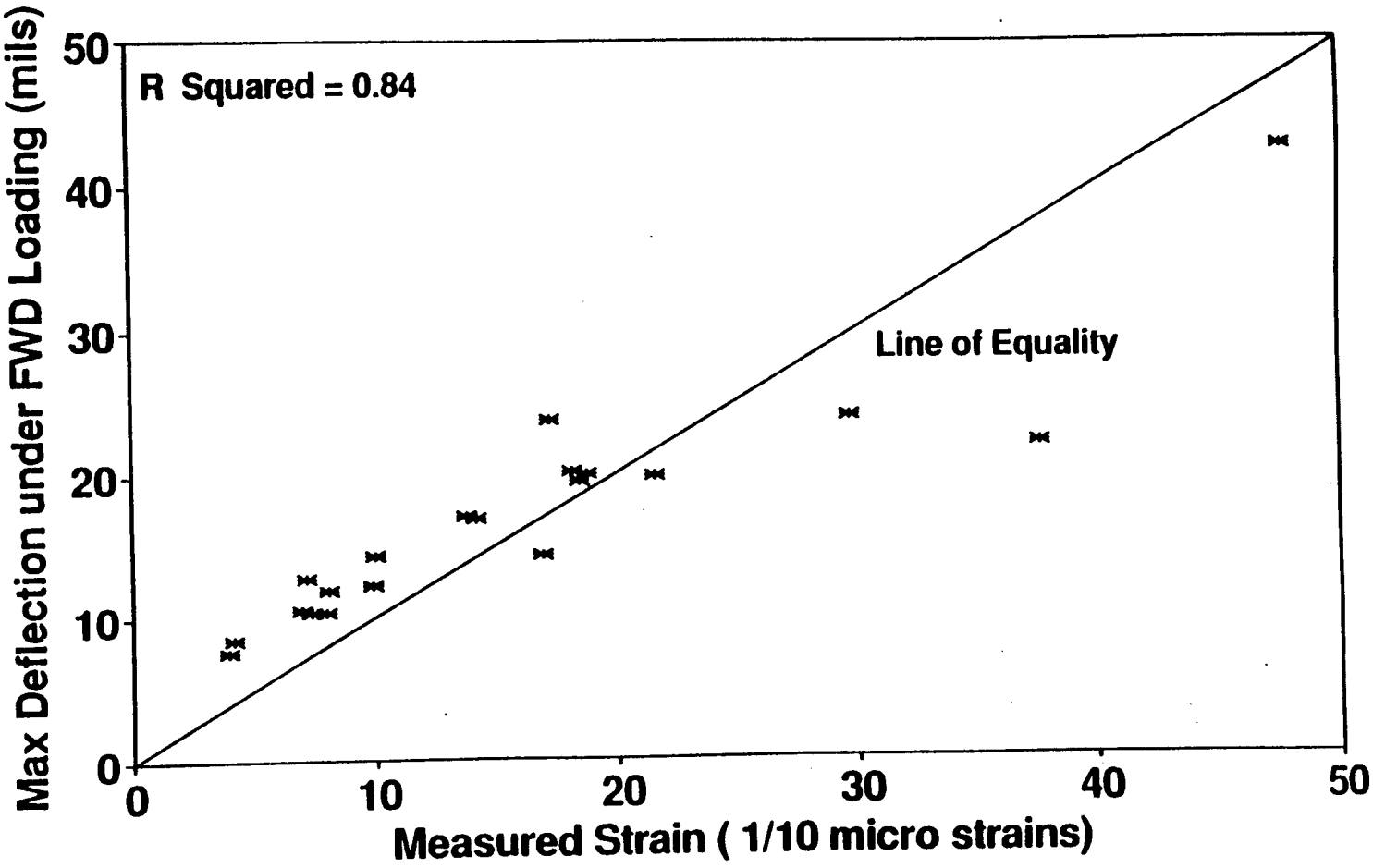

Figure 4.12(c) Relation between pavement surface deflection to pavement strain for full depth AC sections.

4.3 Calculation of Pavement Responses Using WES-5

Multi-layer solutions that calculate stresses, strains and displacements in pavement structures caused by surface loading have been in existence for several decades. However, the use of PC-based software for multi-layer analysis is continually being developed and improved upon. Computation of pavement responses was made using WES-5, a multi-layered elastic theory-based program. This was developed by engineers at the Waterways Experiment station in Mississippi. The selection of the WES-5 program was based on comparisons, conducted using various programs like ELSYM5, WES-5, and CHEVPC. All these programs provide almost identical results. The WES-5 was chosen, due to the easy availability of the source code, which was essential for use in the mechanistic design program (NCFLEX) designed at NCSU.

The WES-5 program contains two separate programs INLEA and WESLEA. The first one takes in the input information and the other, using the input information, generates the response values at the specified locations. The program accepts the following information as input: layer thickness, layer moduli, Poisson's ratio, and interface condition. The program requires a five-layer system. The following method was adopted to arrive at the requisite five-layer format. The fifth layer was considered as hard rock with a modulus value of 30 million psi and Poisson's ratio of 0.1. Surface, base and subgrade layer properties were used as input for the top 4 layers. For systems with only two layers and a subgrade, the subgrade was split into two or more layers to satisfy the five layer criteria. Subgrade thickness calculations were based on depth to bed rock predicted by the backcalculation program MODULUS 4.0. It was decided to use the calculated depths to bedrock to maintain consistency in the analysis. Although the WESLEA program models interface conditions based on Coulombs law, for this analysis, a full friction condition (no slip) was assumed for the interface.

4.3.1 Comparison of Measured versus Predicted Pavement Responses

Dependence on observed performance is necessary because theory alone has not proven sufficient to design pavements realistically. Differences between measured and

predicted pavement performance may arise not just due to limitations in the classical theory but also from inappropriate modeling of loading conditions and layer properties. Data collection to response prediction has been a two-stage process involving backcalculation and followed by a forward calculation routine. The nature of errors in both the steps along with how these errors complement one another, needs to be understood for a clear interpretation of comparison between measured and predicted responses.

The pavement responses including strains at the bottom of asphalt concrete layers, stresses at the top of subgrade, and deflections at different depths were calculated based on the application of a 9 kip (40 KN) load with a circular contact area (Dynatest 8000 FWD loading configuration).

Strain at the bottom of AC layers

Comparisons between the measured and predicted strains at the bottom of AC layers were conducted for the three groups with different base types. Measured strains are averaged values of multiple drops over several gages (typically three). The following observations can be made from the comparison.

For sections with an aggregate base course, a definite trend is noticed where measured strains are smaller than the predicted strains (see Figure 4.13(a)).

A study of sections containing cement treated base reveals that the technique for calculating the pavement responses cannot predict the strains at the bottom of asphalt concrete layers over severely deteriorated cement-treated-base course layers. As shown in Figure 4.13(b), the predicted strains were relatively constant around the value of 30 micro strains whereas the measured values changed drastically. One major reason for this discrepancy could be that the stiffness reduction in the pavement system due to the cracking of CTB layers is not accounted for in the multi-layered elastic theory. More specifically, the multi-layered elastic theory-based calculations assume an individual layer as a continuous layer with a single modulus value whereas in reality, cracks in the CTB layer can cause much larger local displacements.

Previous studies (Van Caulwelaert et al., 1989) have indicated the influence of the

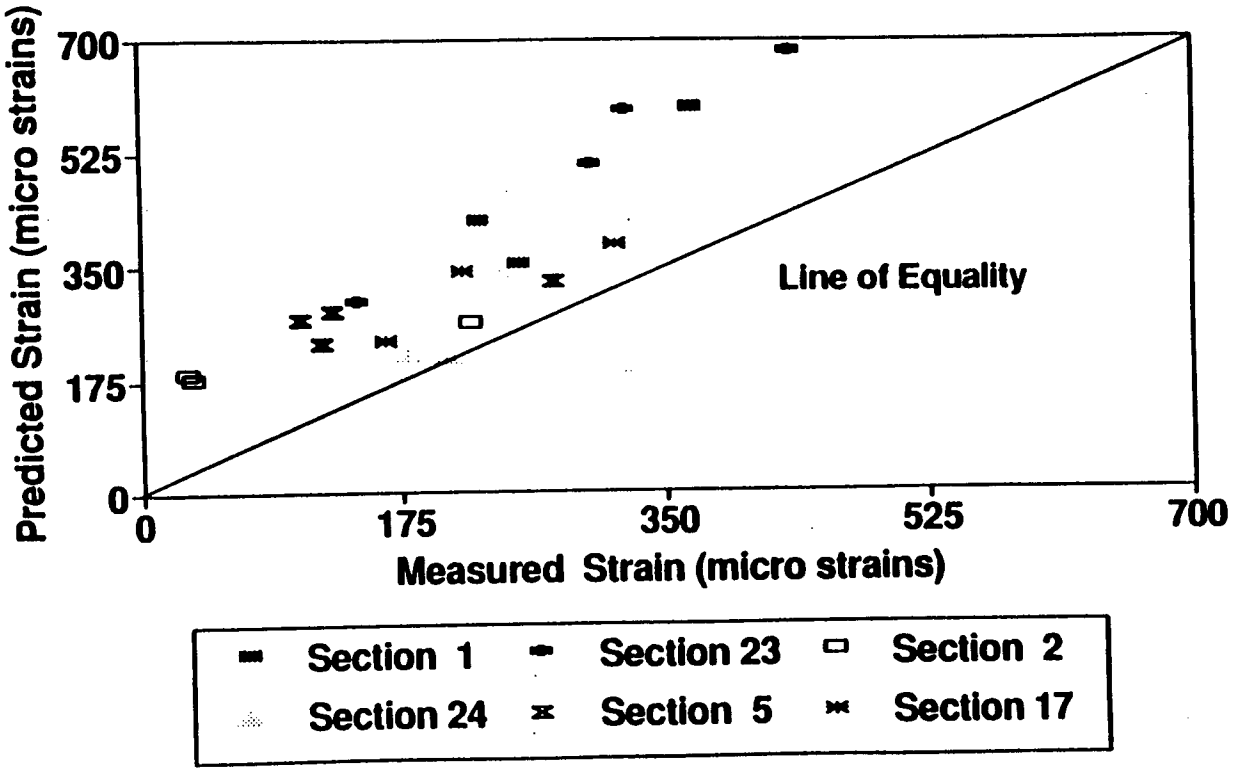

Figure 4.13(a) Measured versus predicted strains for FWD loading on aggregate base course sections.

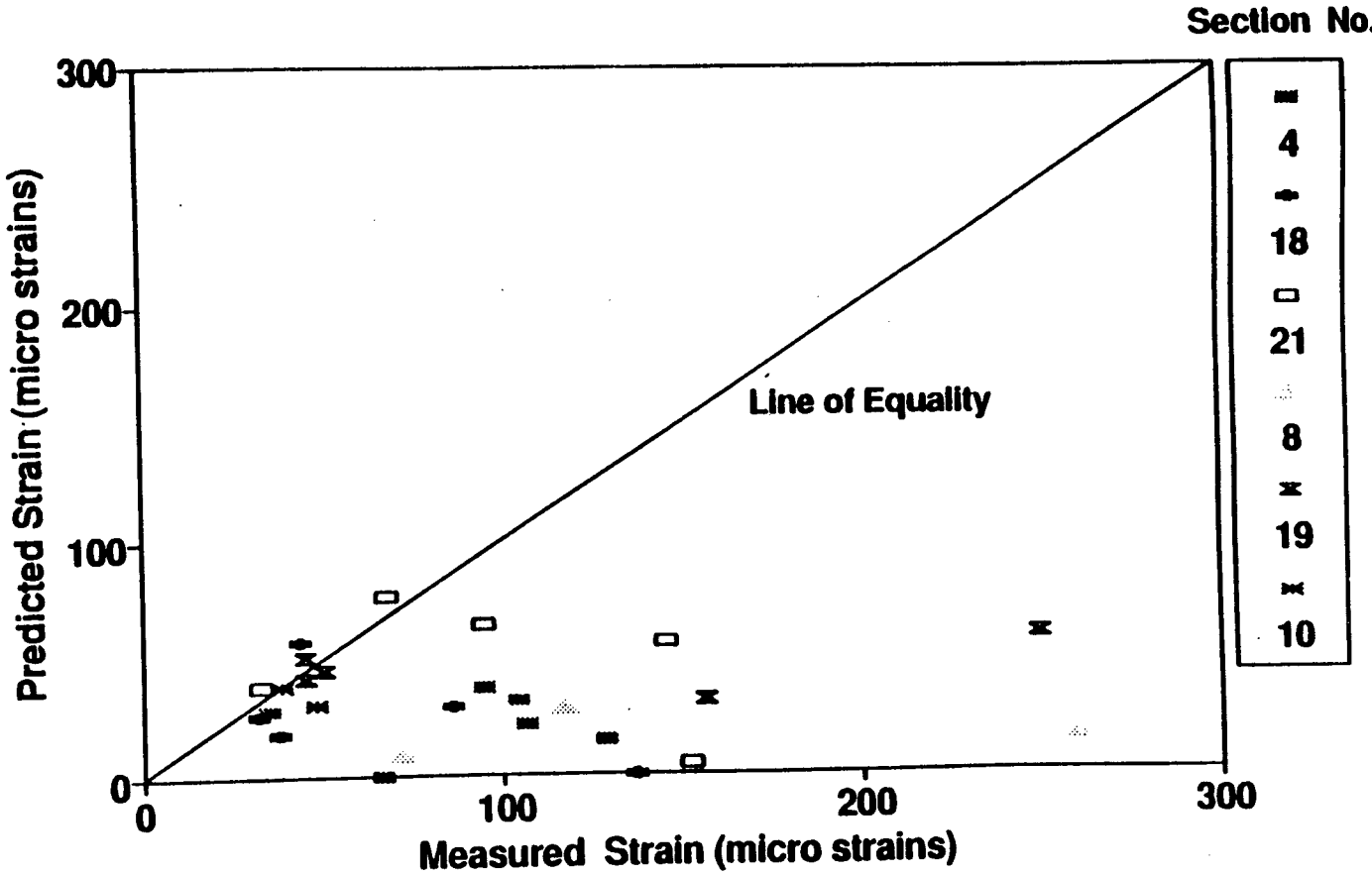

Figure 4.13(b) Measured versus predicted strains for FWD loading on cement-treated base course sections.

presence of stiffer layers below the surface on integration intervals used in forward calculation routines and by that on the accuracy of the predicted responses. There are also problems regarding the assumptions for the interface condition; condition for full friction as assumed in this calculation may not be realistic. Studies have pointed out that the horizontal stress at the bottom of the surface layer of a multi-layered system can vary up to 300% when going from full to zero friction. The disparity between measured and predicted values could also be studied from the viewpoint of the depth at which the response from the installed gages is measured. Gages at a depth of 2 inches (5.08 cm) from the surface may be very close to the surface, making it susceptible to the high impact FWD blows in a way that may not be realistic.

Figure 4.13(c) shows the comparison between measured and predicted strains.

Deflections at different depths

Figures 4.14(a) to 4.14(c) present plots of predicted versus measured depth deflections for three groups categorized by the base type. Sections included in the individual groups
are as follows:

(1) Group 1: Sections 1, 2, and 3.

(2) Group 2: Section 8.

(3) Group 3: Sections 7, 9, and 11.

Although Section 6 has an MDD, it was eliminated from the analysis because of unrealistic moduli values obtained from most of the trips. The distress records clearly indicate that Section 6 had failed due to cracking of the underlying cement treated base course. For brevity the term "depth deflections" is used in this section to denote deflections measured at different depths.

The data in Figures 4.14 represent peak deflections at all depths picked up by a database sorting procedure after verifying the integrity of the signals obtained. For ABC sections (Group 1 in Figure 4.14(a)), overall comparison was somewhat satisfactory, although the accuracy of prediction was section dependent. In this regard, depth deflections in Section

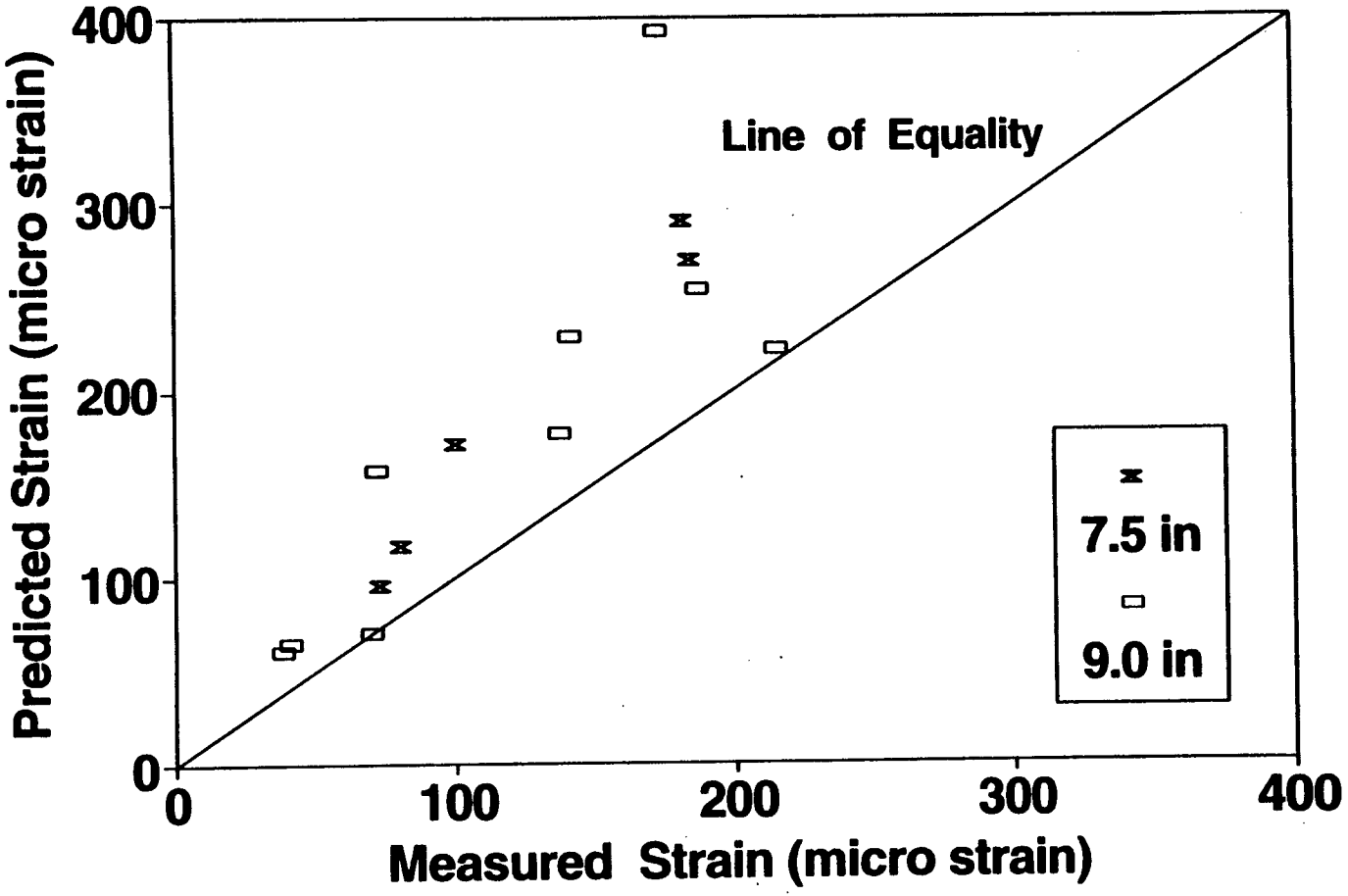

Figure 4.13(c) Measured versus predicted strains for FWD loading on full depth AC sections.

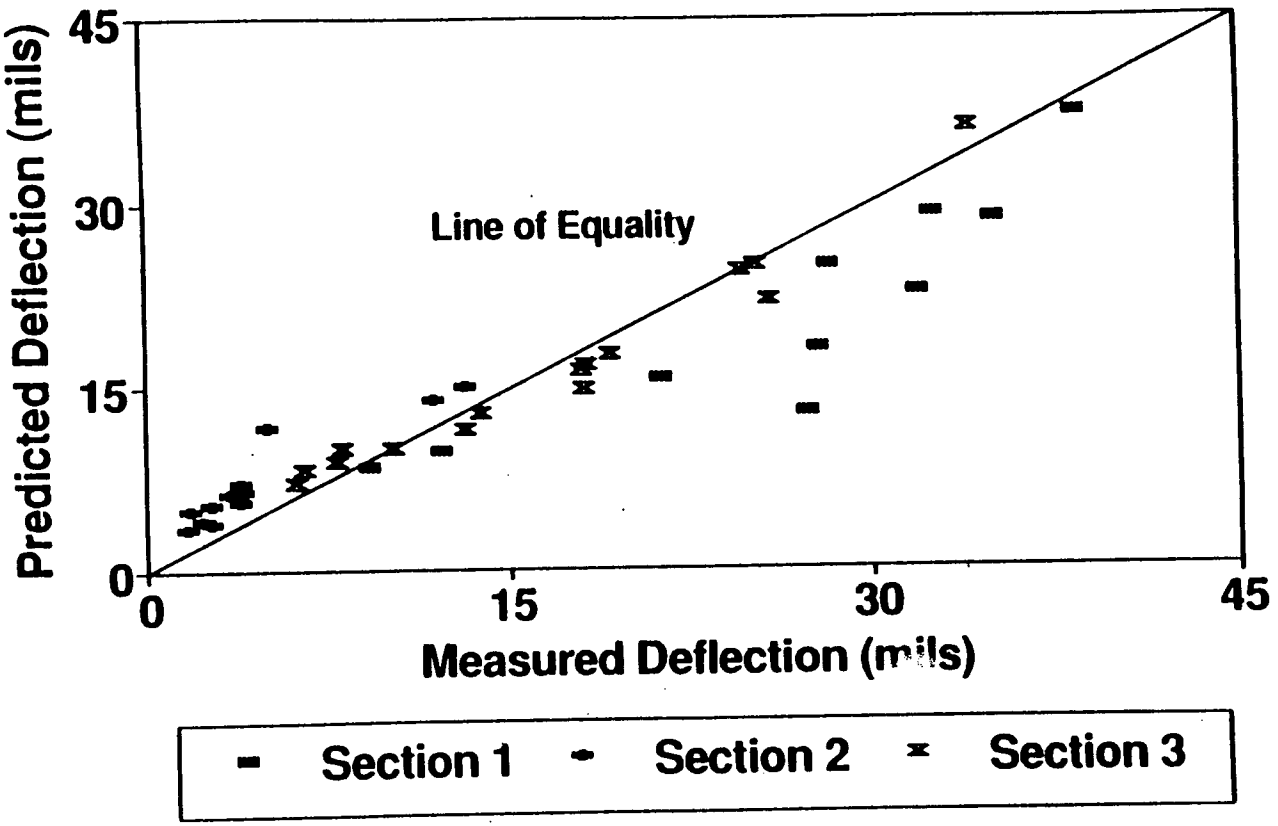

Figure 4.14(a) Measured versus predicted deflections for FWD loading on aggregate base course sections.

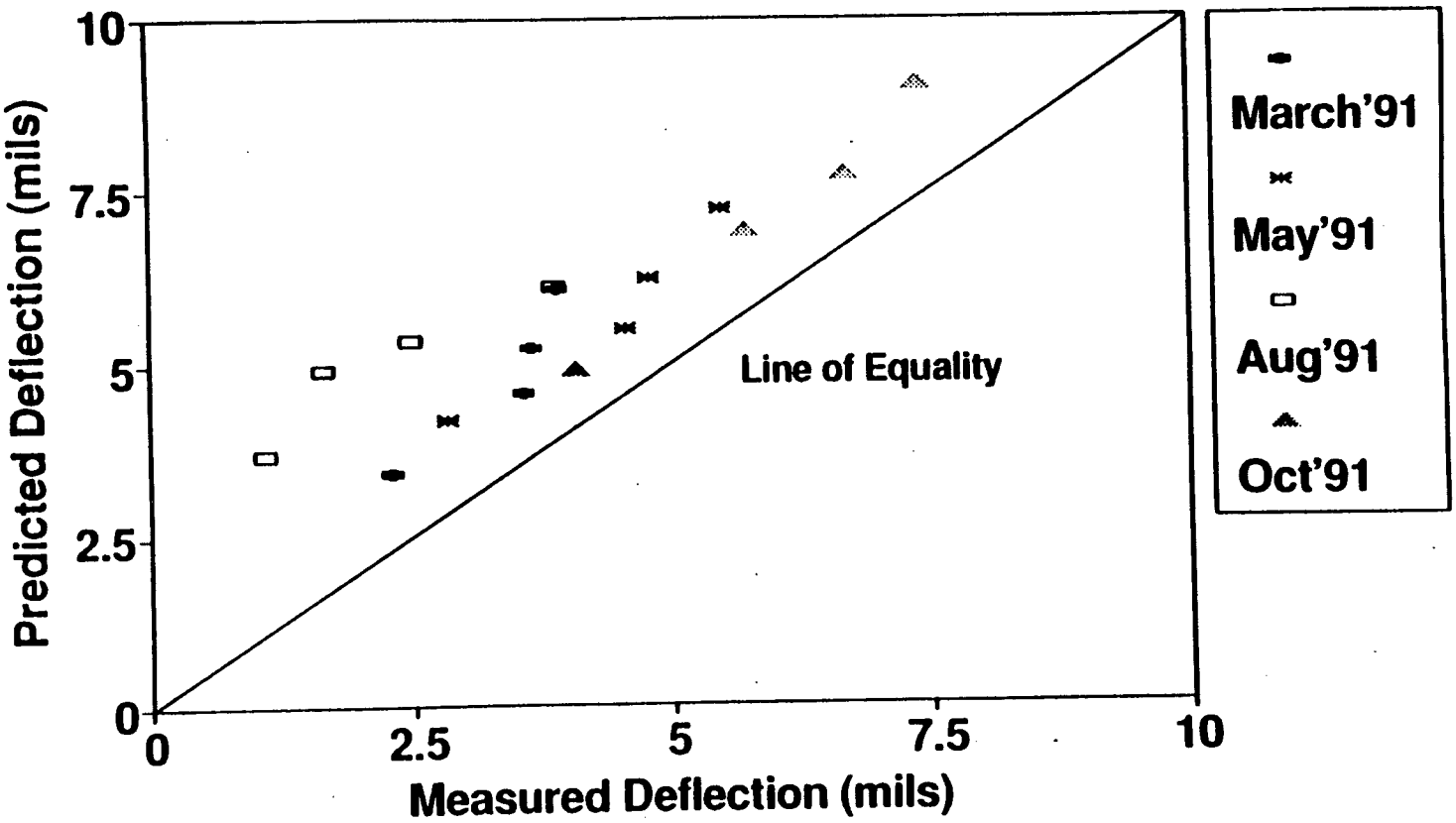

Figure 4.14(b) Measured versus predicted deflections for FWD loading on cement-treated base course sections.

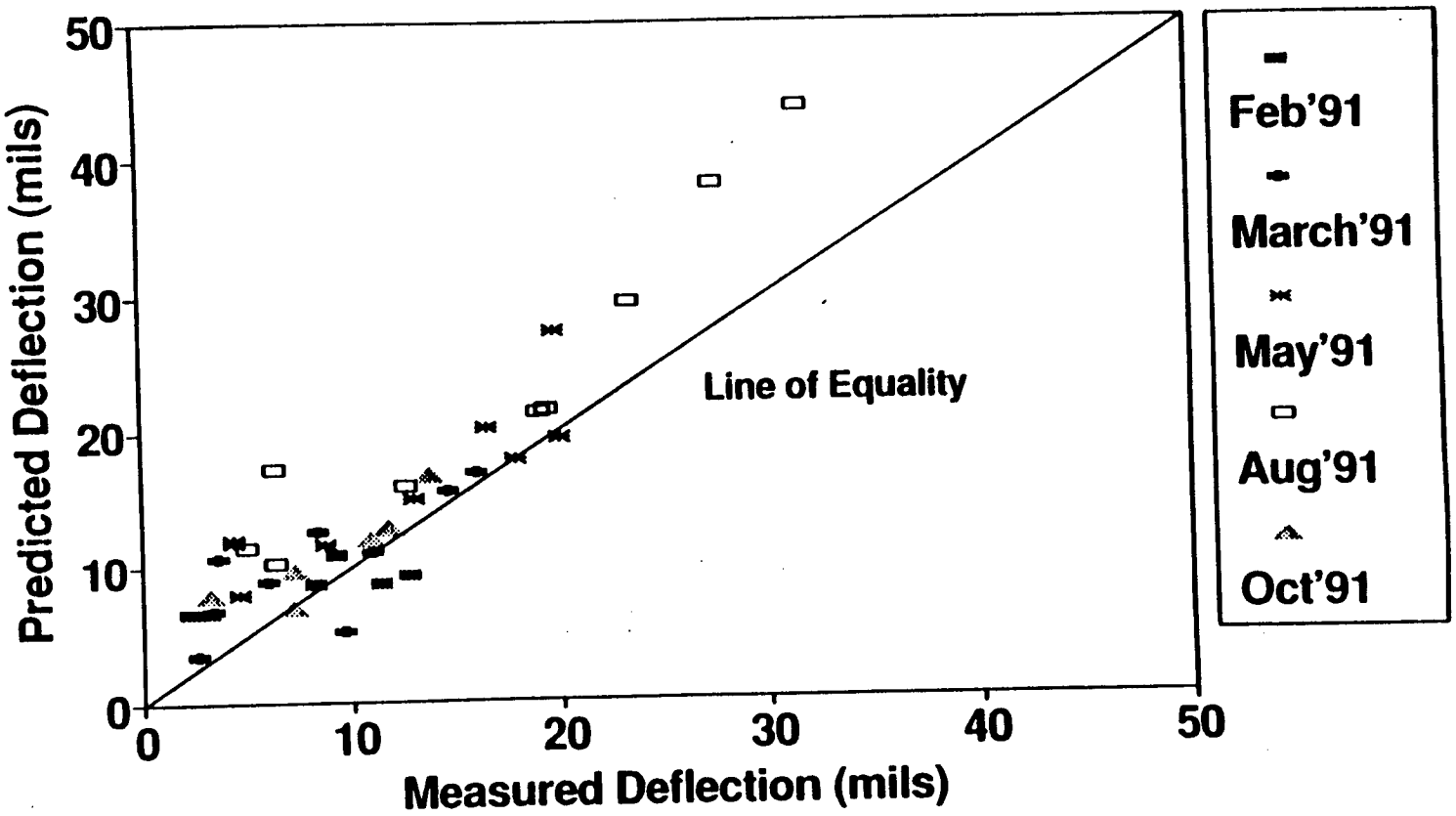

Figure 4.14(c) Measured versus predicted deflections for FWD loading on full depth AC sections.

1 with 3.5 inch (8.9 cm) thick AC layers and unstabilized subgrade were underpredicted whereas those in Section 2 with the stabilized subgrade were over-predicted. Section 3 with 6.3 inch (16 cm) thick AC layer (5 inch (12.7 cm) original AC surface plus 1.3 inch (3.3 cm) AC overlay) showed the best prediction of measured deflections.

Although two CTB sections (Sections 6 and 8) were instrumented with MDD's, only depth deflections from Section 8 were compared because of unrealistic moduli values obtained for Section 6. As shown in Figure 4.14(b), all the predicted deflections for Section 8 were larger than the measured deflections.

The depth deflections in the full-depth AC sections were overestimated by the forward- and back-calculation process employed in this study, as shown in Figure 4.14(c). The discrepancy became generally greater as the pavement temperature increased.

Another important observation as observed in Figure 4.14(c) is that most of the discrepancies between the measured and predicted depth deflections occurred at the subgrade. All of the data for May and August 1991 trips are plotted in Figure 4.15 to illustrate this point better. The interface deflection measured from any LVDT is the sum total of the deformation that occurs in all layers below that interface. It can be observed from Figure 4.15 that the trend among deflections at different depths for a particular section and trip is almost parallel to the line of equality except Section 9 during the May 1991 trip. This observation implies that the discrepancy between measured and predicted deflections for the lowest LVDT (located in the subgrade) contributes the most toward discrepancies in prediction for the interface deflections above the lowest LVDT.

Probably, the discrepancy described above is related to the nonlinearity of subgrade. That is, as temperature increases, asphalt concrete becomes softer and therefore, higher stresses delivered to the subgrade. Since the modulus of fine-grained soils increases as the stresses increase, the actual subgrade modulus becomes larger than the modulus backcalculated using the linear elastic theory. This will result in an underestimation of the subgrade deflection for full-depth AC sections as shown in Figure 4.15. This is more apparent for the trips that encountered higher temperatures.

As discussed before, in spite of complex effects of various parameters a certain

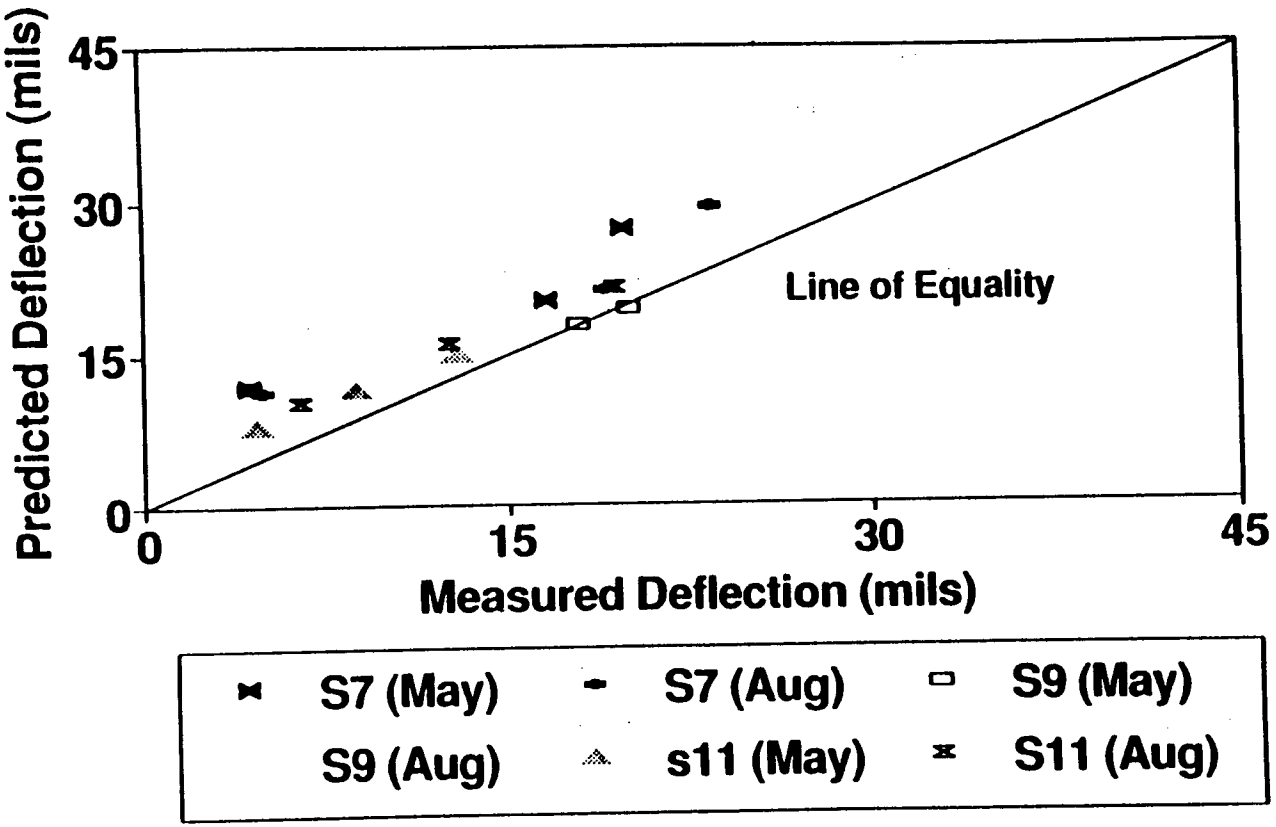

Figure 4.15 Measured versus predicted deflections for FWD loading on full depth AC sections.

consistency in measurements is apparent. More rigorous analysis to include the effects of moisture contents may be carried out when quantitative information on moisture contents is made available. Additionally, the use of dynamic back-calculation procedures may be used to improve prediction. Research on the use of dynamic back-calculation procedures (Ong et al., 1992) has shown that static back-calculation procedures may underestimate subgrade moduli. Any discrepancies in the back-calculation of subgrade parameters affect the prediction of the response variables.

Stress at the top of the subgrade

Stresses at the top of the subgrade were measured using the pressure gages. The gages, being at greater depths, show smaller deviations among different trips. Comparison of measured and predicted stresses are shown in Figures 4.16(a) to 4.16(c) for the three groups - aggregate base, cement treated base and asphalt base courses. Following conclusions can be drawn from these figures:

(1) For sections with an aggregate base course (Figure 4.16(a)), the predicted stress values showed little variation with varying thickness designs, whereas the measured values present considerable differences from section to section. The measured stress values for individual sections represent the performance of the sections very well. For example, Section 3 had to be overlaid at a very early date, the cause for which could be tied to a subgrade failure causing high stresses. Sections 2 and 5 show relatively low stresses on top of the subgrade due to stabilization, which helps to enhance the performance of ABC sections.

(2) For sections with cement treated base course layers (Figure 4.16(b)), the predicted stresses were greater than the measured values except Section 21. The same behavior was observed from the comparison of depth deflections in Figure 4.14(b). The disparity between measured and predicted values can be explained using the pavement distress data, which clearly indicate the failure of the cement treated base courses. The

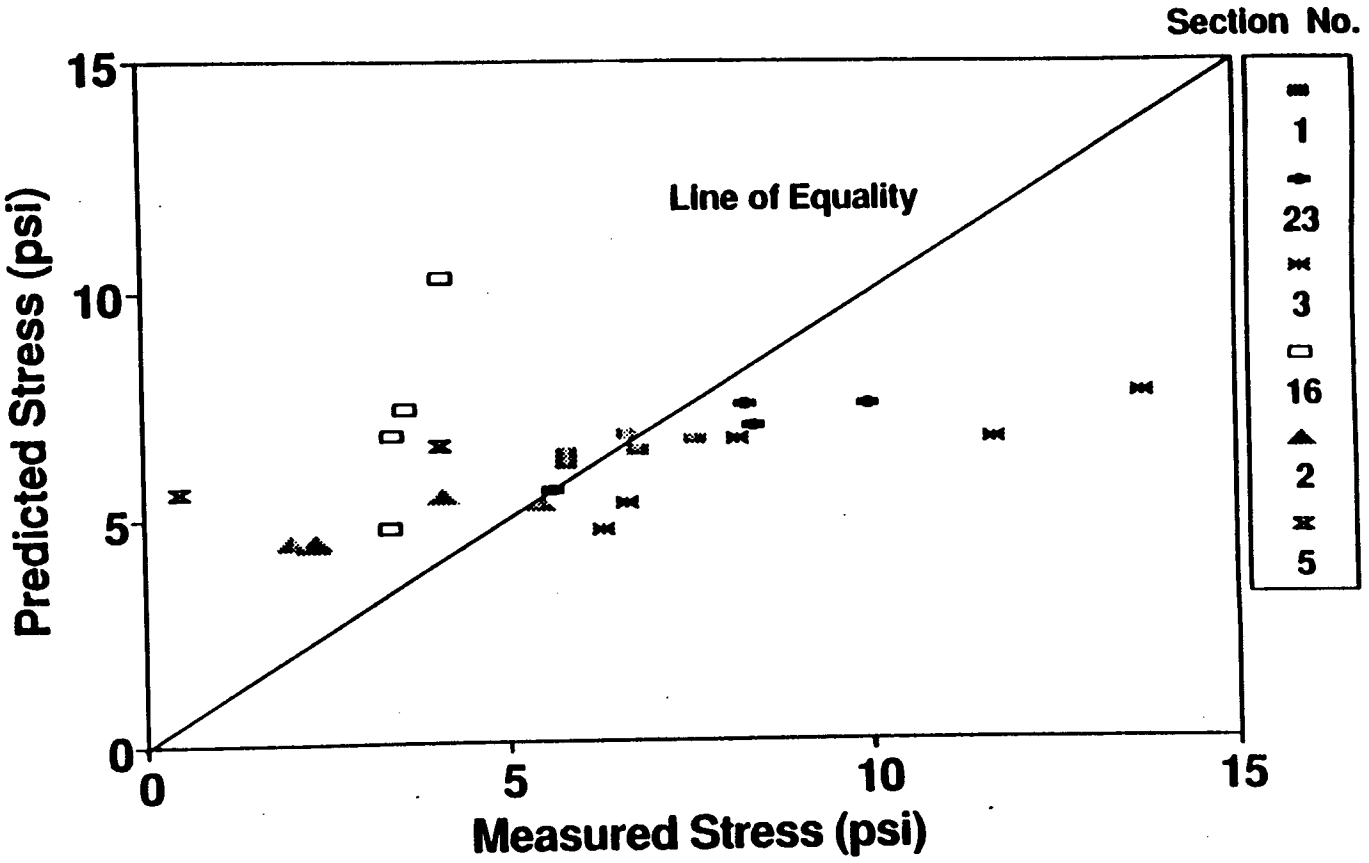

Figure 4.16(a) Measured versus predicted stresses for FWD loading on aggregate base course sections.

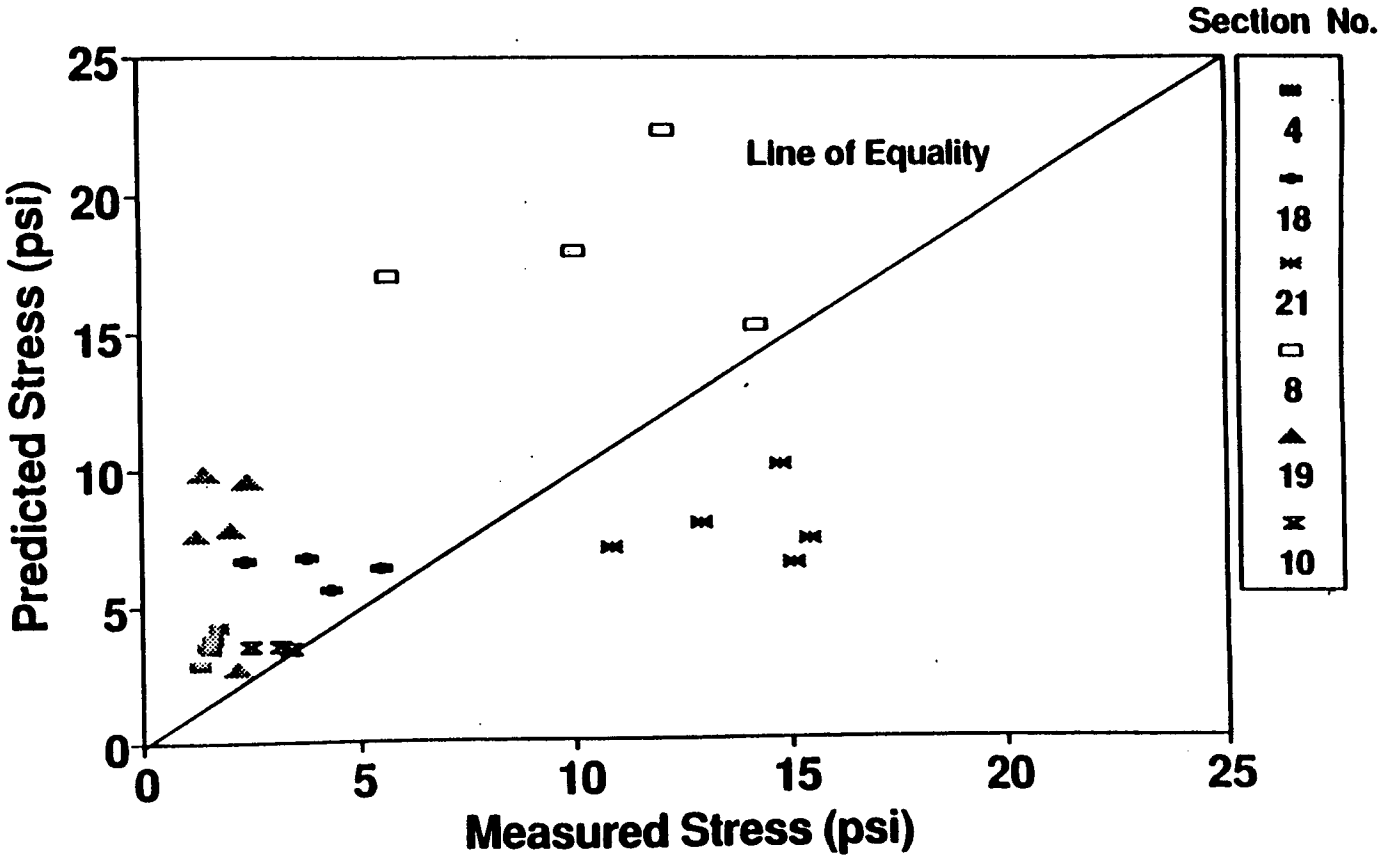

Figure 4.16(b) Measured versus predicted stresses for FWD loading on cement-treated base course sections.

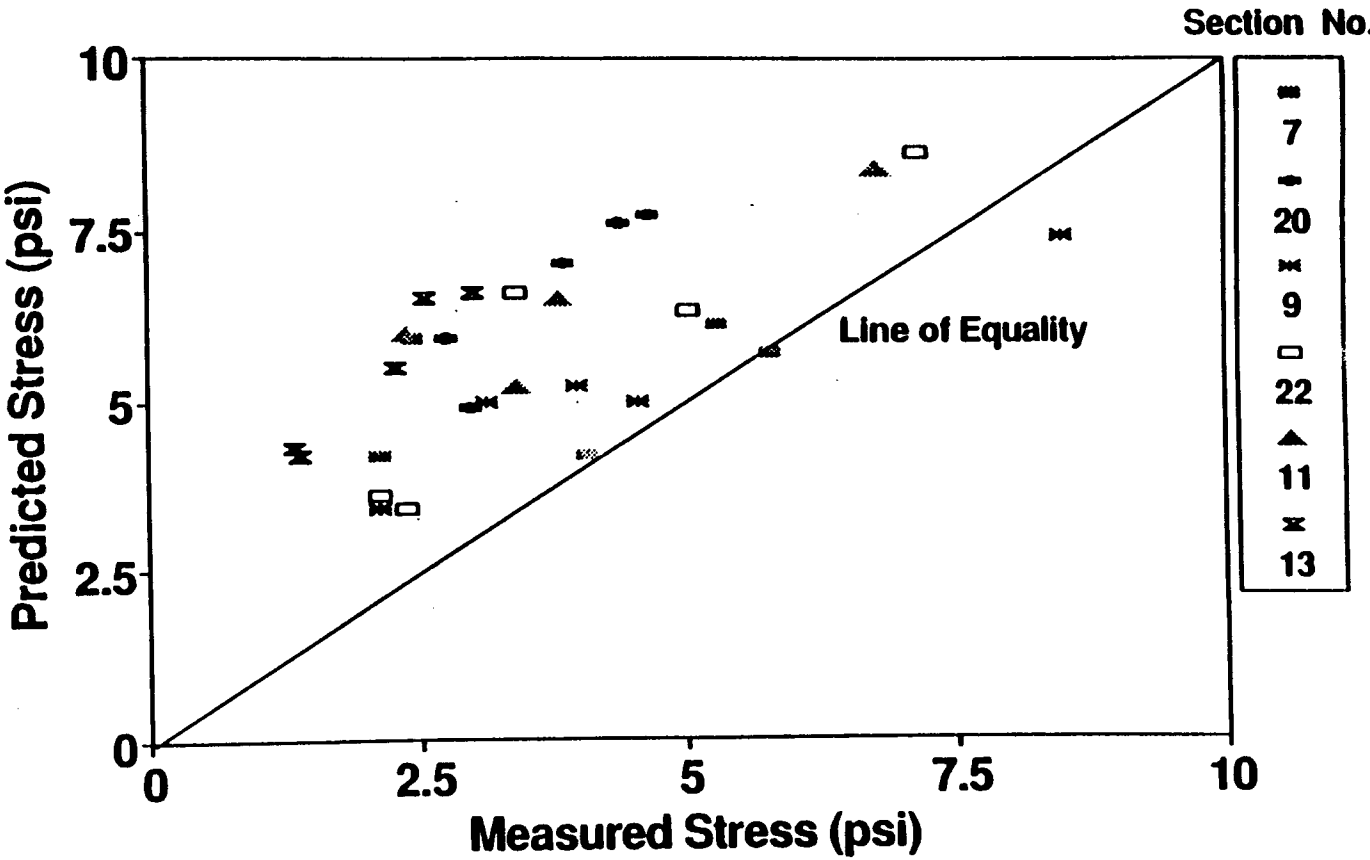

Figure 4.16(c) Measured versus predicted stresses for FWD loading on full depth AC sections.

backcalculated moduli evidently does not truly reflect this loss of support. If they had, it would be more reasonable to observe higher measured values than predicted values.

(3) The analysis scheme using the backcalculated moduli and forward calculation overestimated the stresses at the top of the subgrade of full-depth asphalt concrete sections.

4.3.2 Comparison of Pavement Responses from FWD and Moving Wheel Loads

A truck speed of 55 mph (88 kmph) was considered for comparison as shown in Figures 4.17 (a) to 4.19 (c). The loading duration of 100 msec for the speed of 55 mph (88 Kmph) was relatively closer to the FWD loading duration of around 40 msec, as compared with the 35 mph (56 Kmph) and 10 mph (16 Kmph) speeds that had loading durations between 200 and 800 msecs, respectively. The following observations could be made from these figures:

Measured responses (strains, stresses, and deflections) for the FWD and 18 kip (80 KN) truck, are highly correlated irrespective of the design type and suggest that the FWD loading with 9 kip (40 KN weight can be used to approximate the pavement responses under standard 18 kip axle with dual wheels. However, correlation becomes worse at higher temperatures (e.g., May and August).

4.4 Validation Scheme for Backcalculated Moduli

Considering the different techniques available for backcalculation and the inherent difficulties experienced in terms of a range of output values provided by these schemes, it becomes imperative to verify the backcalculated moduli. The word verification needs to be explained in more detail here. The backcalculation schemes use layered elastic programs for matching deflection bowls. The moduli arrived at, are a measure of relative stiffness rather than a material property. Most efforts to validate backcalculation techniques have compared derived moduli with those obtained in the lab (Lytton et al., 1989; Ong et al., 1992; Scullion et al., 1989). A method to verify backcalculated moduli using surface deflections and also

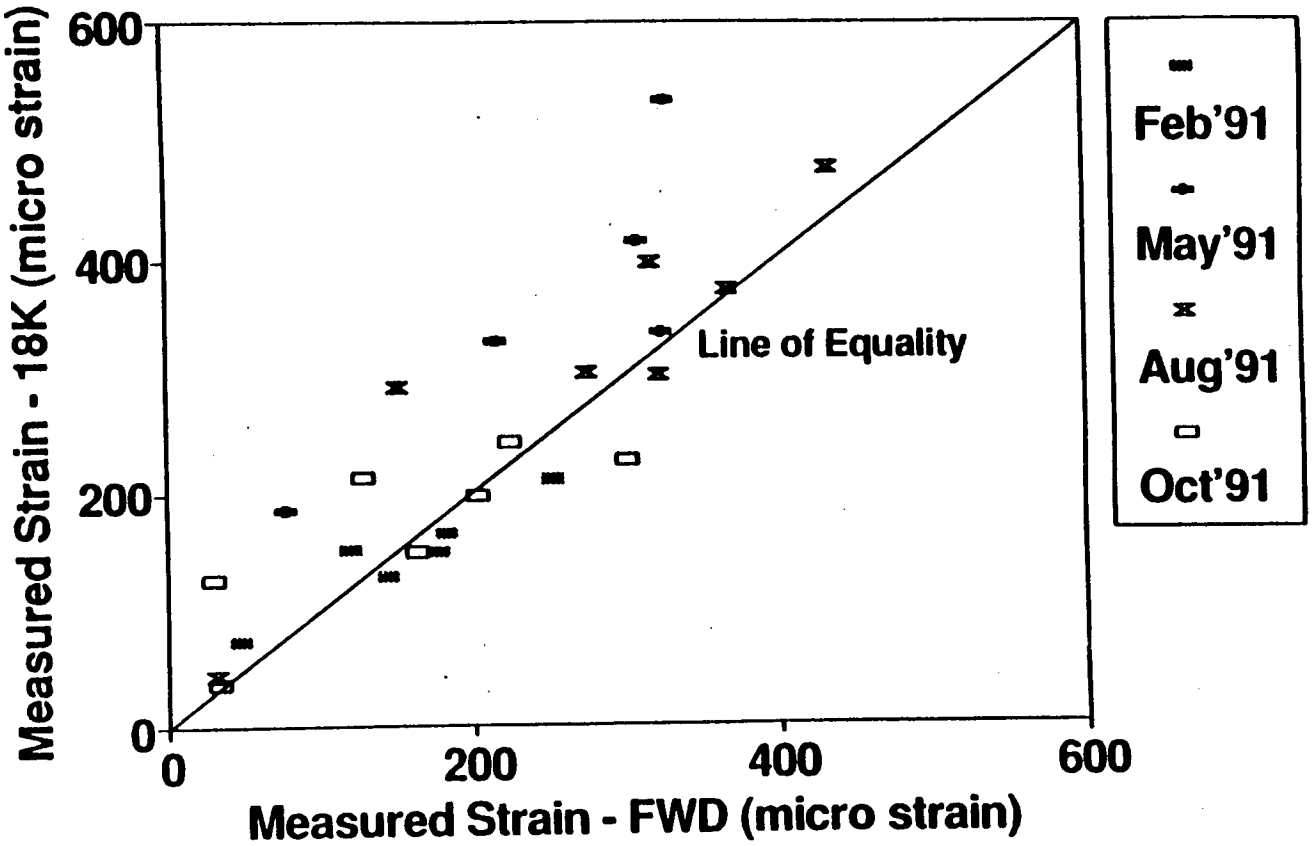

Figure 4.17(a) Comparison of measured strains under FWD and 18 kip truck loading for aggregate base course sections.

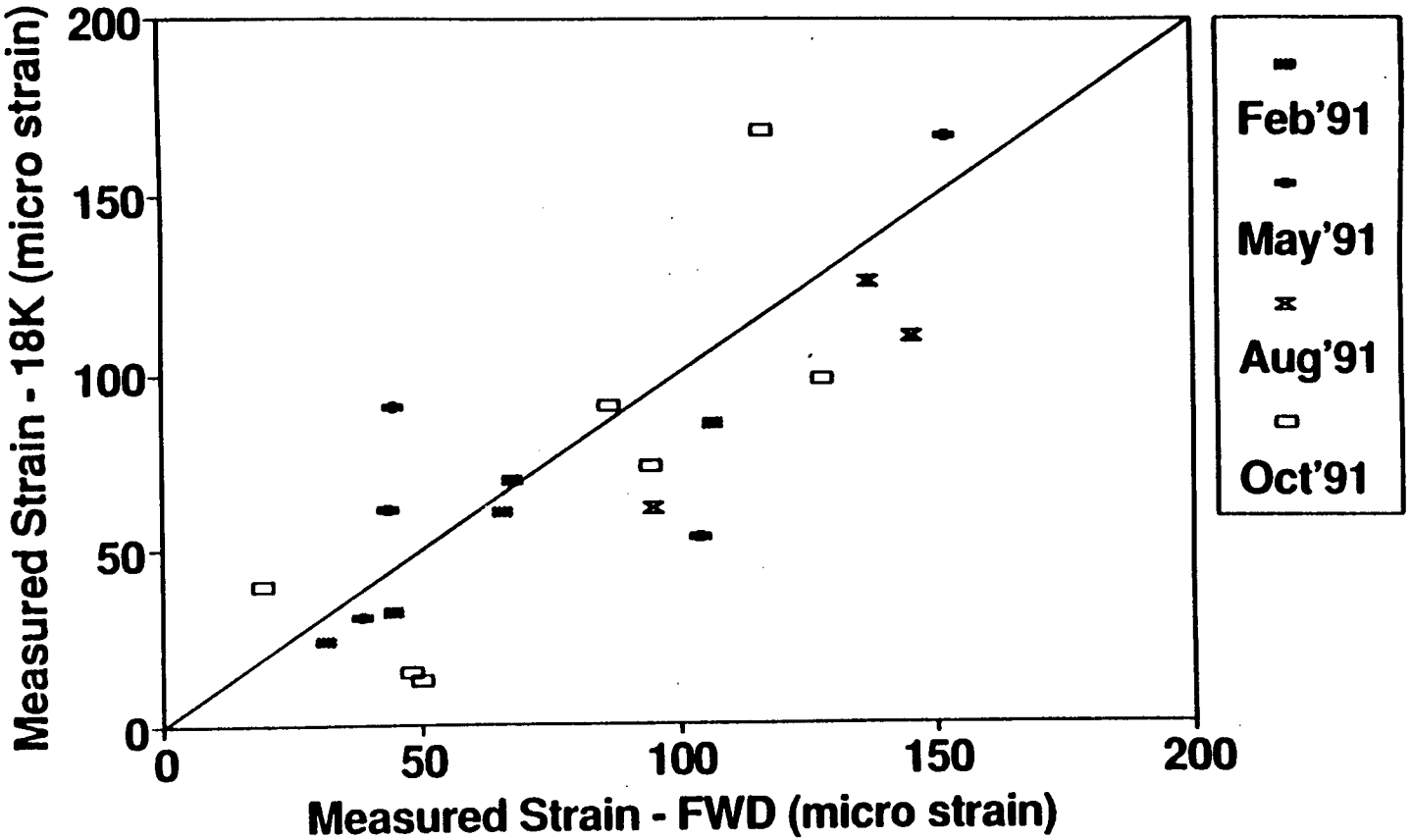

Figure 4.17(b) Comparison of measured strains under FWD and 18 kip truck loading for cement-treated base course sections.

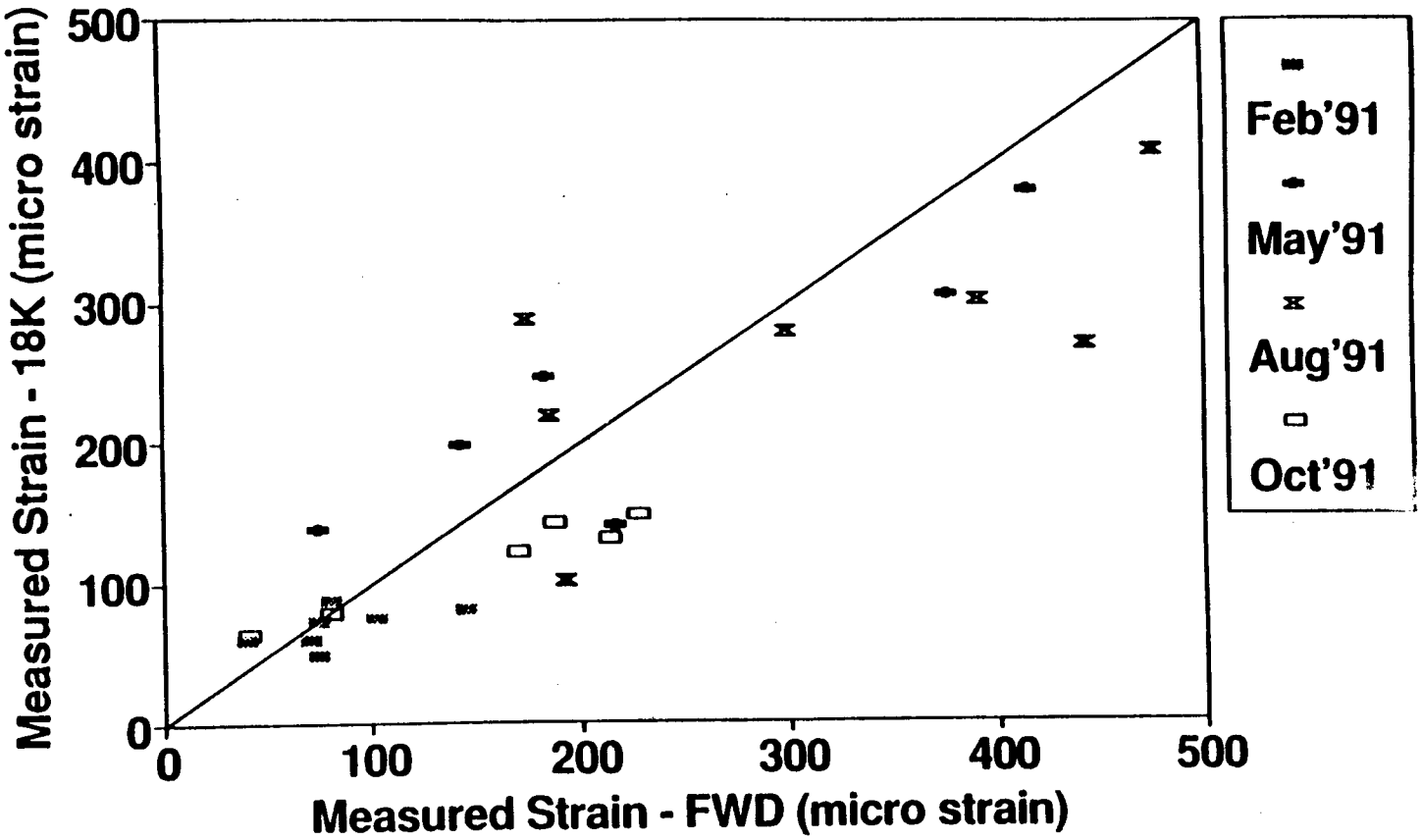

Figure 4.17(c) Comparison of measured strains under FWD and 18 kip truck loading for full depth AC sections.

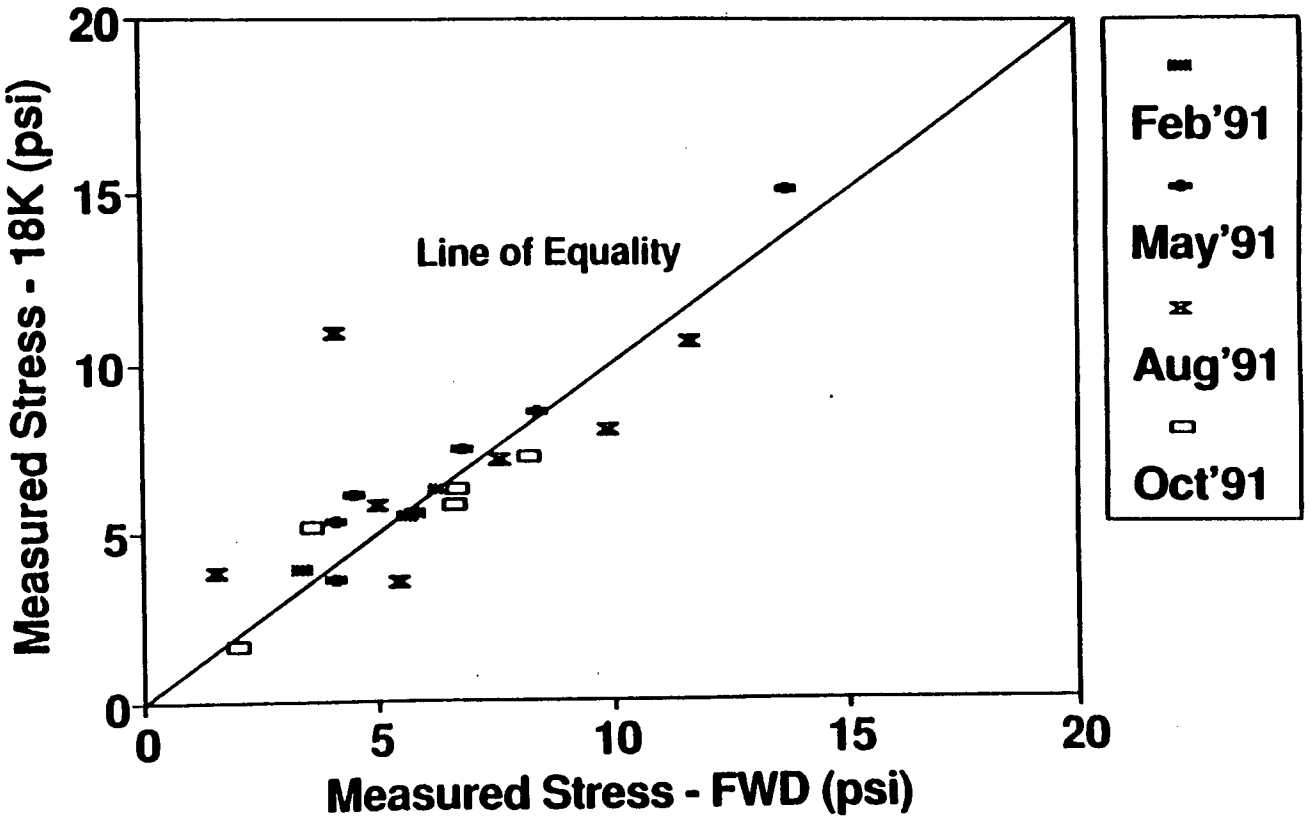

Figure 4.18(a) Comparison of measured stresses under FWD and 18 kip truck loading for aggregate base course sections.

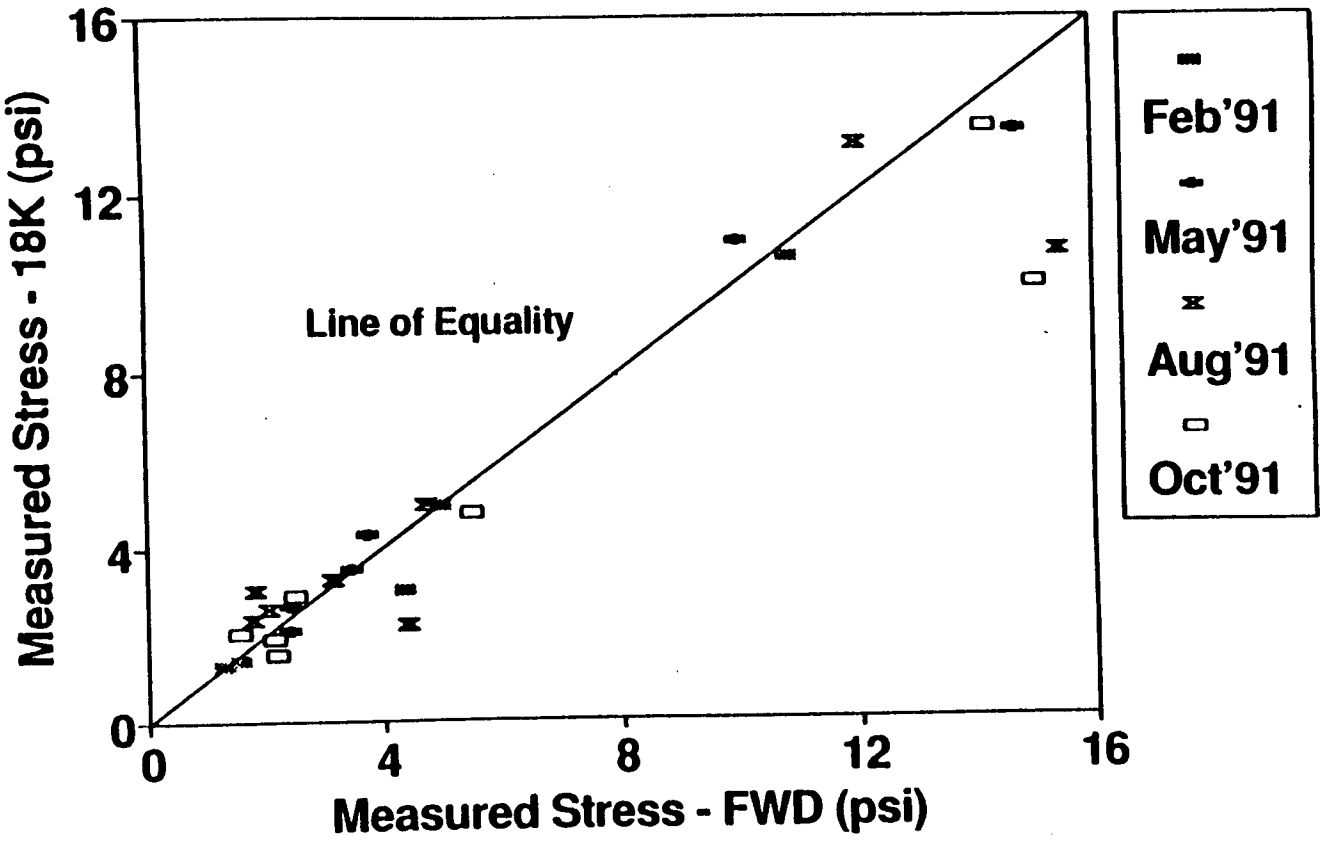

Figure 4.18(b) Comparison of measured stresses under FWD and 18 kip truck loading for cement-treated base course sections.

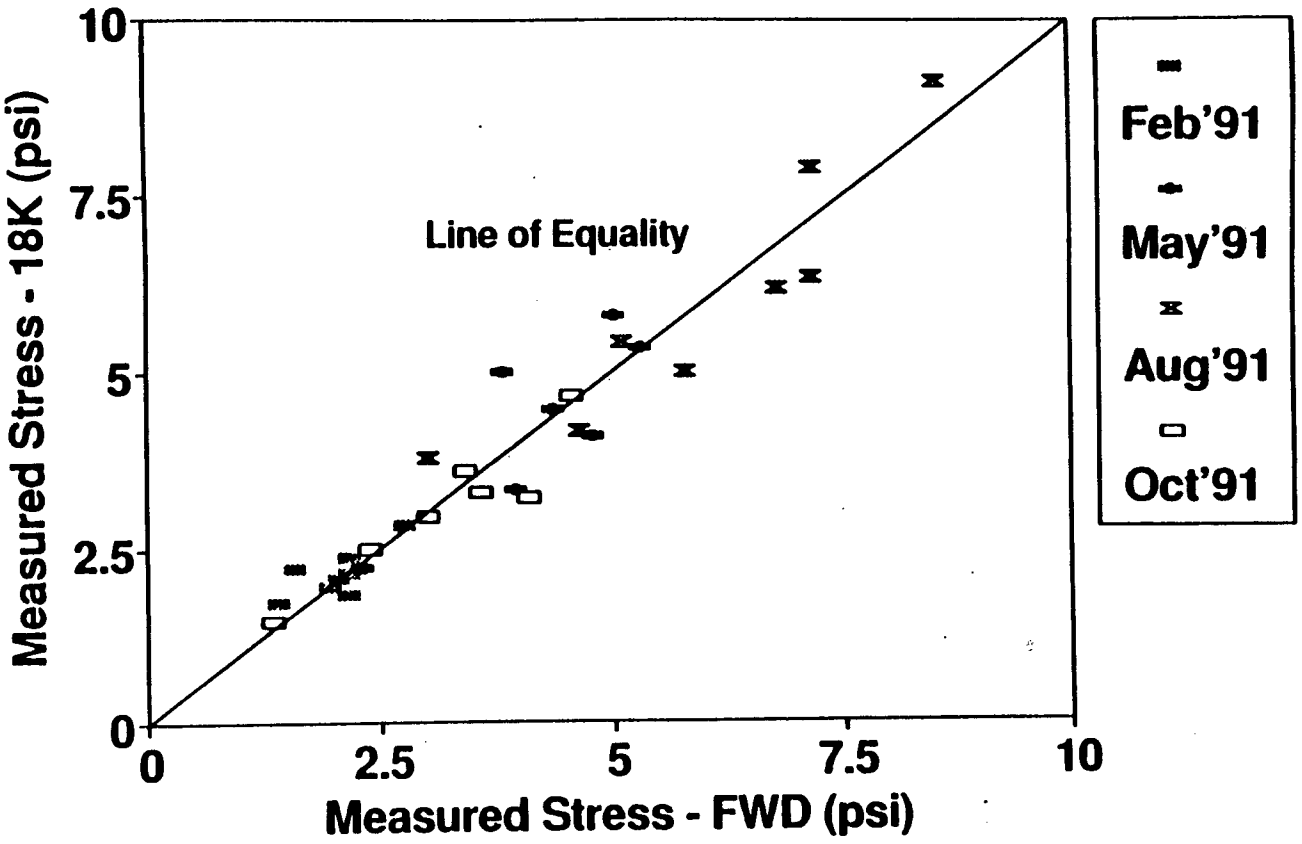

Figure 4.18(c) Comparison of measured stresses under FWD and 18 kip truck loading for full depth AC sections.

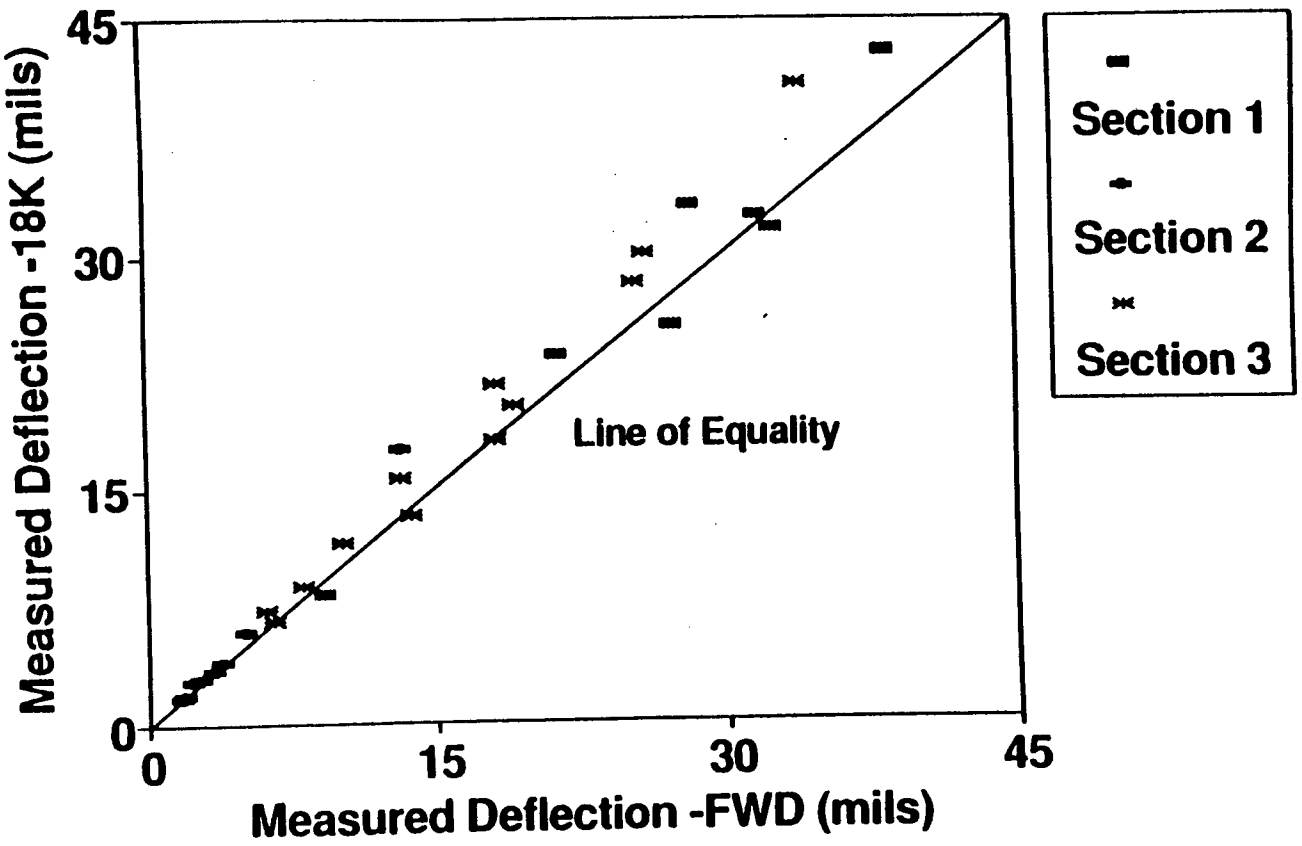

Figure 4.19(a) Comparison of measured deflections under FWD and 18 kip truck loading for aggregate base course sections.

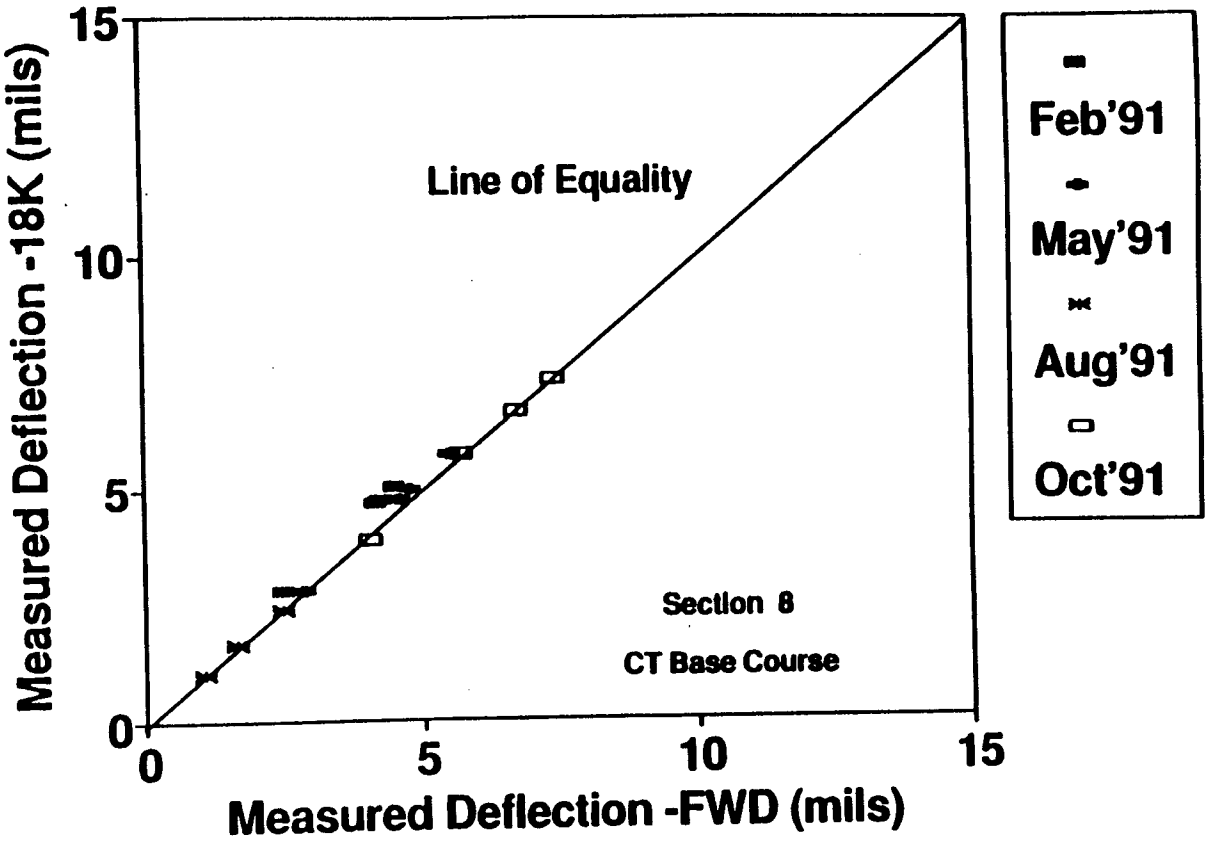

Figure 4.19(b) Comparison of measured deflections under FWD and 18 kip truck loading for cement-treated base course sections.

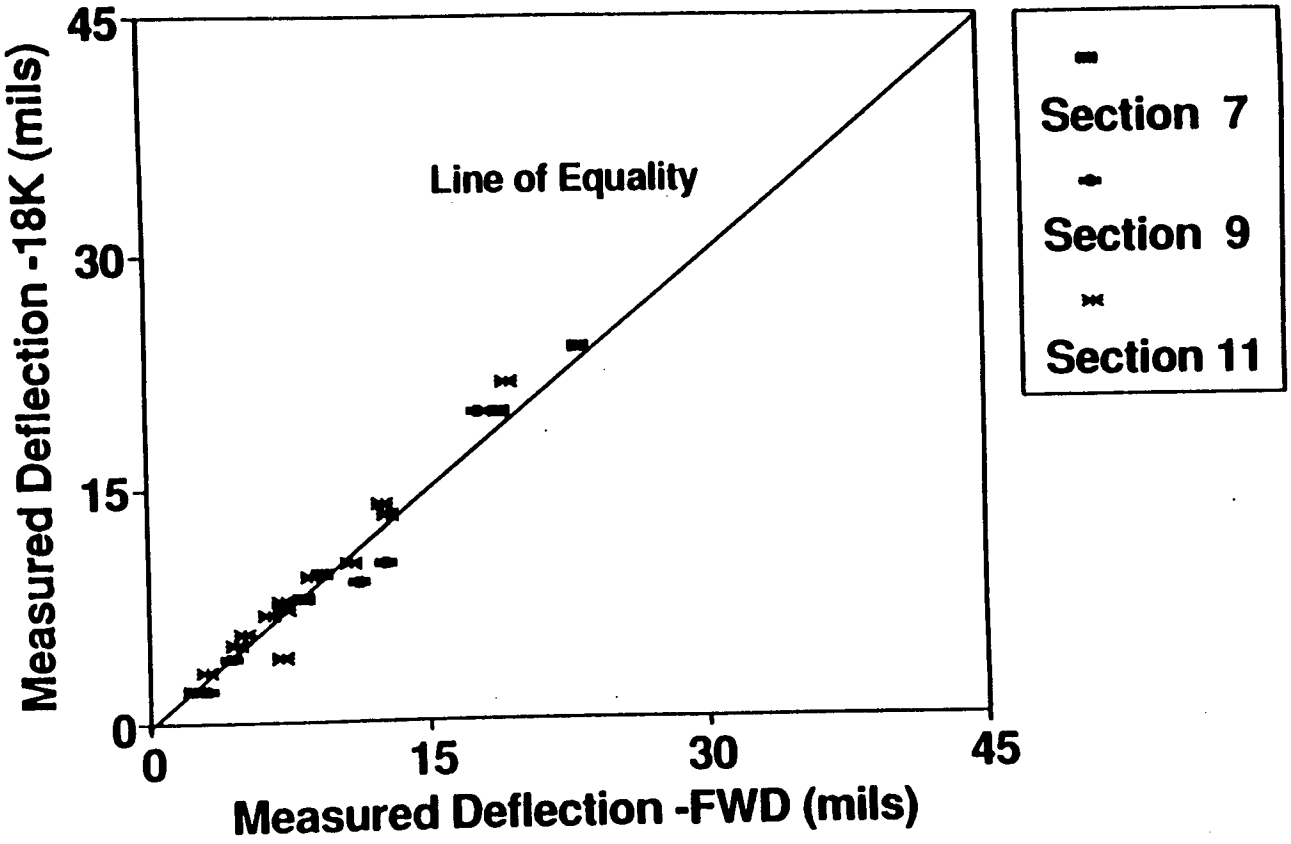

Figure 4.19(c) Comparison of measured deflections under FWD and 18 kip truck loading for full depth AC sections.

deflection at different depths (measured using an MDD) is elaborated below.

Once the modulus of each layer has been determined, deflections at different depths can be calculated from a forward calculation technique using the thickness of layers, assumed Poisson's ratios used in the backcalculation, and the backcalculated layer moduli values. The discrepancies between the measured depth deflections and the predicted depth deflections can be used as an estimate of how valid the backcalculated moduli are for various design types.

Surface and depth deflections at known offset distances and depths were calculated for the June 1990 and May 1991 trips using the WES-5 forward calculation program with the backcalculated moduli. Figures 4.20 through 4.26 show the predicted and the measured deflections of both the trips. The following observations could be made from these figures:

(1) Stabilized layers (subgrade or base) in Sections 2,6 and 8 decreased the surface deflections and deflections at different depths considerably.

(2) Regardless of section type, surface deflections were predicted very accurately for both the trips as shown in subfigure (a)'s of Figures 4.20 to 4.26. However, for Section 6 the discrepancy in predicting surface deflections for the May 1991 trip was due to a general failure of the pavement yielding unreasonable moduli values. Distress records attest to this fact.

(3) The accuracy of deflection prediction inside the subgrade was observed to be much worse in May 1991 data.

Since the depth deflections measured by MDDs could be used in evaluating the accuracy of the backcalculation technique, the influence of making different assumptions with the MODULUS program was investigated. The same deflection basins used to generate moduli values were input to the MODULUS program with different combinations of assumptions 1, 2 and 3 outlined in Section 4.1. The moduli values were backcalculated from the surface deflections with different assumptions, and depth deflections were calculated from the WES-5 forward calculation program. The absolute errors for different cases were calculated and plotted against the depth of LVDT in the last subfigures of Figures 4.20 through 4.26. Five cases were studied with the following conditions:

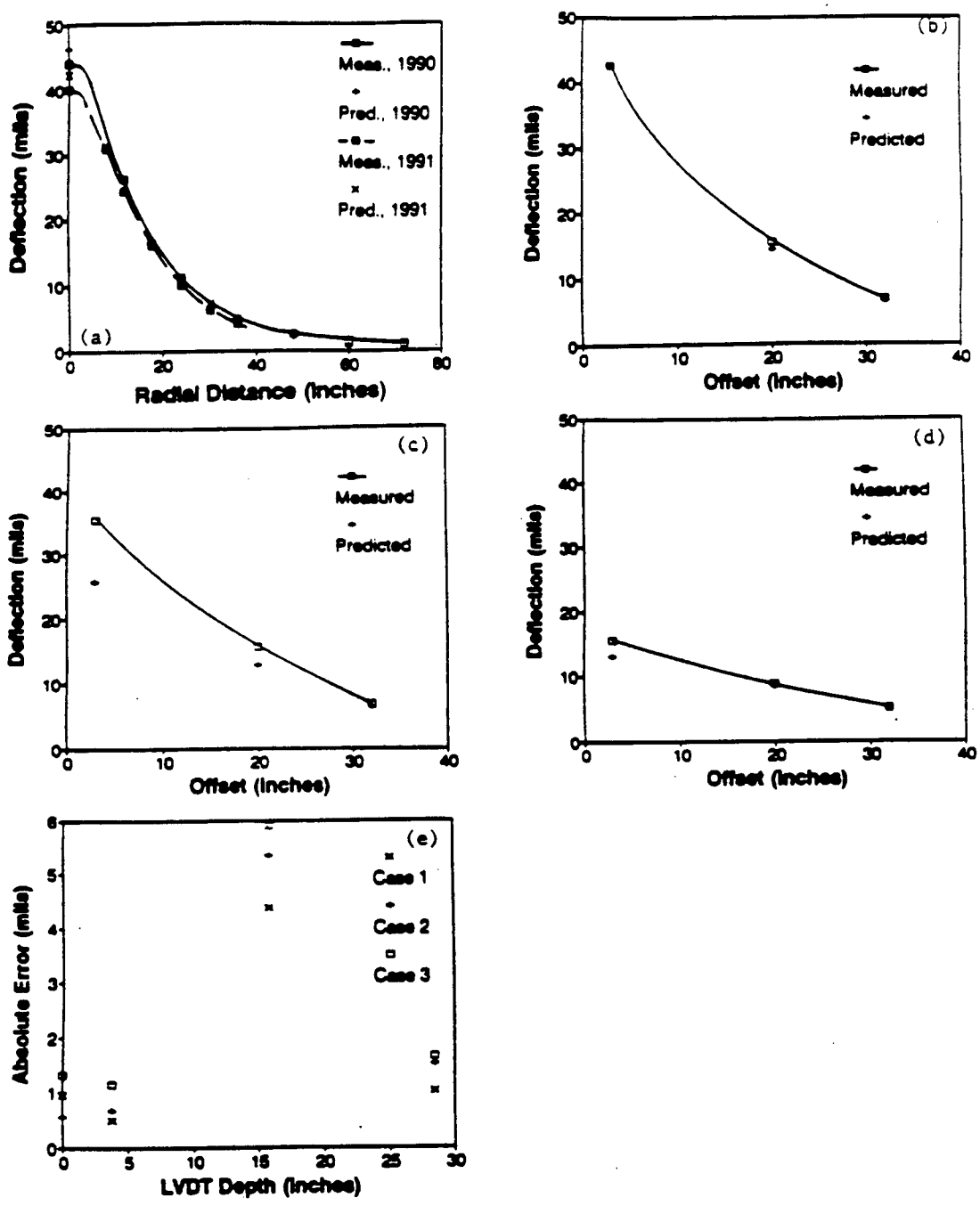

Figure 4.20 June 1990 and May 1991 results of Section 1: (a) Surface deflection, (b) Deflection at the top of the base, (c) Deflection at the top of the subgrade, (d) Deflection 13" into the subgrade, and (e) Absolute error from different assumptions (June 1990).

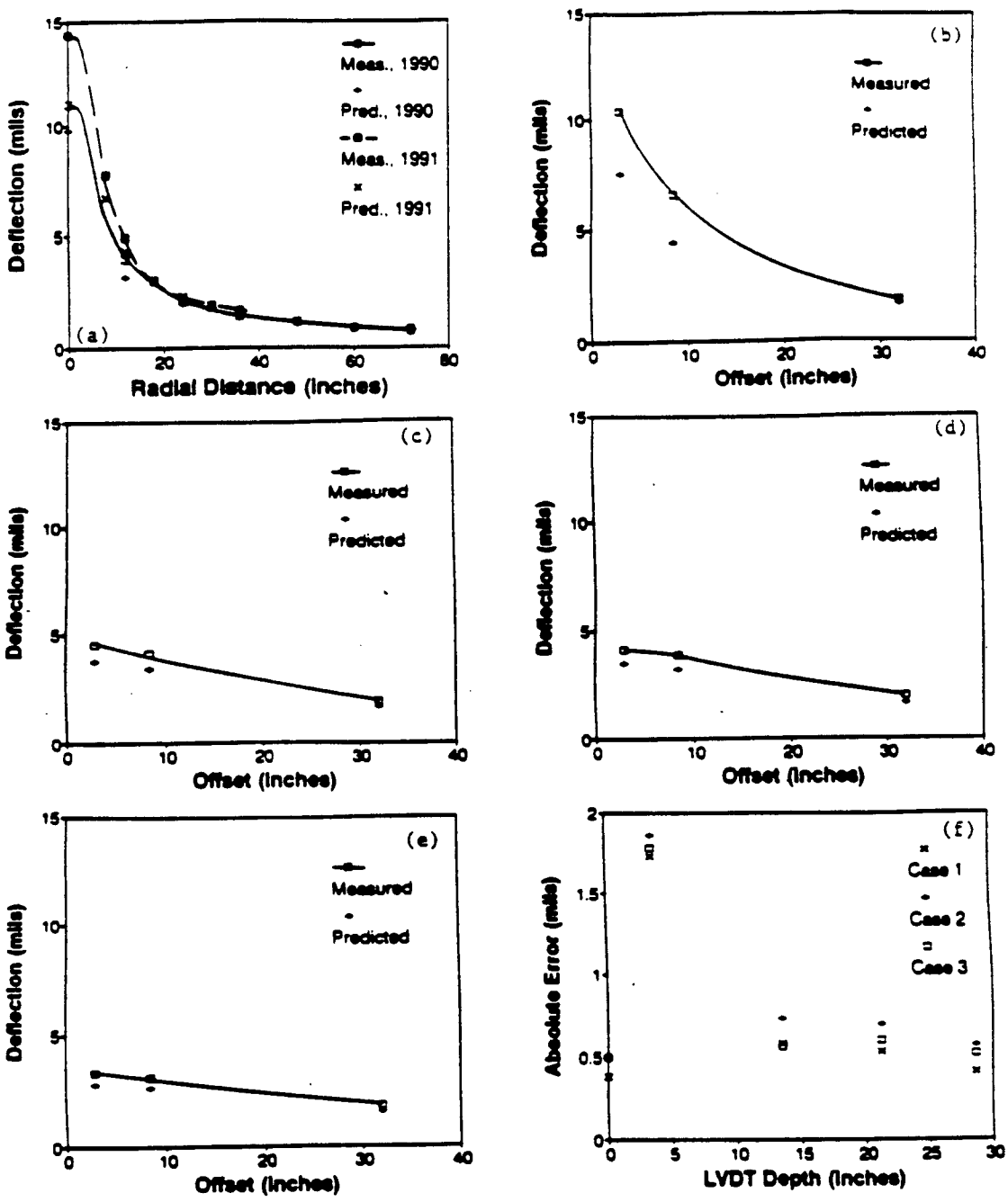

Figure 4.21 June 1990 and May 1991 results of Section 2: (a) Surface deflection, (b) Deflection at the top of the base, (c) Deflection at the top of the stabilized subgrade, (d) Deflection at the top of the subgrade, (e) Deflection 7.7" into the subgrade, and (f) Absolute error from different assumptions (June 1990)

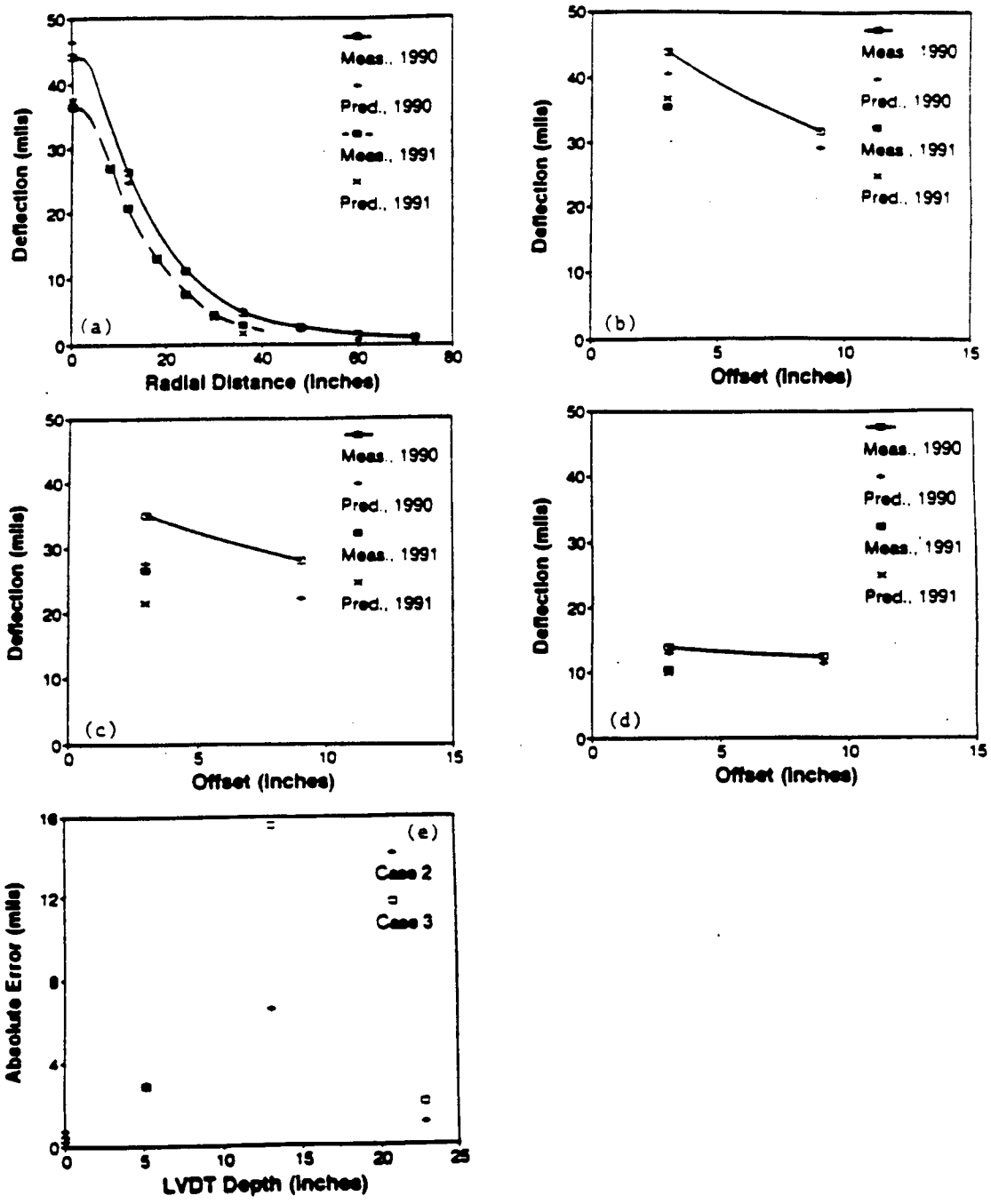

Figure 4.22 June 1990 and May 1991 results of Section 3: (a) Surface deflection, (b) Deflection at the top of the base, and (c) Deflection at the top of the subgrade, (d) Deflection 9.9" into the subgrade, (e) Absolute error from different assumptions (June 1990).

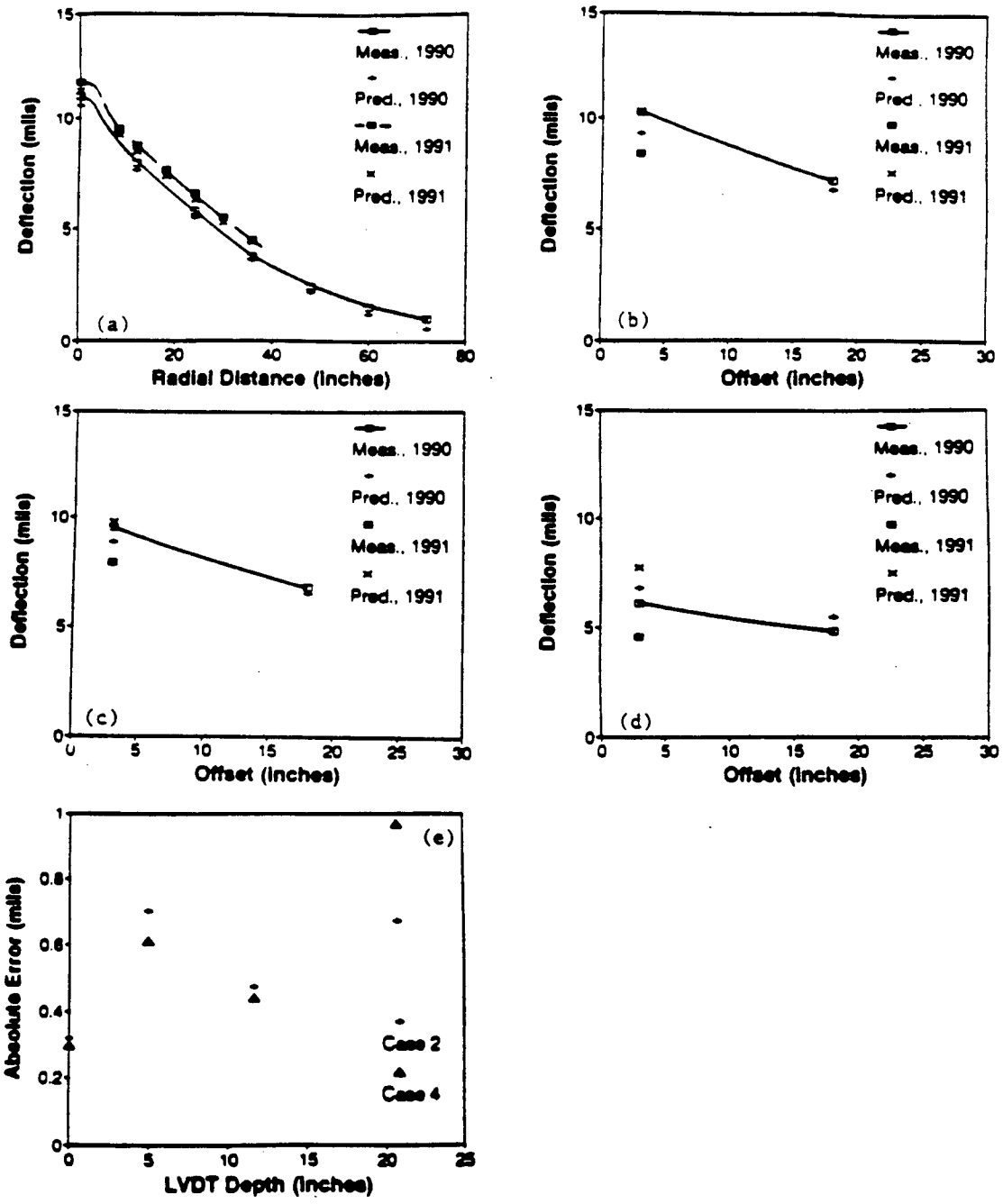

Figure 4.23 June 1990 and May 1991 results of Section 6: (a) Surface deflection, (b) Deflection at the top of the base, (c) Deflection at the top of the subgrade, (d) Deflection 10.2" into the subgrade, and (e) Absolute error from different assumptions (June 1990).

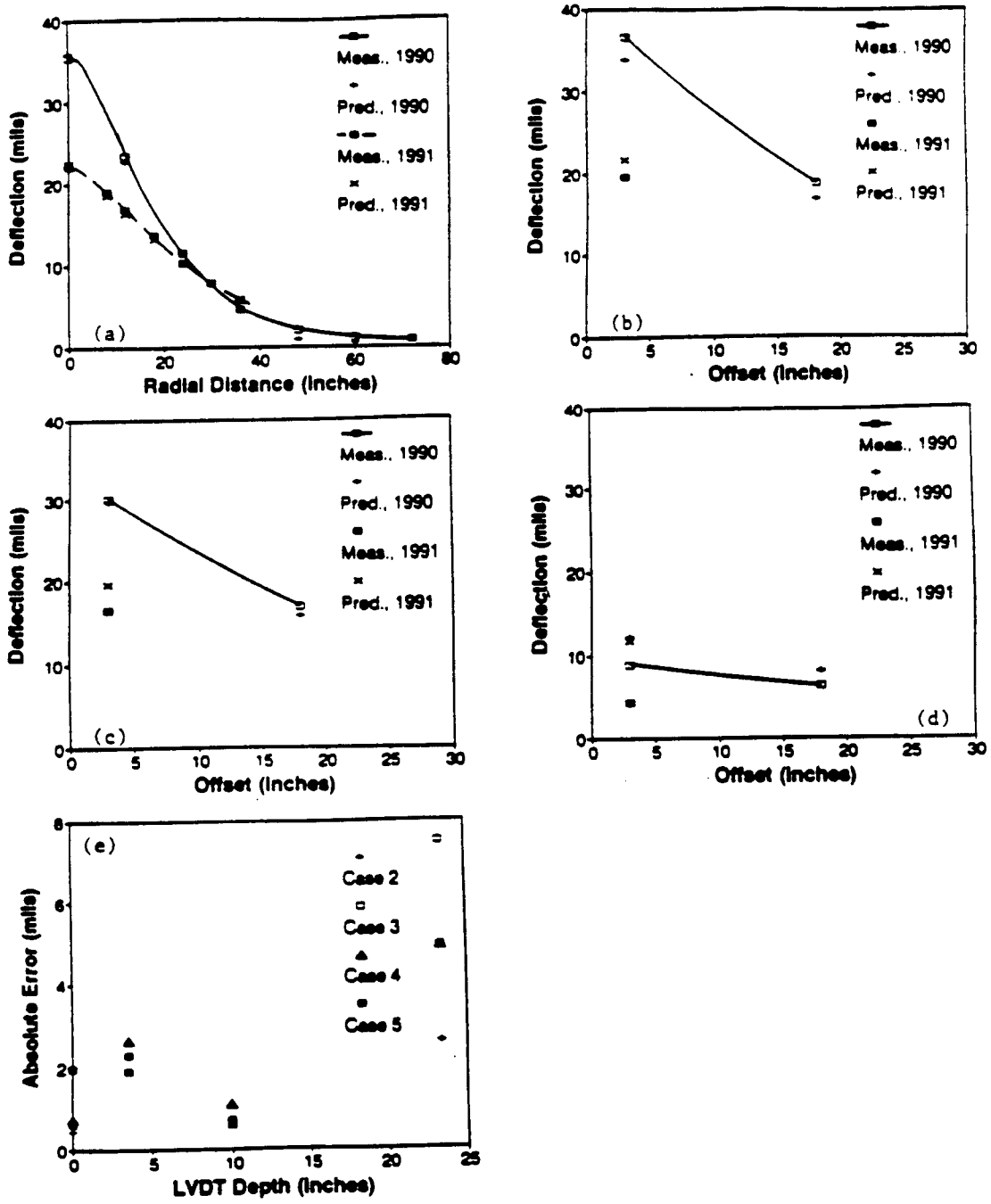

Figure 4.24 June 1990 and May 1991 results of Section 7: (a) Surface deflection, (b) Deflection at the top of the base, (c) Deflection at the top of the subgrade, (d) Deflection 14.4" into the subgrade, and (e) Absolute error from different assumptions (June 1990).

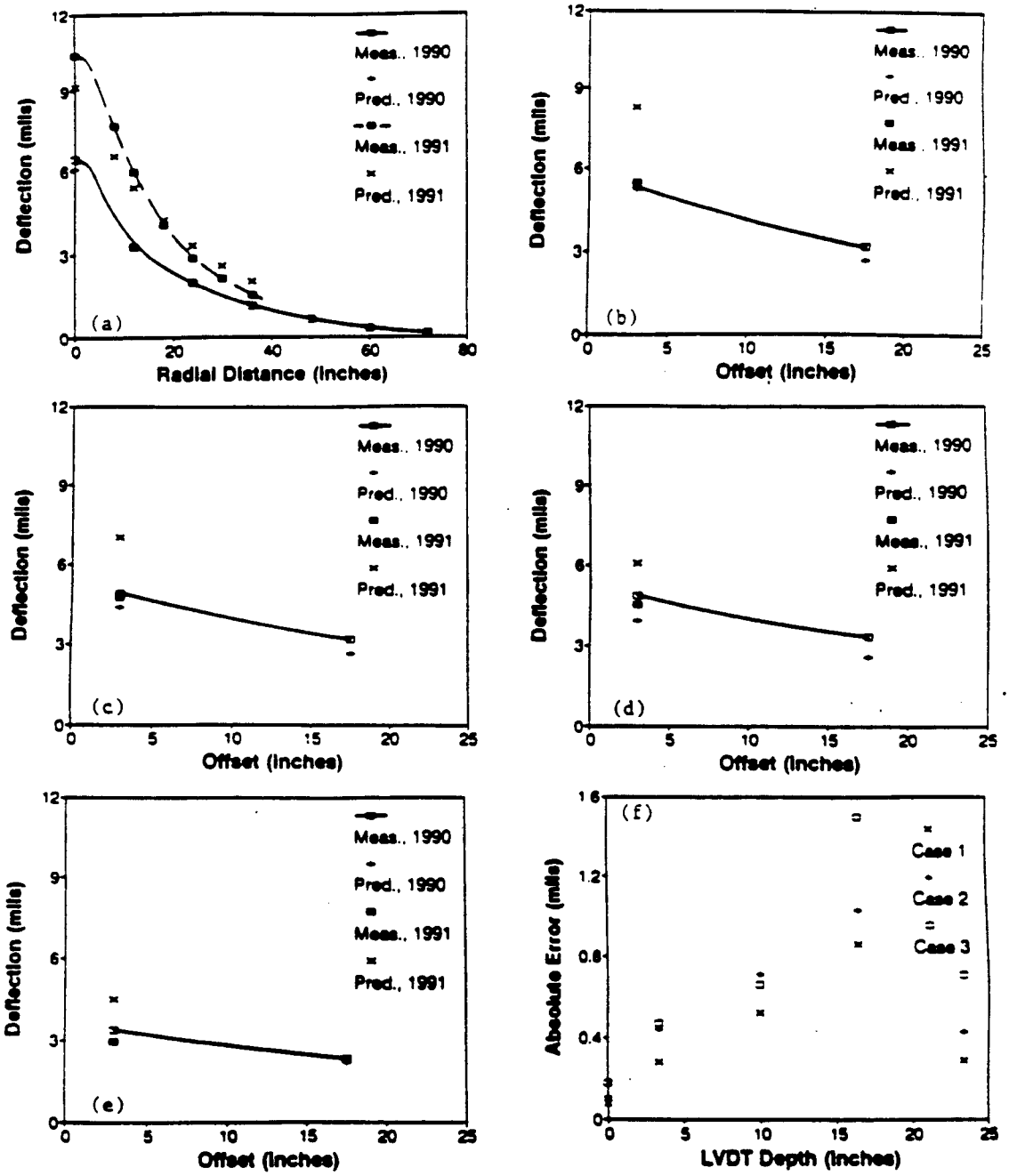

Figure 4.25 June 1990 and May 1991 results of Section 8: (a) Surface deflection, (b) Deflection at the top of the cement-treated base, (c) Deflection at the top of the stabilized subgrade, (d) Deflection at the top of the subgrade, (e) Deflection 6.9" into the subgrade, and (f) Absolute error from different assumptions (June 1990)

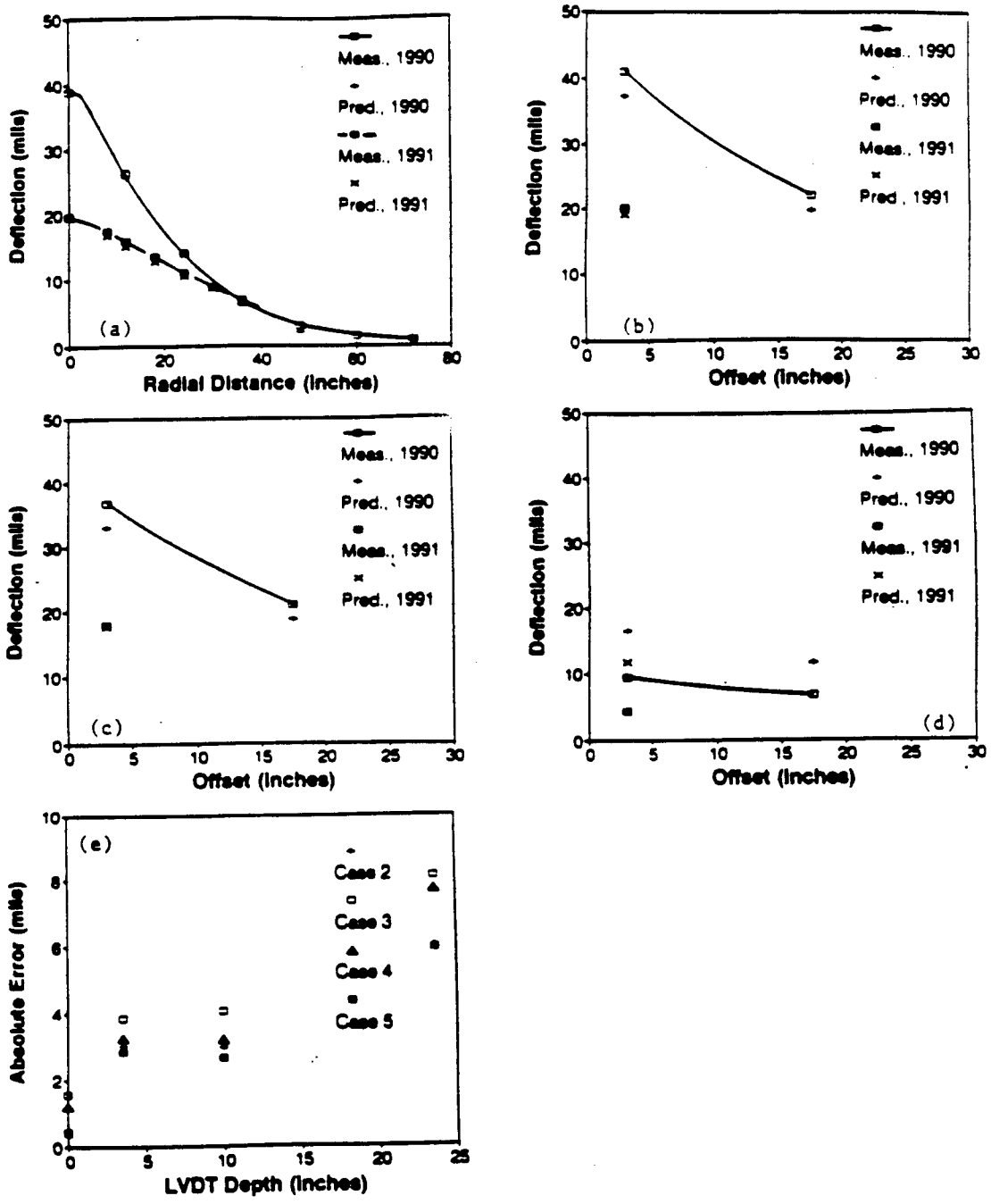

Figure 4.26 June 1990 and May 1991 results of Section 9: (a) Surface deflection, (b) Deflection at the top of asphalt concrete binder course, (c) Deflection at the top of the subgrade, (d) Deflection 14.6" into the subgrade, and (e) Absolute error from different assumptions (June 1990)

CASE 1: The surface modulus of thin surfacing was fixed. Other conditions were the same as in CASE 2.

CASE 2: The surface modulus of thin surfacing was not fixed. The depth to bedrock was left to be calculated by the MODULUS program.

CASE 3: The measured depth to bedrock was input to the MODULUS program. Other conditions were the same as in Section 2.

CASE 4: Top 24 in. of subgrade was considered as a separate layer. Other conditions were the same as in CASE 2.

CASE 5: Asphalt concrete base layer was separated from the surface and binder courses in Sections 7 and 9. Other conditions were the same as in CASE 2.

The first assumption, fixing the modulus for thin surfacing, was applicable to Sections 1, 2 and 8. Comparing Cases 1 and 2 of these sections in Figures 4.20, 4.21 and 4.25, the absolute errors were noticed to be smaller when the surface modulus was fixed. In Figures 4.24 and 4.26 for Sections 7 and 9 respectively, combining the asphalt concrete base layer with these layers (CASE 5). The effect of forcing the measured depth to bedrock in the MODULUS program, Case 3, produced larger errors in depth deflections than in Case 2 (Figures 4.20 to 4.22 and Figures 4.24 to 4.26). Also the consideration of top 24 inches (0.61 m) of subgrade as a separate layer. (CASE 4) increased the absolute error as shown in Figures 4.23, 4.24 and 4.26. These observations verify the validity of the assumptions made in backcalculating the moduli values.

Due to inherent complications arising from the use of FWD and from the assumptions in the theory of elasticity, gaging the accuracy of the backcalculated moduli would be inappropriate. The following observations, along with comparisons of other predicted responses indicate that the verification process should be treated more as a "criteria of acceptability."

4.5 Traffic Analysis

One of the most important factors to be evaluated in the structural design of

pavements is the traffic volume. The most common procedure of relating the traffic data to the design is to convert repetitions of various combinations of axle configuration and weight to the applications of the Equivalent Single Axle Load (ESAL), typically 18-kip (80 KN) for the highway pavement design. The summary of traffic analysis is presented in Tables 4.11.

4.6 Distress Survey Measurement

NCSU crew members have performed pavement distress surveys for both the South and the North bound lanes in all the 24 test sections since August 1991 in cooperation with NCDOT engineers. The primary objective of this task was to monitor the pavement performance for different pavement designs and provide a necessary calibration tool to performance prediction models to be developed from the laboratory study. The pavement distress surveys were conducted according to the SHRP Distress Identification Manual for the long-term Pavement Performance Studies (1990), and the following major distress types were surveyed:

1. Fatigue (Alligator) Cracking (FC),
2. Longitudinal Cracking (LC),
3. Transverse Cracking (TC),
4. Pumping (PP),
5. Patch/Patch Deterioration (P/PD), and
6. Rutting (RT).

Rutting was measured with a five foot straight edge at five locations in each of the two lanes of a test section. Each distress type was categorized into low, moderate, and high severity levels with the extent of each distress type measured according to the SHRP distress manual (1990).

4.7 Assessment of the Effects of Different Designs

Assessment of the effect of different designs on pavement distress could be done by different methods. Such methods are based on the following criteria:

Table 4.11 Traffic data from weigh-in-motion device.

	South Bound Lane		North Bound Lane	
Month	18 kip ESAL#	Cum. ESAL#	18 kip ESAL#	Cum. ESAL#
Jun'90	5,000	5,000	14,052	14,052
Jul'90	4,283	9,284	11,924	25,976
Aug'90	4,861	14,144	11,268	37,245
Sep'90	4,861	19,005	15,123	52,368
Oct'90	4,861	23,866	16,296	68,664
Nov'90	4,861	28,727	17,469	86,133
Dec'90	4,861	33,588	18,642	104,775
Jan'91	4,861	38,448	19,814	124,586
Feb'91	4,861	43,309	20,987	145,577
Mar'91	4,861	48,170	22,160	167,737
Apr'91	4,861	53,031	23,333	191,069
May'91	5,511	58,542	24,505	215,575
Jun'91	4,649	63,191	25,678	241,253
Jul'91	4,894	68,084	30,965	272,218
Aug'91	5,263	73,347	26,419	298,637
Sep'91	5,557	78,905	29,196	327,833
Oct'91	6,115	85,020	30,369	358,203
Nov'91	6,507	91,527	31,542	389,745
Dec'91	3,334	94,861	31,204	420,949
Jan'92	8,846	103,707	34,085	455,033
Feb'92	5,550	109,257	26,754	481,787
Mar'92	5,550	114,806	22,981	504,769
Apr'92	5,550	120,356	19,209	523,978
May'92	3,646	124,002	15,338	539,315
Jun'92	6,373	130,375	12,174	551,489
Jul'92	8,616	138,991	7,057	558,549
Aug'92	8,180	147,171	8,910	567,456
Sep'92	7,322	154,493	8,507	575,963
Oct'92	7,322	161,815	8,507	584,470
Nov'92	6,464	168,279	8,104	592,574
Dec'92	10,115	178,394	11,502	604,076
Jan'93	8,162	186,556	8,584	612,660
Feb'93	7,861	194,417	6,779	619,439
Mar'93	7,716	202,133	6,648	626,087
Apr'93	4,250	206,383	2,286	628,373
May'93	2,206	208,589	1,049	629,422
Jun'93	2,231	210,820	794	630,216
Jul'93	2,150	212,970	848	631,064

1. Average vertical strains
2. Backcalculated moduli values, and
3. Pavement distress measurements (visual).

Method 3 is a common method of studying pavement performance. Method 1 involves field instrumentation and therefore is more of a research tool. Method 2 involves principles of non destructive testing and backcalculation. In the discussion below, Method 3 is used to validate conclusions reached using pavement response measurements (i.e., Methods 1 and 2). This clearly demonstrates the effect of design and distress levels on response measurements, thereby making out a strong case for a "mechanistic design" approach for pavement design. Method one is limited to sections having MDD's.

4.7.1 Average Vertical Strains

The LVDT measurements can be used to calculate the average vertical strain between the LVDT locations. Data from the trips made in June 1990 and May 1991 were used to assess the performance of pavement sections based on average vertical strains. The average vertical strains of multi-layers based on deflection measurements, as shown in Figures 4.27 to 4.29, were utilized in evaluating the effect of different designs (i.e., varying thicknesses and material types) on the pavement response. The following are the noteworthy observations made from these figures.

(1) The first noteworthy observation made from these figures was regarding the beneficial effect of stabilized layers in Sections 2, 6, and 8. In Figure 4.29, the average vertical strain values in the subgrade of Sections 2, 6, and 8 were much lower than those in the other sections due to the stiffening effect of stabilization. The influence of base stabilization could be also studied by comparing the average vertical strains in the surface layer of Sections 2 and 8. Sections 2 and 8 have identical surface layer thicknesses and differ only in the thickness and material type, of the base layer. The results in Figures 4.27 and 4.29 showed that the strains in the asphalt concrete layer and in the subgrade were lower in Section 2 than in Section 8. Furthermore, some

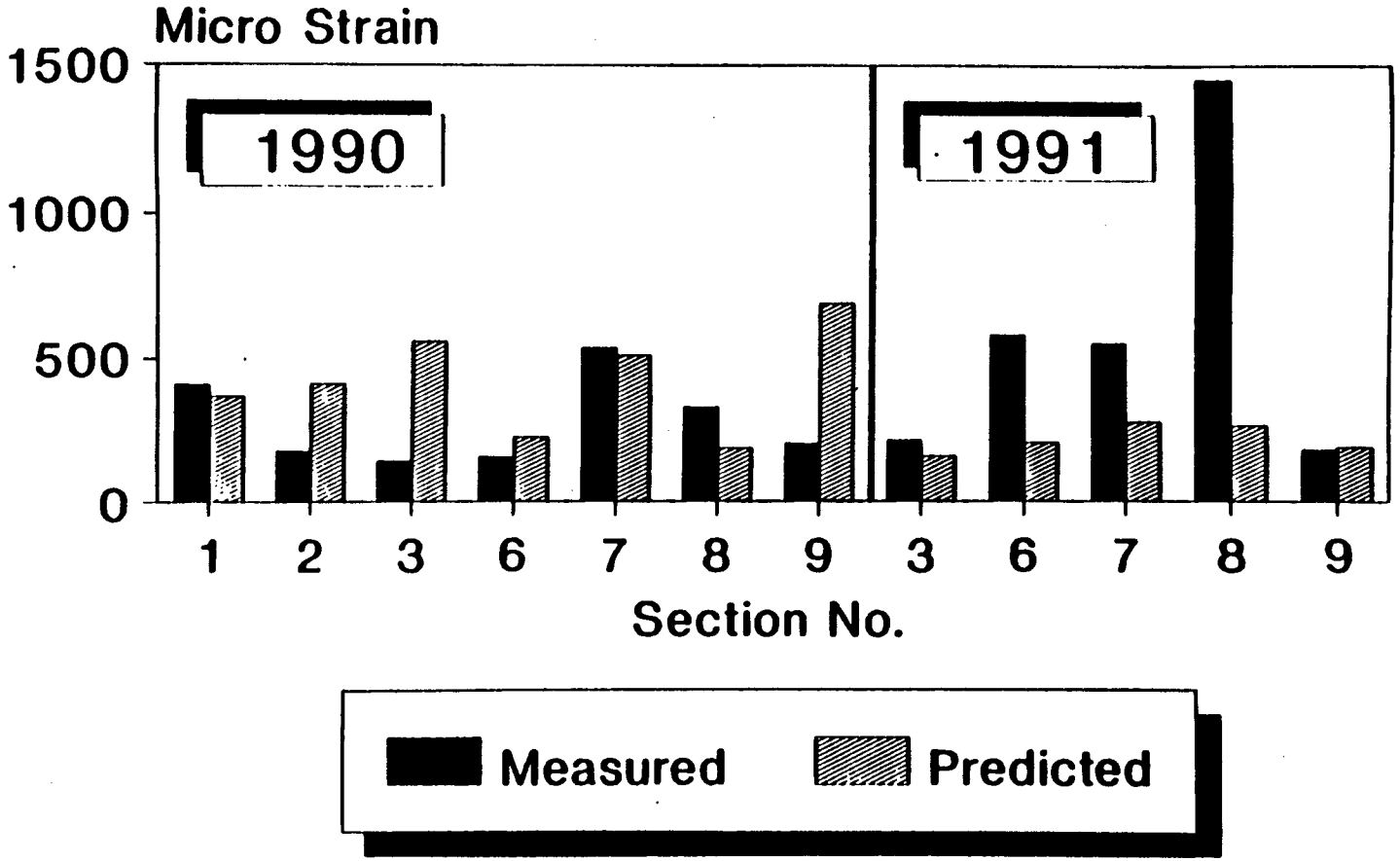

Figure 4.27 Average vertical strains within the asphalt concrete surface layers.

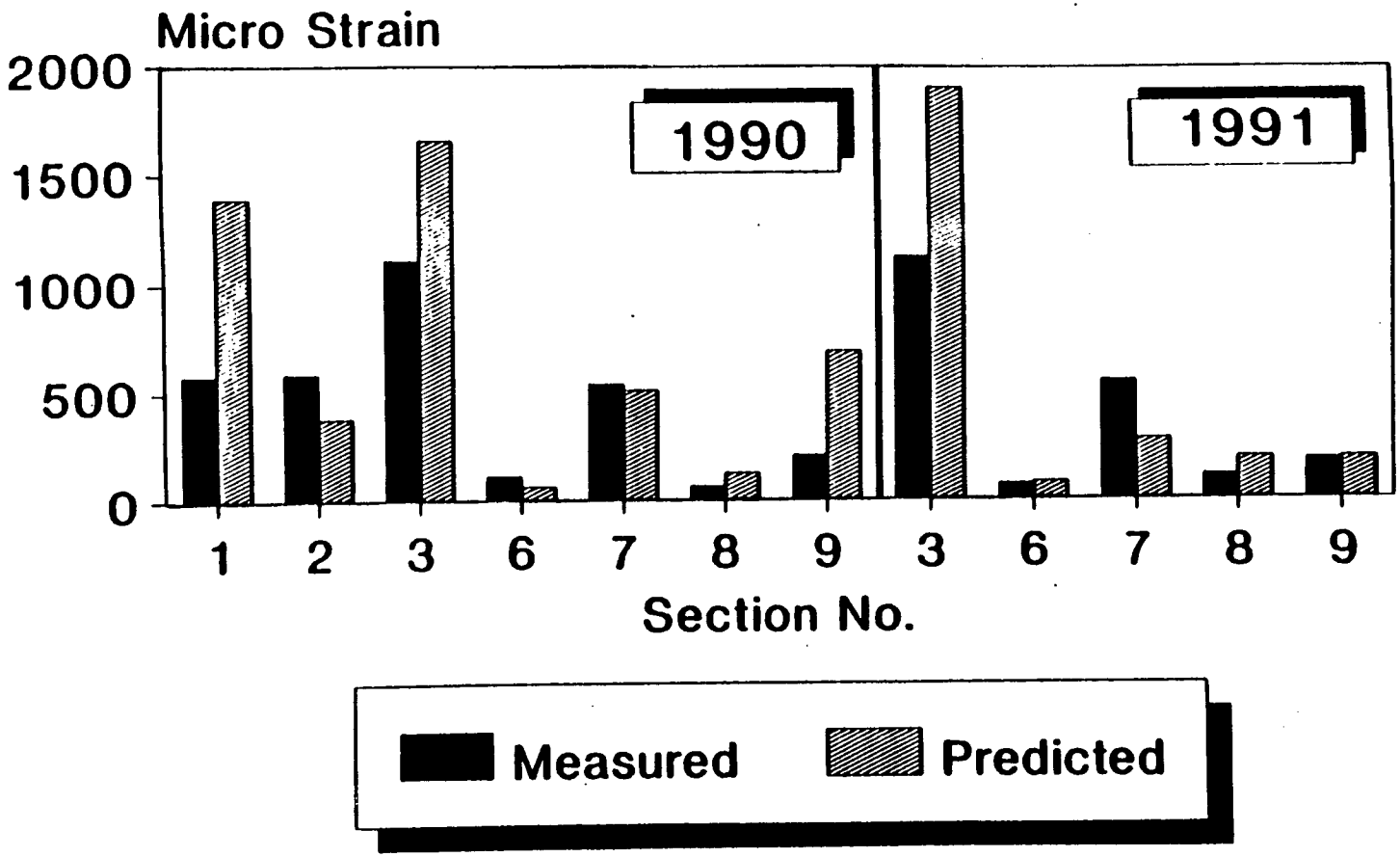

Figure 4.28 Average vertical strains within the base layers.

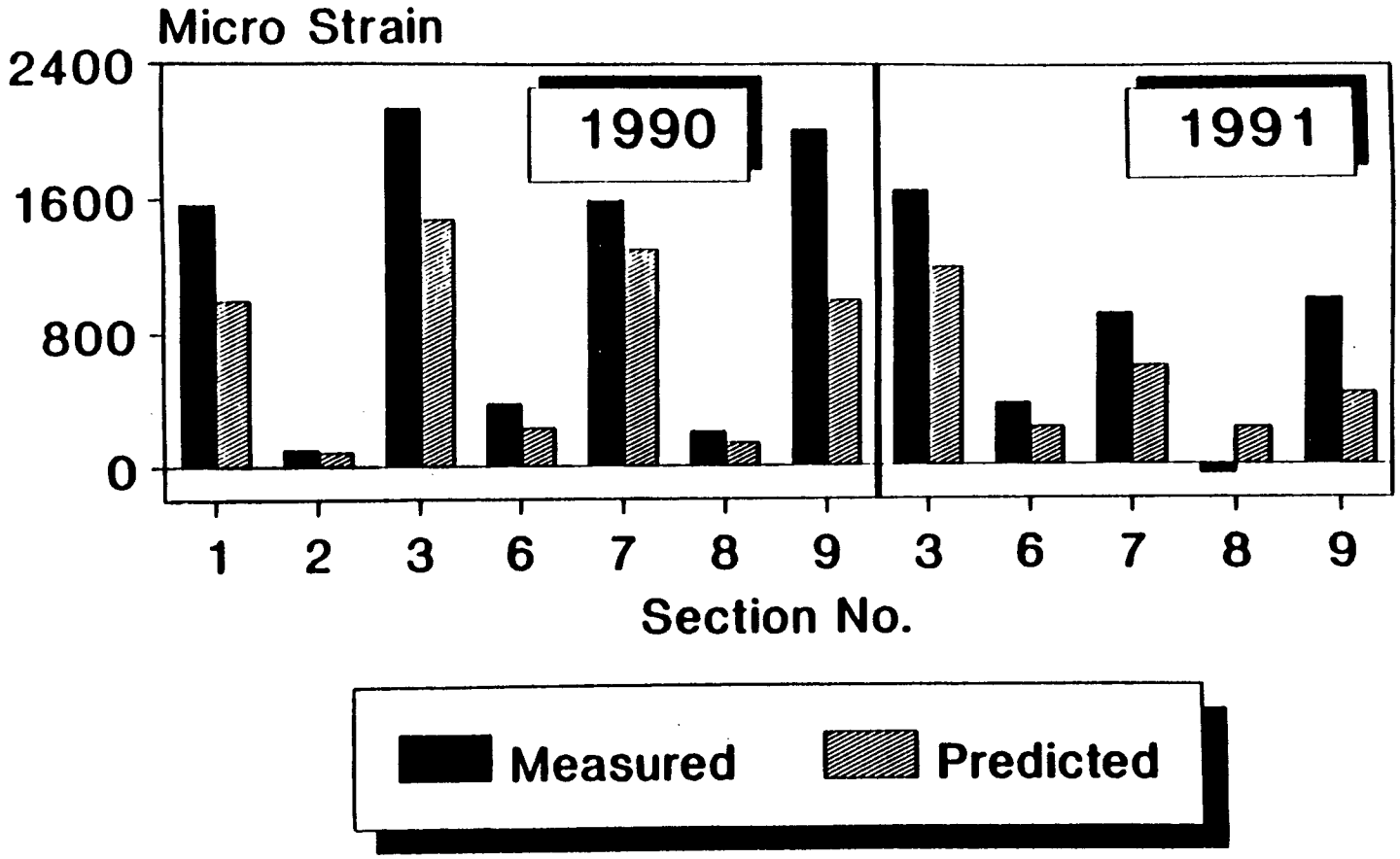

Figure 4.29 Average vertical strains within the subgrades.

block cracking observed in the sections with the cement-treated base courses, after the construction, raised questions about the benefits of the cement-treated base course.

(2) The comparison of the subgrade strains in Sections 1 and 2 yielded more detailed information on the beneficial effect of subgrade stabilization. Section 1 has 3.5-inch (8.9 cm) thick AC surfacing with no stabilization, and in Section 2, the surface course is only 2-inch (5.08 cm) thick but the top 7 inches (17.78 cm) of the subgrade is stabilized with the cement. Although the average vertical strains in the aggregate base layer were almost the same for both the sections as shown in Figure 4.28, the strains in the asphalt concrete and in the subgrade were reduced considerably in Section 2, which is an important factor in minimizing rutting in pavements.

(3) A similar comparison could be made with Sections 6 and 8. Section 6 has 5-inch (12.7 cm) thick AC surfacing with no subgrade stabilization, and Section 8 has only 2-inch (5.08 cm) thick AC surfacing but with the lime-stabilized subgrade. Although the beneficial effects of stabilization of subgrade could not be fully recognized due to the presence of cement-treated base layers in both the sections, the average vertical strains in the base layer and subgrade of Section 8 with the stabilized subgrade were smaller than those in Section 6 without subgrade stabilization.

(4) The average vertical strain data for Sections 1 and 3 in Figures 4.27 through 4.29 provide an interesting comparison. In Section 1, the thicknesses of the surfacing and the aggregate base layer are 3.5 (8.9 cm) and 12 inches (30.48 cm) respectively, whereas Section 3 has 5-inch (12.7 cm) thick AC surfacing and 8 inches (20.32 cm) thick aggregate base course. As a result, the average vertical strain in the AC surfacing was much lower in Section 3 with a thicker AC layer, but the average vertical strains within the aggregate base layer and within the subgrade were lower in Section 1. Therefore, a 1.5-inch (3.81 cm) increase in the AC layer thickness with

4-inch (10.16 cm) reduction of the base layer thickness increased the average vertical strains in the base layer and in the subgrade. This is to say that a pavement section with a 3.5 inch (8.9 cm) AC layer and a 12 inch (30.48 cm) aggregate base layer (Section 1) is not equivalent to a pavement section with a 5 in (12.70 cm)AC layer with an 8 inch (20.32 cm) aggregate base course (Section 3).

(5) The effect of replacing a 12-inch (30.48 cm) thick aggregate base course with 5.5-inch (13.9 cm) thick asphalt concrete base course was investigated by comparing the vertical strains of Sections 1 and 7 in Figure 4.29. The average vertical strains in the subgrade were almost the same for both the sections. This observation indicates that based on the vertical compressive strain in the subgrade, the structural capacity of 5.5-inch (13.9 cm) thick asphalt concrete base is almost the same as that of 12-inch (30.48 cm) thick unbound aggregate base course.

(6) The average vertical strain values from Sections 3, 6, and 9 could be compared to evaluate the effect of different base materials. Sections 3, 6, and 9 have the same thickness for the asphalt concrete surface but varying base course designs. Section 3 has an 8-inch (20.32 cm) thick unbound aggregate base, Section 6 has a 5.5-inch (13.97 cm) thick cement-treated base, and Section 9 has a 4-inch (10.16 cm) asphalt concrete base, respectively. The average vertical strain in the subgrade was lowest in Section 6. In addition, the average vertical strain values in the subgrade for Sections 3 and 9 were comparable. This was evident for both the trips (June 1990 and May 1991) as shown in Figure 4.29. It appears that a 4 inch (10.16 cm) thick asphalt concrete base is equivalent to 8 inch (20.32 cm) of aggregate base course.

In general, Section 2 resulted in the lowest average vertical strain in the subgrade as compared with other sections. Although the thickness of the AC surface was only 2 inches (5.08 cm), cement stabilization of top 7 inches (17.78 cm) of subgrade reduced the subgrade strain effectively. This fact emphasizes the importance of subgrade improvement on

pavement design and rehabilitation.

4.7.2 Backcalculated Moduli Values

Backcalculation was carried out using MODULUS 4.0. Figures 4.30 through 4.33 show moduli values for different layers for 6 different field trips.

Surface moduli values for Section 6 was calculated by the full analysis and appeared to be unreasonably high. It was noticed that the moduli values for the surface were, for most part, very close to the upper limit of the input seed moduli. It must be mentioned here that none of the gages (strain and pressure gages) work any more in this section, suggesting that there must have been a severe deterioration of the CTB layer. Also, the distress survey indicated severe pumping and rutting in Section 6.

Figure 4.33 presents the moduli values of granular base layers for all the trips. One interesting observation to be made here is that the granular base over the stabilized subgrade in Sections 2, 5, 17, and 24 had much higher moduli values than the granular base over the soft subgrade in Sections 1, 3, and 23 demonstrating the effect of confinement and support on granular layer modulus. The differences between the responses of Sections 3 and 16 could probably be explained by an increase in surface course thickness of Section 3 due to an early overlay.

A large variation among the moduli of the CTB layers for different sections are depicted in Figure 4.31 with very large variation among different sections. For example, Sections 4 and 18 have the same thickness design and have been subjected to the same traffic. However, the moduli values of the CTB in Section 4 is 2 to 8 times higher than the CTB moduli of Section 8. These differences may be explained by distress survey results on these sections which show a PCR value of 75 for Section 4 and a PCR of 90 for Section 18. These PCR ratings were for May 1991 trip and were determined by NCDOT.

As shown in Figure 4.32, the analysis of data from the trips revealed that the cement-stabilized subgrades in Sections 2 and 5 were much stiffer than the lime-stabilized subgrade in other sections. This is generally expected because the strength gain due to lime stabilization is mainly dependent upon pozzolanic reaction whereas cement stabilization

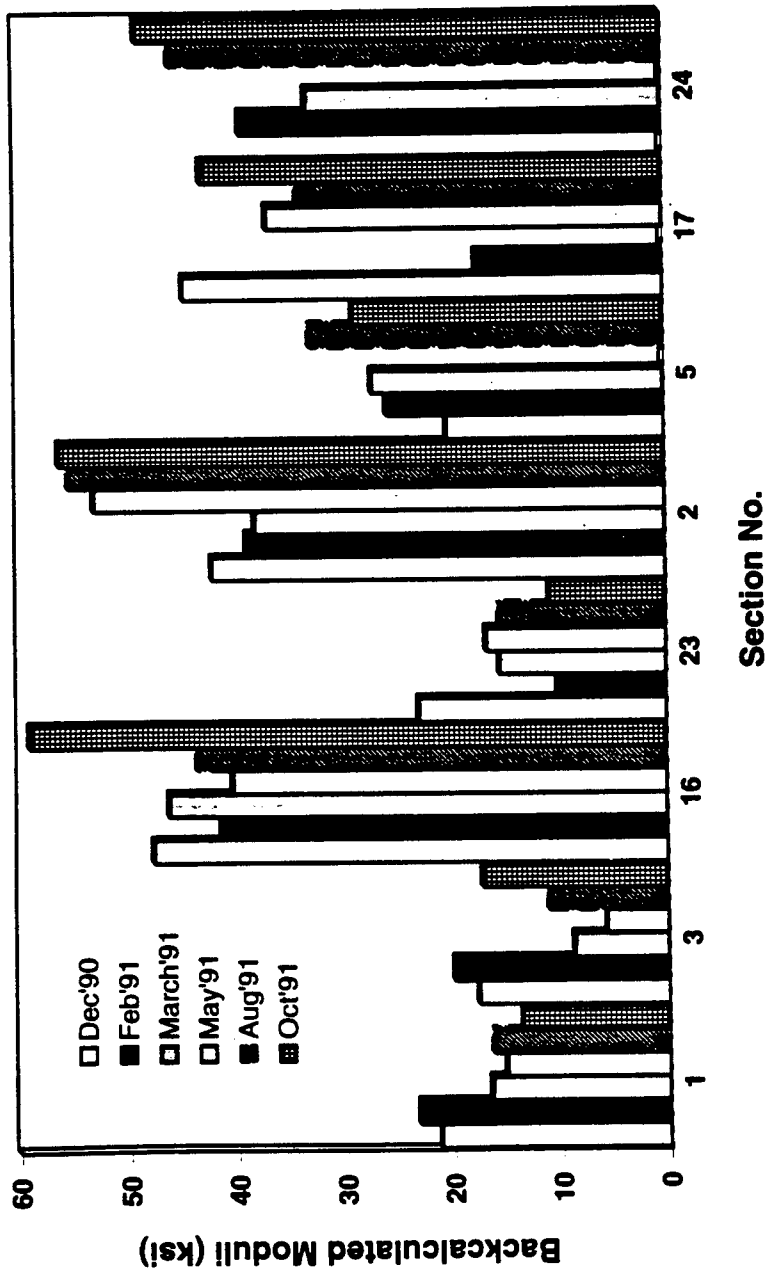

Figure 4.30 Granular base moduli.

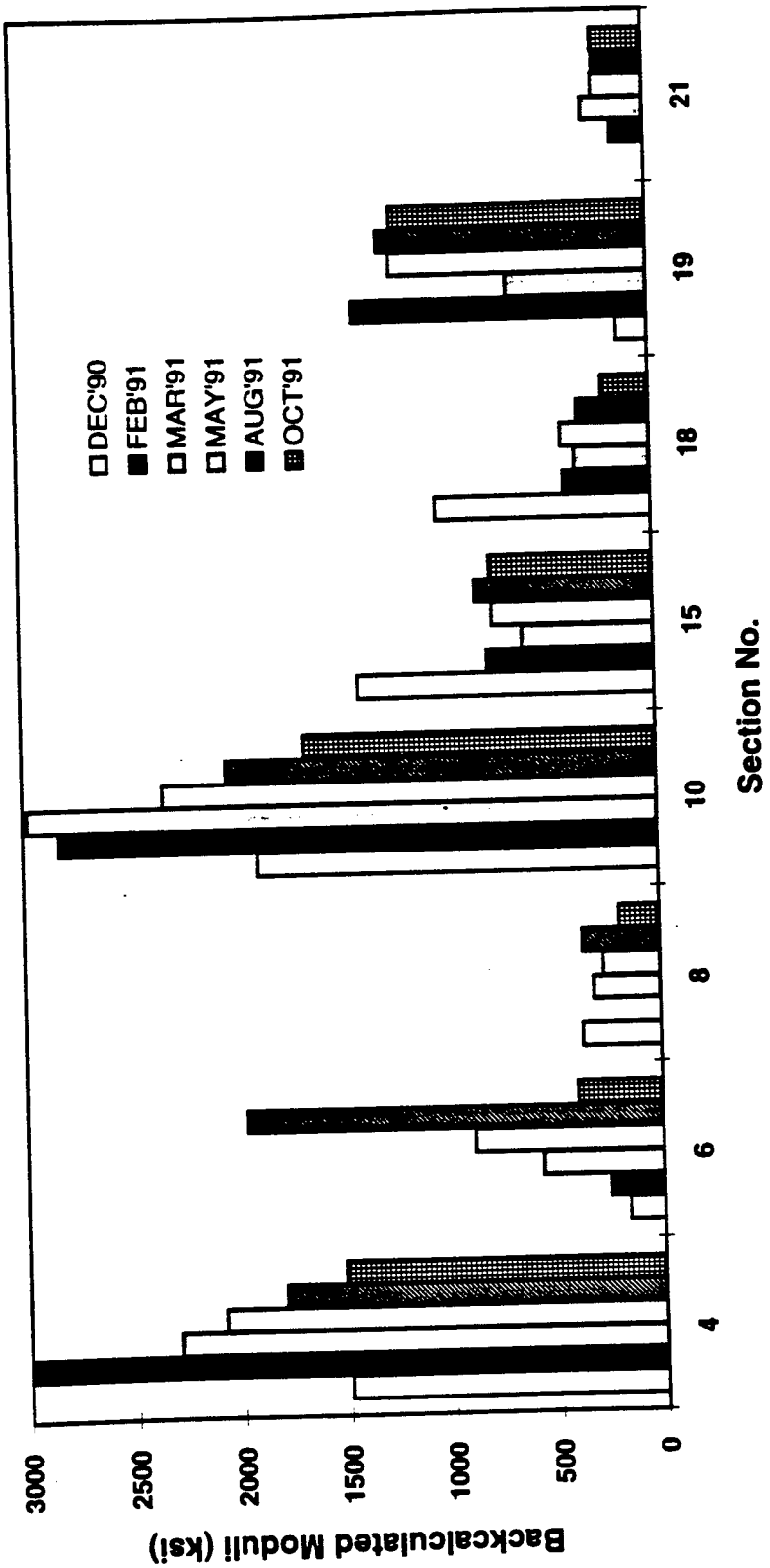

Figure 4.31 Cement-treated base moduli.

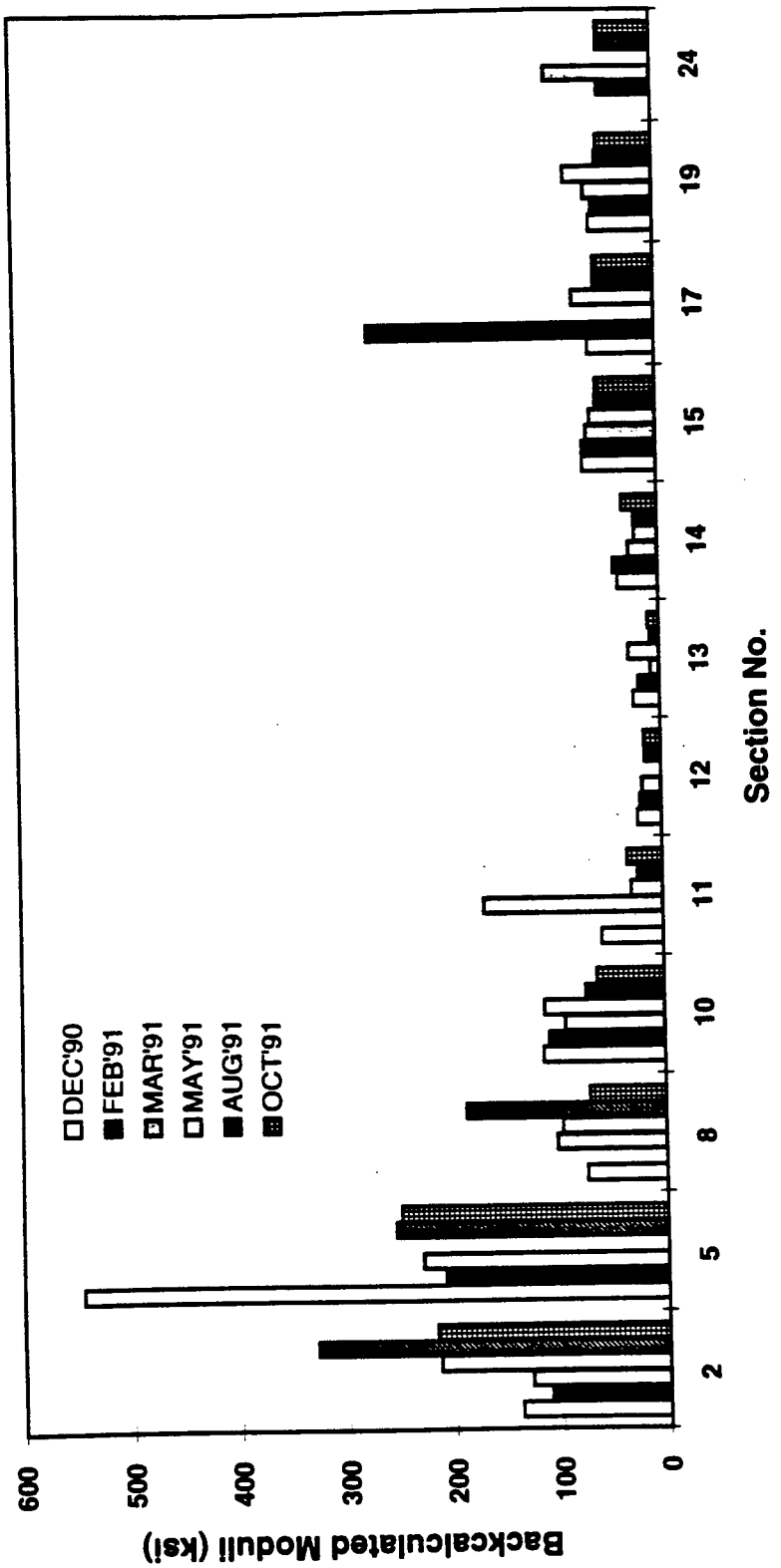

Figure 4.32 Stabilized subgrade moduli.

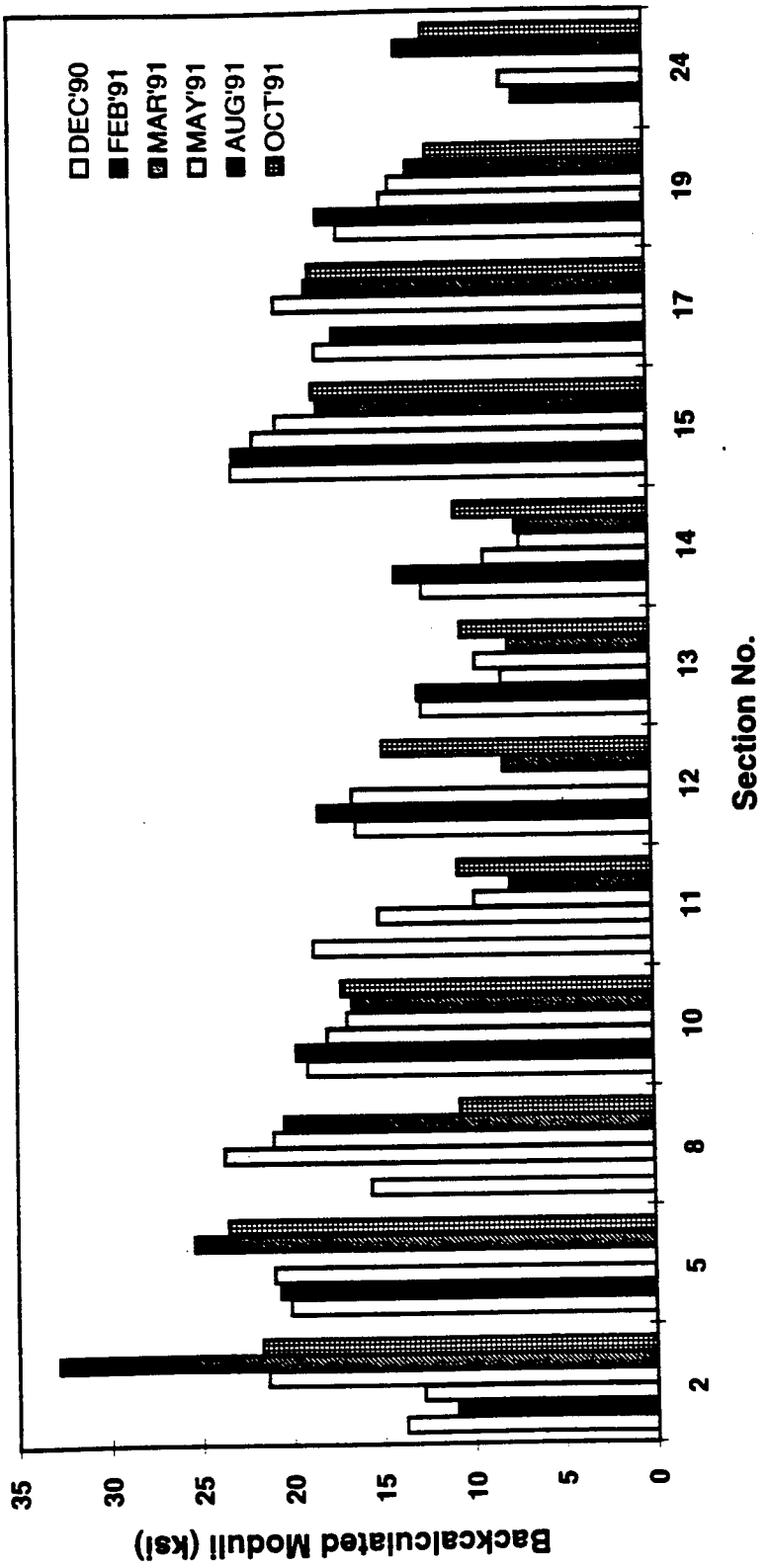

Figure 4.33 Subgrade moduli.

provides additional cementitious reaction forming hydrates of calcium silicate.

Figure 4.33 shows the subgrade moduli values for all the trips. The subgrade moduli values of the sections with the stabilized subbase or CTB layers were higher than those of the sections without any stabilized base or stabilized subbase layer. Perhaps this was due to the low stress state in these layers but, most likely, it was due to the limitation of the multi-layered elastic theory employed in the backcalculation procedure.

As discussed earlier relatively high moduli values of the aggregate base course and subgrade when present with stabilized layers, indicate the limitation of the multi-layered elastic theory. It must be recognized by practicing engineers that the deflection-based moduli backcalculation schemes built on the multi-layered elastic theory measure the effective modulus, not the modulus as the material property.

4.7.3 Pavement Distress Survey Measurements

Performance of the test sections has been monitored separately by the NCDOT and NCSU crew members. NCSU team performed a detailed walk-through distress survey, collecting the extent, severity, and type of surface distresses. Windshield survey results (PCR) are being provided by engineers from NCDOT. A 100 on this scale represents a pavement with very little distress. As a result, the performance of the sections in this report is represented by the detailed distress information during each of the trips in August and October of 1991 and March 1992 and by the Pavement Condition Rating (PCR) which is a composite distress index calculated from the survey data (see Table 4.12). A comparison of pavement performance from different designs was then conducted using the section grouping method, presented in Chapter 3, that categorizes all the 24 sections by the base course type and by the subgrade stabilization. Although quantitative data is available from August 1992 only, a definite trend can be observed. Magnitude of various distresses and specific quantitative distress information has been provided in Tables 4.13(a) to 4.13(c).

The most commonly encountered distress types were longitudinal cracking, fatigue cracking, patching, and rutting. The extent of longitudinal cracks in some sections decreased as the ESAL number increased. This unexpected trend is due to the reason that longitudinal

Table 4.12 Condition Survey by NCDOT

SECTION #	MAY '91	JUL. '91	AUG. '91	NOV. '91	FEB. '92	MAR.'92
1	72	67	67	67	65	65
2	100	100	100	100	100	94
3	100	85	85	85	68	67
4	75	71	71	66	58	57
5	100	100	100	100	100	87
6	100	76	76	76	69	66
7	100	100	96	96	85	76
8	57	57	57	56	71*	56*
9	100	68	67	67	66	66
10	81	58	58	58	54	54
11	100	96	96	96	96	83
12	100	100	100	100	100	91
13	100	100	96	96	96	96
14	100	96	81	81	81	76
15	71	71	71	71	100*	100*
16	75	58	58	58	57	55
17	100	100	100	100	100	100
18	90	86	66	66	59	59
19	85	85	50	50	100*	100*
20	100	91	91	91	91	87
21	100	100	100	100	100	76
22	100	87	76	76	76	76
23	68	60	59	58	58	57
24	100	96	96	96	91	78

*PCR values after overlay

Table 4.13(a) Magnitude of various distresses for Group 1 pavements.

		Group 1								
		Longitudinal Cracking (ft.)								
		18K ESAL	Sec. 1	Sec. 23*	Sec. 3*	Sec. 16	Sec. 2	Sec. 24**	Sec. 5	Sec. 17
SBL	Aug'91	68084	26	93	3	2	0	32	0	0
	Oct'91	78905	30	110	9	2	0	37	0	0
	Mar'92	109257	182	207	0	34	7	129	0	0
	Jun'92	124002	100	223	0	30	80	208	22	0
	Oct'92	154493	160	230	630	40	95	280	22	0
	Feb'93	186556	250	0	780	100	0	250	25	0
	Jun'93	208589	390	-	930	140	55	210	55	130
	Aug'93	212970	390	-	930	250	60	260	45	180
NBL	Aug'91	272218	74	88	30	31	0	0	0	0
	Oct'91	327833	58	89	35	27	0	0	0	0
	Mar'92	481787	45	96	270	5	0	96	264	0
	Jun'92	539315	15	99	284	12	0	182	271	0
	Oct'92	575963	20	0	809	0	20	218	290	13
	Feb'93	612660	20	0	210	30	20	114	335	0
	Jun'93	629422	20	-	260	0	0	20	370	0
	Aug'93	631064	20	-	260	10	0	50	385	0
		Fatigue Cracking + Patching (sq. ft.)								
		18K ESAL	Sec. 1	Sec. 23*	Sec. 3*	Sec. 16	Sec. 2	Sec. 24**	Sec. 5	Sec. 17
SBL	Aug'91	68084	5	430	30	0	0	0	0	0
	Oct'91	78905	5	675	82	0	0	0	0	0
	Mar'92	109257	28	1146	249	0	0	0	0	0
	Jun'92	124002	262	1571	564	0	24	0	0	0
	Oct'92	154493	540	1915	564	0	24	0	0	0
	Feb'93	186556	580	2470	564	0	345	100	0	0
	Jun'93	208589	1675	-	564	570	550	230	30	0
	Aug'93	212970	1675	-	3785	570	700	300	90	0
NBL	Aug'91	272218	162	409	287	569	0	1	0	0
	Oct'91	327833	438	597	412	617	0	1	0	0
	Mar'92	481787	936	2531	413	1100	0	6	0	0
	Jun'92	539315	1518	4228	1091	1794	6	25	0	0
	Oct'92	575963	1988	5725	1210	2225	12	51	0	0
	Feb'93	612660	4250	7170	1360	2348	30	521	85	45
	Jun'93	629422	5430	-	2040	3198	385	1276	435	295
	Aug'93	631064	5430	-	2040	3443	385	1436	465	295
		Rutting (in.)								
		18K ESAL	Sec. 1	Sec. 23*	Sec. 3*	Sec. 16	Sec. 2	Sec. 24**	Sec. 5	Sec. 17
SBL	Aug'91	68084	-	-	-	-	-	-	-	-
	Oct'91	78905	0.21	0.21	0.19	0.15	0.19	0.12	0.18	0.09
	Mar'92	109257	0.21	0.21	0.24	0.18	0.20	0.13	0.18	0.13
	Jun'92	124002	0.21	0.24	0.25	0.20	0.20	0.13	0.18	0.16
	Oct'92	154493	0.21	0.24	0.25	0.22	0.22	0.14	0.19	0.17
	Feb'93	186556	0.21	0.24	0.25	0.22	0.22	0.14	0.19	0.17
	Jun'93	208589	0.21	-	0.25	0.22	0.22	0.14	0.19	0.17
	Aug'93	212970	0.21	-	0.25	0.22	0.22	0.14	0.19	0.17
NBL	Aug'91	272218	-	-	-	-	-	-	-	-
	Oct'91	327833	0.19	0.28	0.25	0.23	0.15	0.16	0.20	0.19
	Mar'92	481787	0.19	0.29	0.25	0.23	0.16	0.16	0.20	0.22
	Jun'92	539315	0.20	0.31	0.25	0.25	0.17	0.16	0.21	0.23
	Oct'92	575963	0.22	0.33	0.29	0.25	0.19	0.19	0.21	0.24
	Feb'93	612660	0.28	0.33	0.29	0.25	0.19	0.19	0.22	0.24
	Jun'93	629422	0.31	-	0.29	0.25	0.21	0.19	0.22	0.24
	Aug'93	631064	0.33	-	0.29	0.26	0.23	0.19	0.23	0.26

Note: * Overlaid completely. ** Overlaid in part.

Table 4.13(b) Magnitude of various distresses for Group 2 pavements.

			Group 2							
			Longitudinal Cracking (ft.)							
		18K ESAL	Sec. 4	Sec. 18**	Sec. 6*	Sec. 21	Sec. 8*	Sec. 19*	Sec. 10	Sec. 15*
SBL	Aug'91	68084	15	252	40	0	10	27	1	317
	Oct'91	78905	60	254	12	0	9	0	111	301
	Mar'92	109257	287	156	181	180	0	-	169	-
	Jun'92	124002	170	162	181	200	84	-	175	-
	Oct'92	154493	170	182	181	200	56	-	150	-
	Feb'93	186556	100	210	-	150	-	-	184	-
	Jun'93	208589	0	50	-	0	-	-	0	-
	Aug'93	212970	0	50	-	0	-	-	0	-
NBL	Aug'91	272218	37	63	184	0	2	114	163	153
	Oct'91	327833	50	26	122	0	20	74	349	35
	Mar'92	481787	316	366	406	238	136	-	403	-
	Jun'92	539315	200	469	218	243	50	-	386	-
	Oct'92	575963	30	589	222	243	75	-	368	-
	Feb'93	612660	25	130	-	137	-	-	100	-
	Jun'93	629422	30	10	-	37	-	-	0	-
	Aug'93	631064	30	10	-	47	-	-	590	-
			Fatigue Cracking + Patching (sq. ft.)							
		18K ESAL	Sec. 4	Sec. 18**	Sec. 6*	Sec. 21	Sec. 8*	Sec. 19*	Sec. 10	Sec. 15*
SBL	Aug'91	68084	42	18	244	119	137	1600	0	0
	Oct'91	78905	128	18	762	156	237	2130	0	0
	Mar'92	109257	508	396	1286	198	225	-	0	-
	Jun'92	124002	769	510	1540	234	375	-	0	-
	Oct'92	154493	900	510	1580	320	414	-	50	-
	Feb'93	186556	1780	780	-	555	-	-	440	-
	Jun'93	208589	3785	1105	-	1415	-	-	1178	-
	Aug'93	212970	3785	1105	-	1415	-	-	1178	-
NBL	Aug'91	272218	3	478	95	0	627	1022	10	397
	Oct'91	327833	4	481	328	0	948	2771	41	1452
	Mar'92	481787	473	843	1356	48	398	-	708	-
	Jun'92	539315	1449	1268	2184	48	687	-	804	-
	Oct'92	575963	2210	2225	2370	48	1720	-	772	-
	Feb'93	612660	4300	2068	-	450	-	-	1610	-
	Jun'93	629422	7480	3198	-	960	-	-	4228	-
	Aug'93	631064	7480	4678	-	1020	-	-	5628	-
			Rutting (in.)							
		18K ESAL	Sec. 4	Sec. 18**	Sec. 6*	Sec. 21	Sec. 8*	Sec. 19*	Sec. 10	Sec. 15*
SBL	Aug'91	68084	-	-	-	-	-	-	-	-
	Oct'91	78905	0.21	0.16	0.19	0.11	0.18	0.08	0.15	0.14
	Mar'92	109257	0.20	0.17	0.22	0.21	0.17	-	0.18	-
	Jun'92	124002	0.20	0.20	0.21	0.20	0.18	-	0.18	-
	Oct'92	154493	0.20	0.22	0.21	0.20	0.18	-	0.17	-
	Feb'93	186556	0.20	0.22	-	0.20	-	-	0.17	-
	Jun'93	208589	0.20	0.22	-	0.20	-	-	0.17	-
	Aug'93	212970	0.20	0.22	-	0.20	-	-	0.19	-
NBL	Aug'91	272218	-	-	-	-	-	-	-	-
	Oct'91	327833	0.20	0.15	0.24	0.14	0.21	0.13	0.17	0.19
	Mar'92	481787	0.22	0.21	0.24	0.18	0.23	-	0.17	-
	Jun'92	539315	0.22	0.21	0.24	0.20	0.24	-	0.18	-
	Oct'92	575963	0.22	0.22	0.25	0.21	0.24	-	0.18	-
	Feb'93	612660	0.22	0.23	-	0.21	-	-	0.20	-
	Jun'93	629422	0.22	0.23	-	0.21	-	-	0.20	-
	Aug'93	631064	0.22	0.23	-	0.21	-	-	0.21	-

Note: * Overlaid completely. ** Overlaid in part.

Table 4.13(c) Magnitude of various distresses for Group 3 pavements.

Group 3										
Longitudinal Cracking (ft.)										
		18K ESAL	Sec. 7	Sec. 20	Sec. 9	Sec. 22	Sec. 11	Sec. 14	Sec. 12	Sec. 13
SBL	Aug'91	68084	0	0	2	0	0	11	0	0
	Oct'91	78905	0	0	3	0	0	12	0	0
	Mar'92	109257	0	0	3	48	0	21	0	0
	Jun'92	124002	1	0	5	48	54	27	0	0
	Oct'92	154493	7	0	5	45	33	34	0	0
	Feb'93	186556	5	0	70	80	50	50	0	0
	Jun'93	208589	0	0	80	70	40	20	0	0
	Aug'93	212970	0	0	80	70	70	20	0	0
NBL	Aug'91	272218	7	28	40	169	7	80	21	16
	Oct'91	327833	122	34	74	134	33	179	41	23
	Mar'92	481787	133	74	139	119	67	77	127	46
	Jun'92	539315	135	76	170	151	223	88	127	61
	Oct'92	575963	136	30	0	183	220	130	127	81
	Feb'93	612660	190	30	220	120	175	110	150	11
	Jun'93	629422	150	20	190	177	155	120	175	15
	Aug'93	631064	100	30	190	177	160	140	190	40
Fatigue Cracking + Patching (sq. ft.)										
		18K ESAL	Sec. 7	Sec. 20	Sec. 9	Sec. 22	Sec. 11	Sec. 14	Sec. 12	Sec. 13
SBL	Aug'91	68084	71	0	0	0	0	0	0	0
	Oct'91	78905	154	0	0	2	0	0	0	0
	Mar'92	109257	323	0	0	2	0	0	0	0
	Jun'92	124002	419	0	0	6	60	0	0	0
	Oct'92	154493	485	0	84	10	60	0	0	0
	Feb'93	186556	794	0	189	30	60	0	0	0
	Jun'93	208589	1159	0	489	119	111	64	0	0
	Aug'93	212970	1159	30	489	119	111	60	0	0
NBL	Aug'91	272218	2	0	200	34	0	0	0	279
	Oct'91	327833	13	0	395	62	0	0	0	279
	Mar'92	481787	232	0	694	344	0	12	0	294
	Jun'92	539315	249	0	861	500	51	26	0	294
	Oct'92	575963	292	180	1166	510	60	20	0	294
	Feb'93	612660	1103	180	1905	680	210	190	20	494
	Jun'93	629422	1204	298	4336	935	370	300	20	494
	Aug'93	631064	1758	298	4336	935	370	340	30	494
Rutting (in.)										
		18K ESAL	Sec. 7	Sec. 20	Sec. 9	Sec. 22	Sec. 11	Sec. 14	Sec. 12	Sec. 13
SBL	Aug'91	68084	-	-	-	-	-	-	-	-
	Oct'91	78905	0.14	0.09	0.20	0.19	0.13	0.17	0.15	0.17
	Mar'92	109257	0.15	0.12	0.20	0.20	0.16	0.18	0.17	0.18
	Jun'92	124002	0.18	0.12	0.21	0.22	0.17	0.19	0.17	0.18
	Oct'92	154493	0.17	0.14	0.22	0.24	0.18	0.19	0.19	0.20
	Feb'93	186556	0.18	0.14	0.22	0.24	0.18	0.19	0.19	0.20
	Jun'93	208589	0.18	0.14	0.22	0.24	0.19	0.19	0.20	0.20
	Aug'93	212970	0.19	0.14	0.22	0.24	0.21	0.19	0.21	0.20
NBL	Aug'91	272218	-	-	-	-	-	-	-	-
	Oct'91	327833	0.20	0.20	0.24	0.23	0.15	0.24	0.19	0.24
	Mar'92	481787	0.20	0.22	0.24	0.25	0.19	0.25	0.19	0.25
	Jun'92	539315	0.22	0.22	0.24	0.26	0.19	0.25	0.19	0.26
	Oct'92	575963	0.22	0.22	0.27	0.26	0.20	0.26	0.22	0.27
	Feb'93	612660	0.22	0.22	0.27	0.27	0.20	0.26	0.22	0.27
	Jun'93	629422	0.22	0.22	0.27	0.27	0.20	0.26	0.24	0.27
	Aug'93	631064	0.24	0.22	0.27	0.27	0.20	0.28	0.25	0.27

cracks progress toward fatigue cracks as the pavements deteriorate further.

Clearly, the sections with cement-treated base course, regardless of subgrade stabilization, performed worst among the three groups. Sections 15 and 19 had to be overlaid completely in early 1992 due to severe deterioration, which implied that sections had "failed" in so far as the objective of this research project was concerned. Some difficulties were also encountered in analyzing and presenting the performance data from Sections 8 and 18 because they had been partially overlaid. To maintain some consistency in comparison, the distress survey results from these sections, after the overlay, were not used in the analysis.

4.8 Summary of Performance of Different Test Sections

For the ABC sections, it was the subgrade stabilization that further enhanced the performance of this design type. Sections with cement-stabilized subgrade performed relatively better than the lime-stabilized sections due to stronger bonds developed by the cement stabilization. Among all the ABC sections, Section 2 with cement stabilized subgrade demonstrated the best performance. No longitudinal cracks, fatigue cracks, and patching were observed in this section. The performance of test Section 5 with cement stabilized subgrade, also demonstrated good performance in terms of fatigue cracking and patching. However, the rutting performance of Section 5 was not as good as that of Section 2. The same trend was found from the comparison of Sections 17 and 24. Based on the study of the section designs, it was concluded that 2 in. AC over 12 in. ABC in Sections 2 and 24 resulted in less rutting than 3.5 inch (8.9 cm) AC over 8 inch (20.35 cm) ABC in Sections 5 and 17. The effect of base course thickness on pavement performance could not be studied independently due to the confounding influence of AC binder course thickness.

The beneficial effects of subgrade stabilization could be demonstrated from the comparison of the performance among full-depth AC sections. The sections with lime-stabilized subgrade (Sections 11 to 14) performed better than the sections without subgrade stabilization (Sections 7, 9, 20, and 22) in terms of both the fatigue cracking and rutting. Also, the comparison between Sections (7, 20) and Sections (9, 22) revealed that, with the same thickness of full depth AC, better performance could be expected by having

relatively thicker HB base course. A summary of general performance of different designs (Table 4.14) surveyed in March 1992 support the conclusions made using the methods of average vertical strain and layer moduli comparisons.

Figures 4.34 (a)-(c) show percentage fatigue cracking observed in the various pavement sections as a function of ESALs (NBL). Sections with an asphaltic base course showed less cracking as compared to sections with cement treated base courses. The Sections 1 and 23 with aggregate base course, although being similar in design, showed significantly different fatigue characteristics. Sections 2 and 24, and 3 and 16 which were similar in design showed similar fatigue characteristics. Most of the full-depth sections showed very low levels of fatigue cracking, except for section 9.For the CTB sections, only section 21 seemed to show reduced levels of fatigue cracking. This could be attributed to the thick ac surface and binder course present. Although Section 6 is similar in design to Section 21, its early failure can only be explained by lack of adequate quality control during construction. It is felt that results from Section 6 should be treated more as an exception and that the thick ac and binder course should have prevented any reflective cracking, allowing the sections to perform well. To relate the good performance of Section 21 to prevailing subgrade conditions, proved to be difficult due to lack of reliable information from the moisture gages.

Subgrade stabilization seemed to be an important factor for reducing distress in flexible pavements. The asphalt and aggregate bases performed better than the cement treated base courses. This was due to the extensive cracking in the early service life of the sections with CTB course. Effect of stabilization of the subgrade under CTB courses is difficult to realize because of the extensive failure of the CTB courses. Sections 10 and 15 (both CTB sections), with stabilized subbases did not effectively prevent early failure of the two sections. It would therefore seem that the thickness of the cover provided over CTB layers may play a more important role in preventing early failure than subbase stabilization.

Table 4.14 Summary of general performance of different designs surveyed in March 1992

Design Type	Group 1					
Base Course	Aggregate Base					
Subgrade Stabilization	Cement		Lime		None	
Test Section #	2	5	24	17	(1,23)*	(3,16)*
Longitudinal Cracking (ft)	A	B	B	A	B	B
Fatigue Cracking + Patching (sq.ft.)	A	A	A	A	C	C
Rutting (in.)	A	B	A	B	C	C
PCR (NCDOT)	94	87	78	100	61	61

Design Type	Group 2			
Base Course	Cement-Treated Base			
Subgrade Stabilization	Lime		None	
Test Section #	(8, 19+)*	(10,15+)*	(4, 18)*	(6, 21)*
Longitudinal Cracking (ft)	C	C	C	C
Fatigue Cracking + Patching (sq.ft.)	C	C	B	C
Rutting (in.)	B	A	B	B
PCR (NCDOT)	56	54	58	71

Design Type	Group 3			
Base Course	Asphalt-Stabilized Base			
Subgrade Stabilization	Lime		None	
Test Section #	(11, 14+)*	(12.13+)*	(7.20)*	17
Longitudinal Cracking (ft)	A	B	B	A
Fatigue Cracking + Patching (sq.ft.)	A	A	A	A
Rutting (in.)	A	B	A	B
PCR (NCDOT)	80	94	82	71

where

Distress Type	Grade		
	A	B	C
Longitudinal Cracking (ft)	0 - 100	100 - 200	200 -
Fatigue Cracking + Patching (sq . ft)	0 - 500	500 - 1000	1000 -
Rut Depth (inches)	0 - 0.20	0.20 - 0.25	0.25 -

Note:

* Sections in the parenthesis have the same thickness design.

\+ The performance of these test sections are not considered since they were overlaid completely.

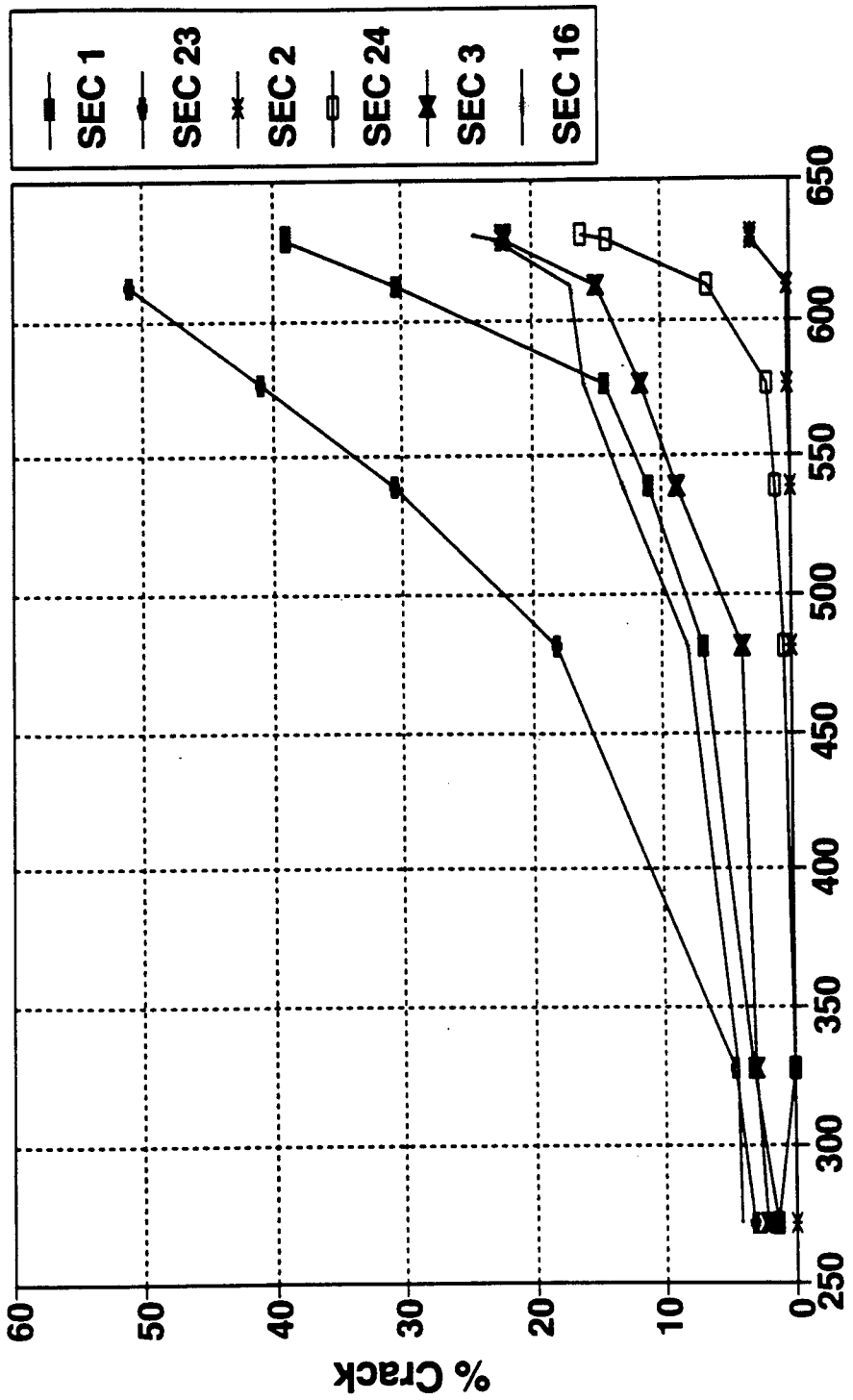

Figure 4.34(a) Percentage fatigue cracking observed in aggregate base course sections as a function of ESALs.

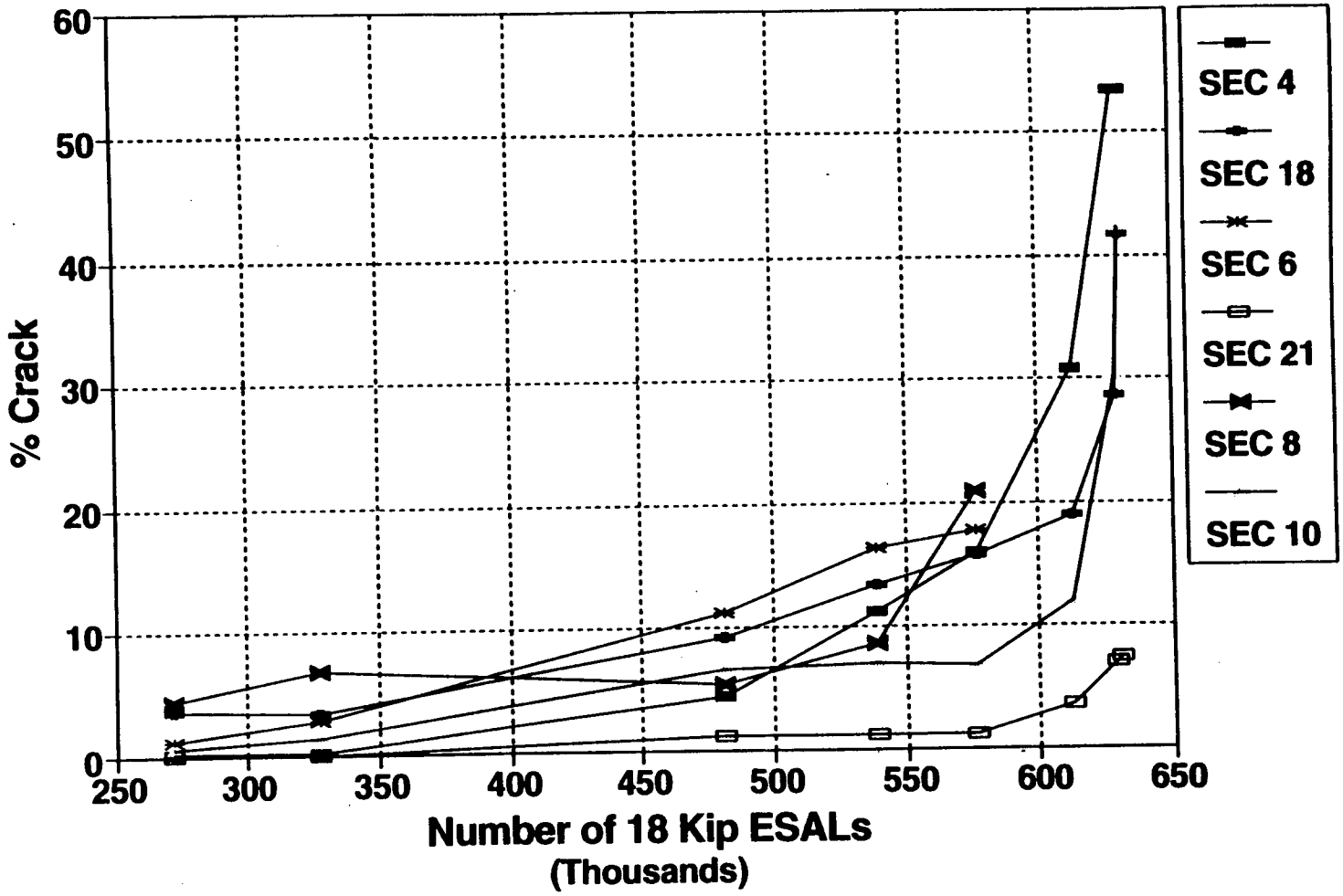

Figure 4.34(b) Percentage fatigue cracking observed in cement treated base course sections as a function of ESALs.

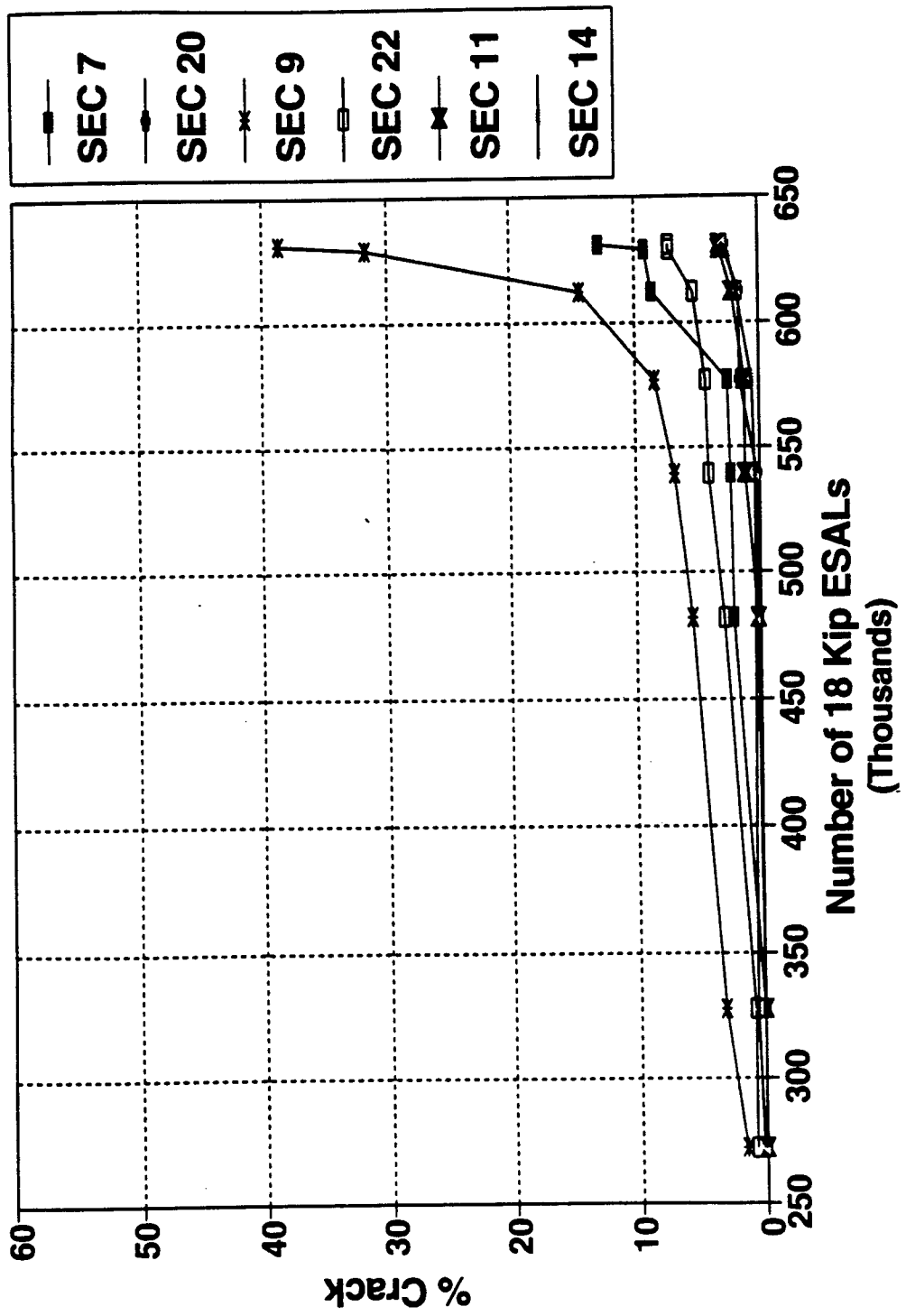

Figure 4.34(c) Percentage fatigue cracking observed in full depth ac sections as a function of ESALs.

CHAPTER 5

MATERIAL TESTING AND CHARACTERIZATION

5.1 Introduction

Laboratory tests were performed on the materials constituting the various layers in the pavement systems to evaluate representative layer properties. Layer properties, in essence, refers to the layer moduli. To make these input layer moduli consistent with the structural analysis scheme (elastic analysis) used, it was decided to use the resilient modulus as the parameter for layer stiffness.

The resilient modulus (M_r) of a material is defined as the ratio between applied stress and the recoverable strain (strain measured after removal of applied stress). It can be expressed as:

$$M_r = \frac{\sigma}{\varepsilon_r} \qquad (5.1)$$

where M_r = resilient modulus,

σ = applied stress, and

ε_r = recoverable strain.

No specific tests were performed to determine Poissons ratio's as they could be assumed fairly accurately. After preparing the sample, specific tests to obtain various material properties were performed on each of the layer materials. Detailed descriptions are provided in the following subsections.

5.2 Tests on Asphalt Concrete

5.2.1 Aggregate Sieve Size Analysis

The aggregates used in this research were #67, #467, #78M, SCRG., and sand. To get three types of mixtures (HDS, HBD, and HB), these aggregates were blended in certain proportions. Table 5.1 presents the sample gradations and properties of each aggregate type.

Table 5.1 Sample aggregate gradations and aggregate properties.

Aggregate Type	Sieve Size	Percent Passing by Weight			Specific Gravity
		Sample #1	Sample #2	Sample #3	
#67	1"	100	100	100	2.75
	3/4"	92	94	96	
	1/2"	58	55	59	
	3/8"	28	29	28	
	#4	7	8	5	
	#8	2	3	1	
	#200	1	1	0.4	
Sand	#8	100	100	100	2.65
	#40	49	48	47	
	#80	7	7	6	
	#200	0.1	0.1	0.1	
SCRG.	#4	100	100	100	2.75
	#8	80	78	75	
	#40	42	40	38	
	#80	26	26	25	
	#200	11.8	12	12.4	
#467	1.5"	100	100	100	2.73
	1"	89	82	83	
	3/4"	67	59	64	
	1/2"	31	27	29	
	3/8"	12	12	11	
	#4	3	4	2	
	#8	1	2	1	
	#200	0.3	0.2	0.1	
#78M	1/2"	100			2.75
	3/8"	94			
	#4	27			
	#8	6			
	#40	2			
	#80	1			
	#200	0.8			

The aggregate sources and the selected blending proportions for each mixture are shown in Table 5.2. Also, the selected gradations, along with North Carolina specification limits for the three mixtures are presented in Table 5.3 and in Figures 5.1 through 5.3. The tests on aggregates were performed by Blythe Industries, Inc., Staley, North Carolina.

Wet-sieve analysis was conducted to meet the requirements of aggregate gradations. The following procedure was adopted.

(1) The percent-weight passing each sieve and the percent-weight retained on each individual sieve was determined. The sample was then batched.

(2) The batched sample was washed through a #200 sieve according to ASTM standard C117-80. The weight of the material washed through the #200 was calculated by drying the retained material to constant weight. The differences in weight were determined.

(3) The material retained on the #200 sieve was sieved again. The weight of material passing the #200 sieve from the wet sieve analysis was added to that from the dry sieving.

(4) The cumulative percent weight passing each sieve and the percent weight retained on each sieve were calculated.

(5) The results were compared, and appropriate changes were made in the batching process if required.

(6) Steps (1) through (4) were repeated until the sample gradation satisfied the requirements for mix design.

More detailed information on calculating batching weights can be found elsewhere (Harvey et al.,1990; Kim,1991). The actual sample gradations selected after the calculation of batching weight (wet-sieve analysis) are shown in Table 5.3.

5.2.2 Optimum AC Content Determination

The asphalt cement used in this research was an AC-20 asphalt, and the asphalt content for the asphalt cement was determined by Blythe Industries, Inc., Staley, North Carolina. According to the construction record maintained by the NCDOT, the optimum

Table 5.2 Aggregate sources and blending proportions for each mixture.

	Aggregate Sources and blending Percentage (%)		
Mix Type	Shipping Point	Materials	Amount(%)
HDS	E. Forsyth Quarry	#78M	45.0
	E. Forsyth Quarry	SCRG.	35.0
	Kelly Pit	Sand	20.0
HDB	E. Forsyth Quarry	#67	55.0
	E. Forsyth Quarry	SCRG.	30.0
	Kelly Pit	Sand	15.0
HB	E. Forsyth Quarry	#467	63.0
	E. Forsyth Quarry	SCRG.	21.0
	Kelly Pit	Sand	16.0

Table 5.3 Selected aggregate gradations for each mixture.

Mix Type	JMF Combined Sieve Size	Percent Passing (%) NC Spec. Limits	Selected Gradation
HDS	3/4"	100	100
	1/2"	96 - 100	98
	#4	55 - 80	67
	#8	40 - 60	51
	#40	11 - 38	25
	#80	4 - 20	11
	#200	2 - 8	4.1
HDB	1"	100	100
	3/4"	90 - 100	95
	1/2"	67 - 88	77
	#8	25 - 45	40
	#200	1 - 7	4
HB	2"	100	100
	1.5"	90 - 100	95
	3/4"	60 - 85	75
	#4	25 - 50	37
	#8	25 - 40	33
	#200	0 - 6	2.9

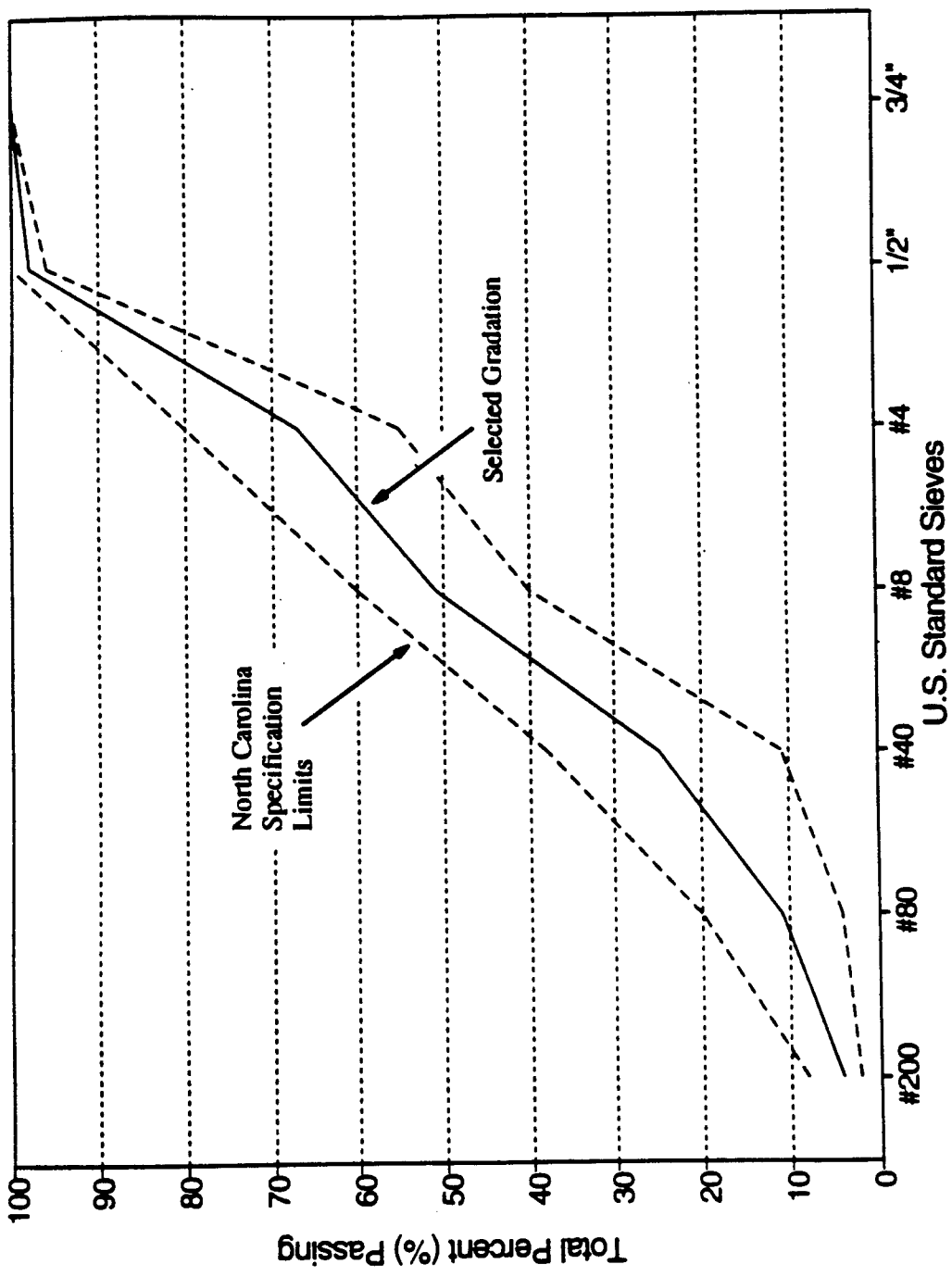

Figure 5.1 Selected aggregate gradation for HDS mixture.

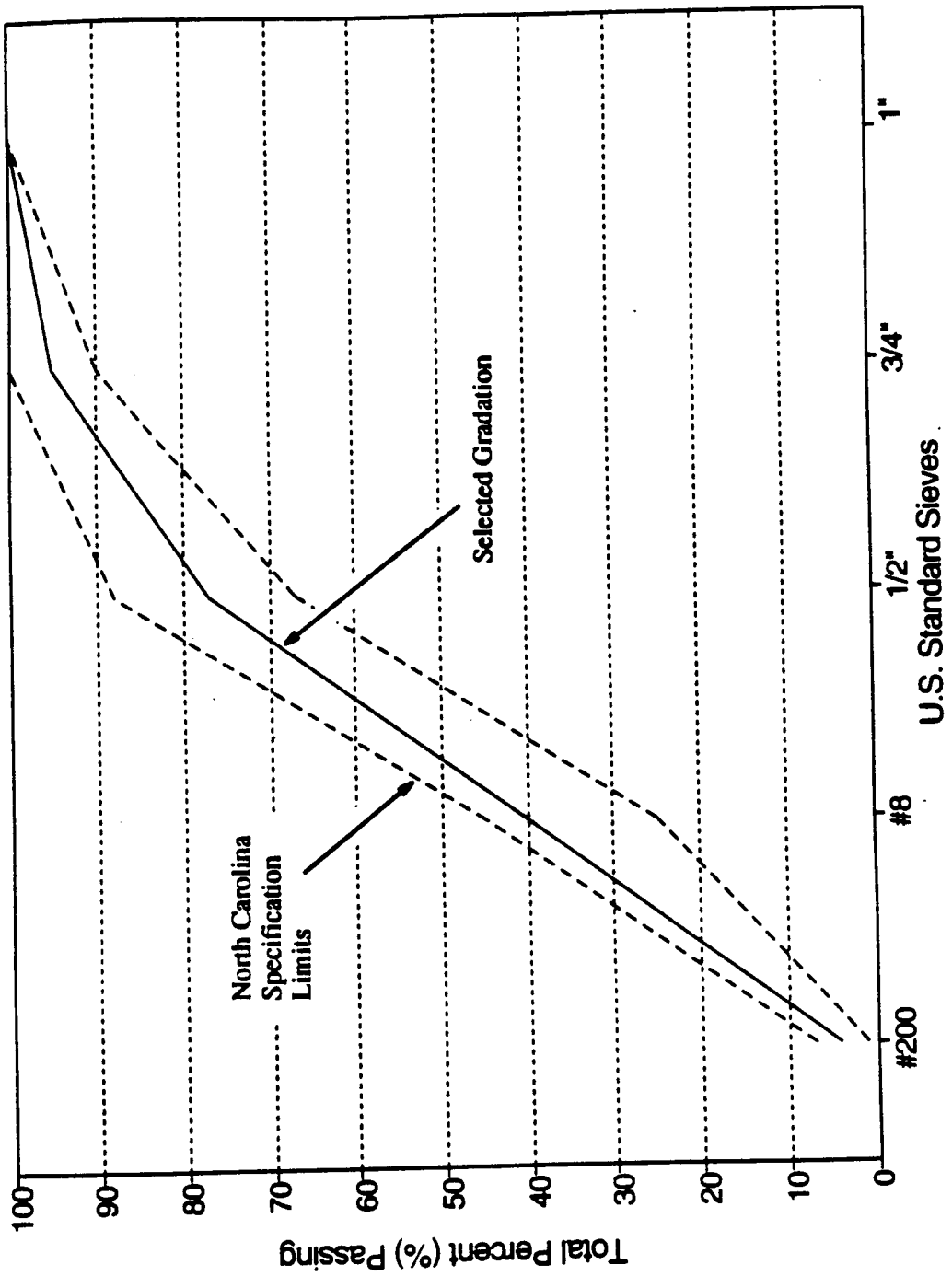

Figure 5.2 Selected aggregate gradation for HDB mixture.

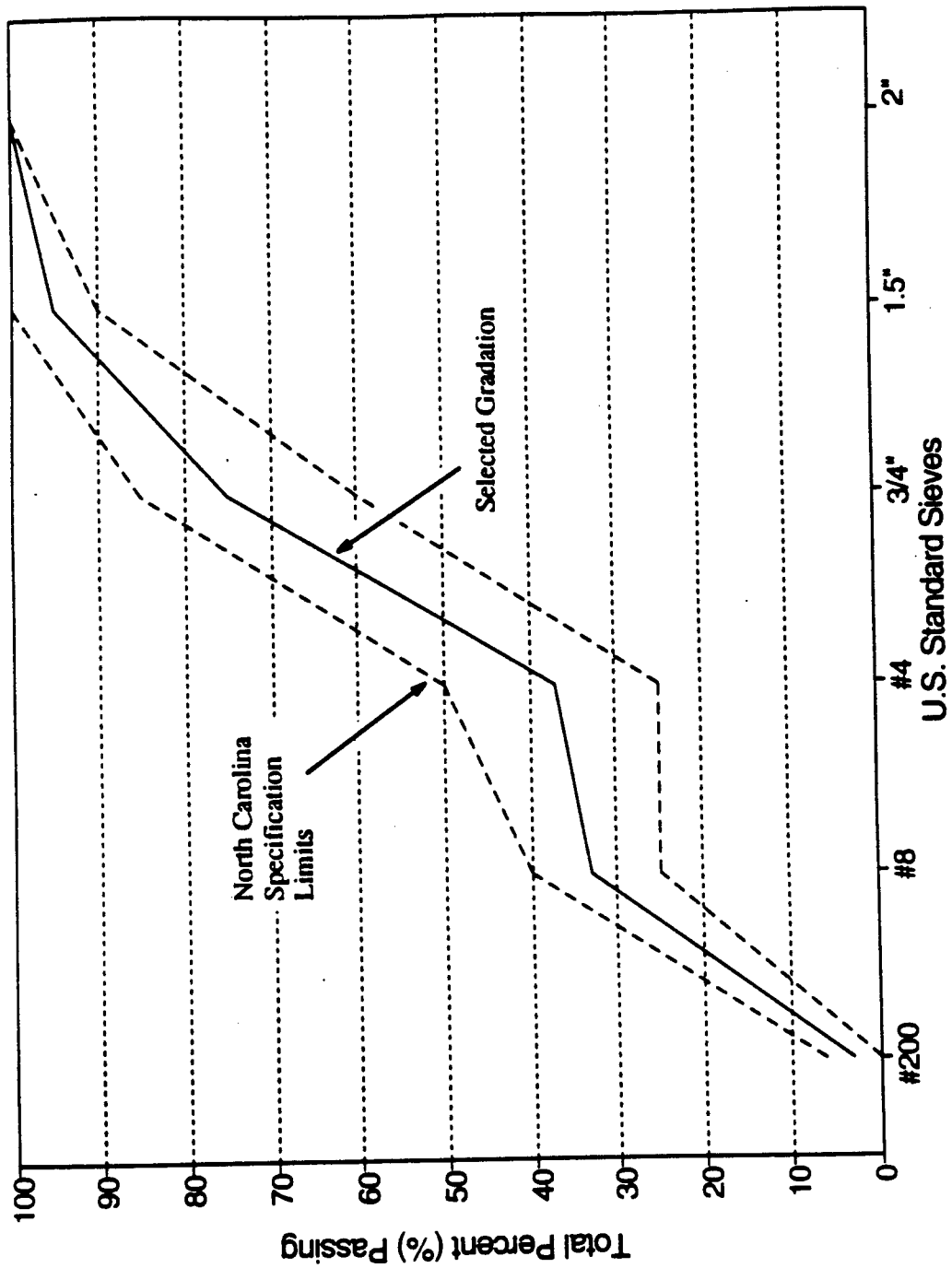

Figure 5.3 Selected aggregate gradation for HB mixture.

asphalt contents of the heavy duty surface (HDS) and the heavy duty binder (HDB) courses were determined using the U.S. Army Corps of Engineers (Marshall) 75-blow procedure (ASTM D 1559). This procedure required a minimum Marshall stability of 1,500 lbs (6.67 KN).

On the other hand, the optimum asphalt content of the asphalt-stabilized base course (HB) was determined using the U.S. Army Corps of Engineers (Marshall) 50-blow procedure. The procedure required a minimum Marshall stability of 800 lbs (3.56 KN). Table 5.4 summarizes the asphalt cement properties tested by both North Carolina State University and Blythe Industries. Also, the selected optimum asphalt contents of each asphalt concrete are presented in Table 5.5.

5.2.3 AC Specimen preparation

The sample preparation procedures for heating of aggregate and asphalt, mixing, and curing were conducted according to the "Asphalt Concrete Specimen Preparation Protocol" (Harvey, 1990) prepared at the University of California, Berkeley as a part of the SHRP Project A-OO3A. Based on the construction records maintained by the NCDOT, a mixing temperature of 285°F (140.6°C) was selected for the three mixtures (HDS, HDB, and HB).

5.2.3.1 Heating of Materials for Mixing

Aggregate

The aggregate was heated (first heating) overnight at 285°F (140.6°C) to remove any moisture that may be present. It was cooled down at room temperature (approximately 77°F (25°C)), then it was sieved in a Gilson type machine. The aggregate was heated again (second heating) for a minimum of about 90 minutes at mixing temperature, 285°F (140.6°C).

Asphalt

The asphalt was heated (first heating) and distributed into small cans from a five-gallon bucket. The asphalt in the cans was heated again (second heating) at the mixing

Table 5.4 Asphalt cement (AC-20) properties.

Properties	NCSU	Blythe Inc.
Absolute Viscosity (poises) at 140°F	1605.2	2153.7
Kinematic Viscosity (centistokes) at 275°F	420.6	431.0
Penetration (0.1 mm) at 77°F(100 gm, 5 sec)	70.7	69.0

Table 5.5 Selected optimum asphalt contents of each mixture.

Mixture Type	Optimum Asphalt Content (%) (by weight of aggregate)
Heavy Duty Surface (HDS)	5.5
Heavy Duty Binder (HDB)	4.7
Asphalt-Stabilized Base (HB)	4.0

temperature (285°F (140.6°C)). To reach uniform temperature, the cans were heated for a minimum of about 90 minutes. If the asphalt was not used within 3.5 hours from the start of heating, it was discarded. The heating of the asphalt was done in a single continuous process.

5.2.3.2 Mixing and Curing

The asphalt and aggregate were heated at the mixing temperature of 285°F (140.6°C). The mixing time used was approximately three minutes, and the mixing bowl was heated using a torch, to maintain the mixing temperature during mixing. After mixing, the asphalt concrete was placed in an oven for 15 hours at a temperature of 140°F (60°C). This operation, called curing, allows for any asphalt absorption by the aggregate prior to compaction.

5.2.3.3 Compaction

Equipment

Figure 5.4 is a front view of model 6B/4C/I Gyratory Testing Machine (GTM) used as a compactor in this research. Figure 5.5 is a schematic drawing of the gyratory mechanism and instrumentation. Mold A, containing a test specimen is clamped in position in the flanged mold chuck B. Vertical pressure on the test specimen is maintained by the upper ram E and lower ram F acting against heads G and H, respectively. Since the mold is securely held by the chuck, a gyratory motion (shear strain) is imparted to chuck B by rollers C and D as they travel around the flanged portion of the chuck, these bearing surfaces being lubricated surfaces. Roller C is adjustable in elevation to permit the setting of any desired gyratory angle.

It is generally maintained at a fixed elevation during the operation of the machine. Roller D maintains an essentially fixed elevation when using the oil-filled cell, but may vary slightly in elevation when using the air-filled cell. Upper roller D, containing the pressure cell, emits signals that are recorded by recorder M and digitized by digital panel meter N. The gyratory motion is sensed by the angular transducer I, registered by panel meter K and recorded by recorder E. This recording of gyratory motion is referred to as a Gyrograph.

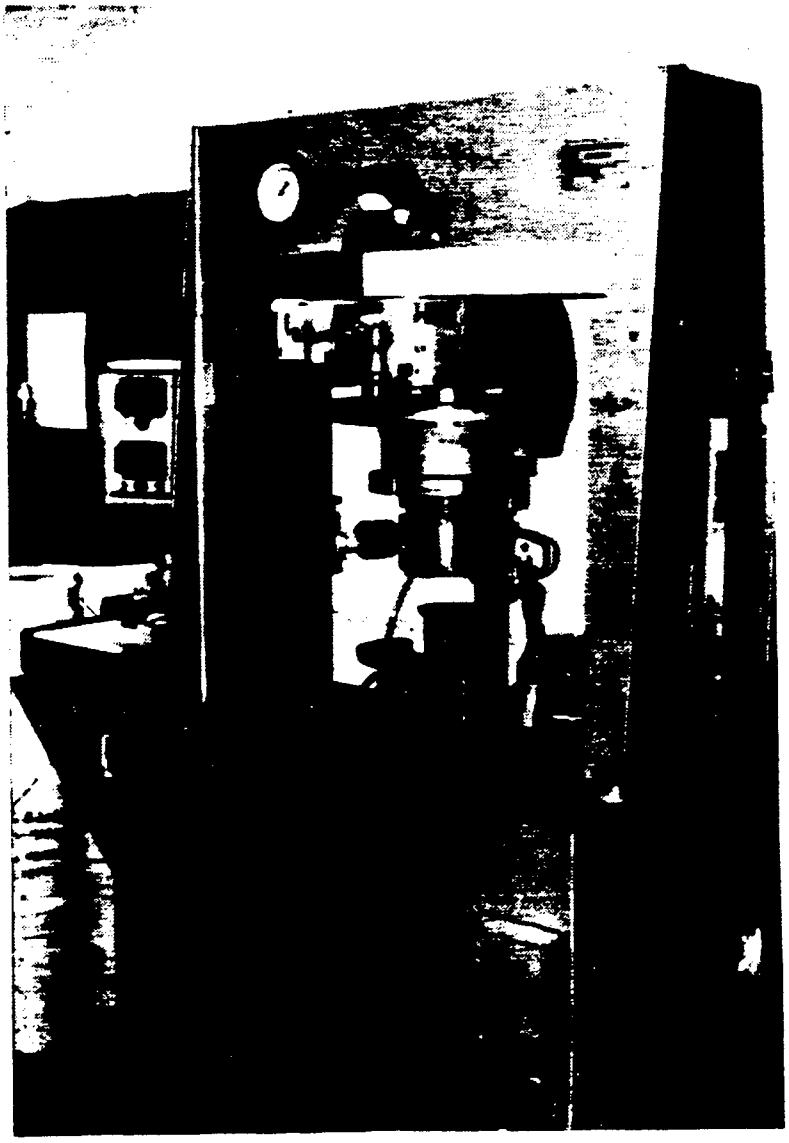

Figure 5.4 Gyratory testing machine model 6B/4C/I.

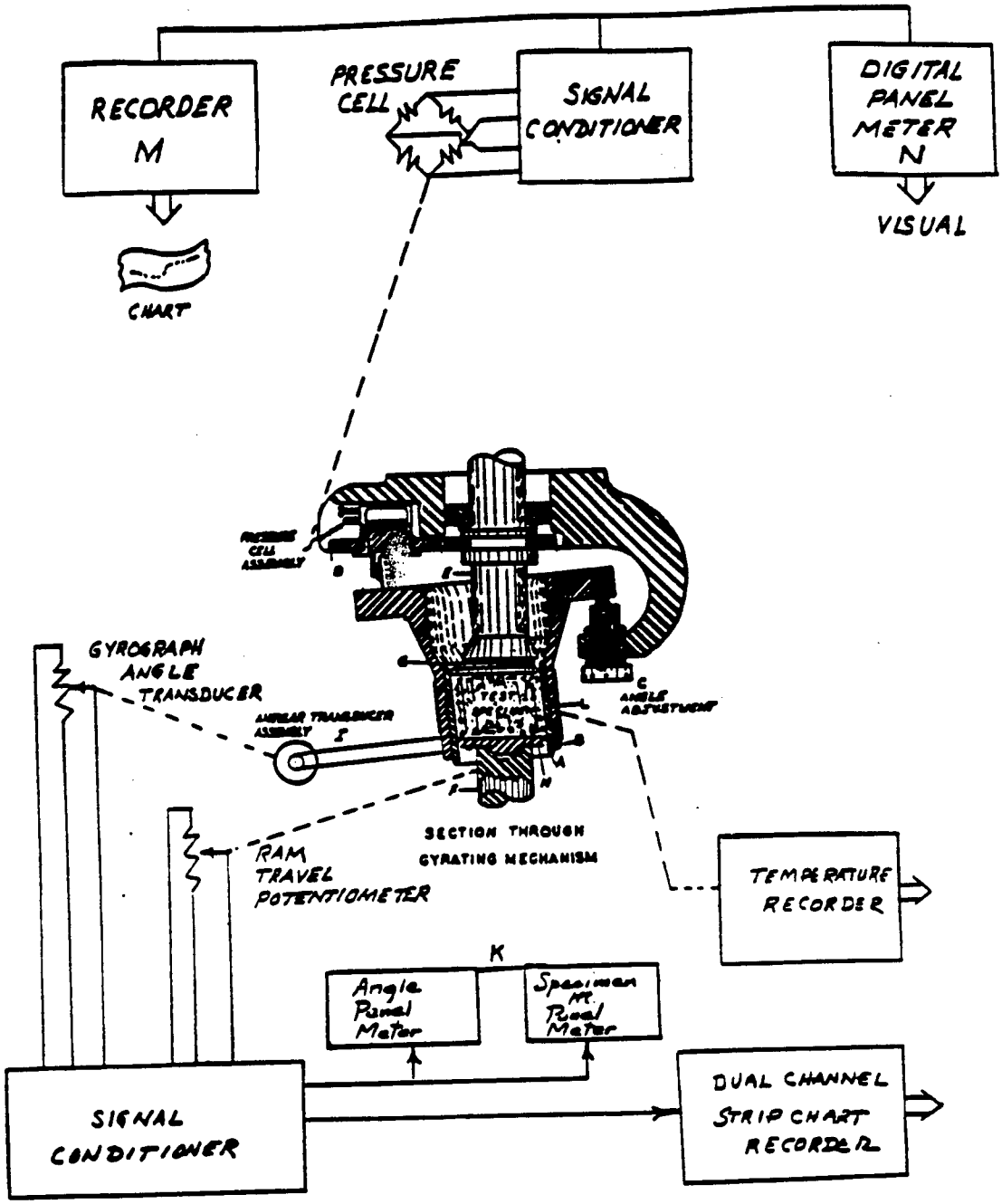

Figure 5.5 Schematic drawing for gyratory mechanism.

This gyratory testing machine is a combination of a compaction and a shear testing machine for bituminous-type paving materials.

Heating of Mixture

The mixture was placed in pans in a forced air oven for a minimum of about 90 minutes to reach uniform temperature. The mixture was heated to a mixing temperature of 285°F (140.6°C). Mixtures not used within 3.5 hours after being placed in the oven were discarded. The heating of the mixture was continuous and was done only once. All molds and tools that came in contact with the mixture during compaction were maintained at the compaction temperature as far as possible.

Compaction Procedure

(1) After curing, the asphalt concrete mixture and compaction molds were placed in a forced air oven at a temperature of 285°F (140.6°C) until they reached a uniform temperature throughout. Also, care was taken to switch on the GTM heating system at least 30 minutes before the start of compaction.

(2) Using the angle adjustment, the gyratory angle was fixed at one degree for both the 4"x2.6" (10.16x6.60 cm) samples and the 6"x3.75" (15.24x9.53 cm) samples.

(3) After heating, the asphalt concrete mixture was poured into the mold with care to avoid the segregation of aggregates. Large aggregate particles were pulled away from the mold wall with a spatula before beginning the compaction.

(4) About 250 - 300 psi (1.72 - 2.07 MPa) of GTM compression and 10 - 25 revolutions of gyration were used for the 4"x2.6" (10.16x6.60 cm) samples depending upon the mixture type used. Table 5.6 shows the information about the compaction forces and gyration numbers for the different sample identifications.

(5) When the sample height reached 2.65 inches for the 4"x2.6" (10.16x6.60 cm) sample and 3.80 inches for the 6"x3.75" (15.24x9.53 cm) sample, the gyration angle was readjusted to zero for the leveling of the samples.

(6) After overnight cooling, the Wet-With-Parafilm (WWP) air voids content was

Table 5.6 Compressive forces and gyration numbers used in gyratory compaction.

Mix Type	Specimen Size (inch)	Compression Forces (psi)	Gyration Number (revolution)
HDS	4x2.6	250	10-15
HDS	6x3.75	350	20-30
HDB	4x2.6	300	20-25
HDB	6x3.75	400	30-40
HB	6x3.75	400	40-50

Table 5.7 Maximum specific gravity of each mixture.

Mixture Type	Maximum Specific Gravity
Heavy Duty Surface (HDS)	2.51
Heavy Duty Binder (HDB)	2.55
Asphalt-Stabilized Base (HB)	2.55

measured.

The compaction efforts were adjusted based on the target air void content of the specimen. In this research, the target air void content of the specimen was 6 percent when measured with a Wet-With-Parafilm (WWP) measurement procedure regardless of the specimen size or mixture type. This target air voids content of the specimen was selected based upon the air voids content measurements from the field core specimens. Generally, the air voids content from the field core specimens were between five and 7 percent.

5.2.3.4 Air Voids Content Measurement

The air voids content measurement was done in accordance with the new method, "Wet-With-Parafilm (WWP)" developed by the researchers at the University of California, Berkeley as a part of the SHRP Project A-003A. The maximum specific gravity of different asphalt concrete mixtures were measured at Blythe Industries, Inc. and are shown in Table 5.7. More detailed information and procedures for air voids content measurement using parafilm can be found elsewhere (Harvey, 1990; Kim, 1991).

5.3 Resilient Modulus Testing

The resilient modulus of asphalt concrete mixtures play an important role in the mechanistic analysis of pavement systems. That is, it is a direct input for most mechanistic pavement analysis programs that use multi-layered elastic theory. As a result, in the mechanistic design procedures, the resilient modulus of asphalt concrete mixture exerts a strong influence on the overall pavement performance. The elastic modulus (Young's modulus, E) of a material, is defined as:

$$E = \frac{\sigma}{\varepsilon} \qquad (5.2)$$

where E = elastic modulus,

σ = stress, and

ε = strain.

When characterizing viscoelastic materials, however, the same relationship applies but loading duration and temperature must be defined because of the rate-dependent nature of asphalt mixtures. A modulus that is time dependent is referred to as stiffness modulus.

One of the commonly used stiffness measurements in pavement design computations is the resilient modulus (M_r). It can be expressed as:

$$M_r = \frac{\sigma}{\varepsilon_r} \qquad (5.3)$$

where M_r = resilient modulus,

σ = applied stress, and

ε_r = recoverable strain.

The value of resilient modulus (M_r) for a given specimen will vary to some degree depending upon the testing temperature, magnitude and duration of loading, recovery between loading cycles, etc. Thus, clear and precise guidelines must be established so that researchers are able to obtain consistent and comparable results (Fairhurst et al., 1990).

The diametral resilient modulus test method was developed by Schmidt and is described in the ASTM standard D 4123-82. However, the resilient modulus testing procedure used in this research occasionally deviated from the ASTM D 4123-82. The main reason for the modifications of the testing procedure from the ASTM D 4123-82, results from the moving wheel load (truck) test results presented in Chapter 4. Based on the truck test results, it was concluded that the 0.05 second of loading time could be a representative highway traffic loading time.

As a result, the resilient modulus test was conducted by applying a repeated vertical haversine loading (loading duration of 0.05 second) on a Marshall size (4 inch dia.x2.6 inch height (10.16x6.60 cm)) sample for the HDS and HDB mixtures. A larger sample with dimensions of 6 inch (15.24 cm) diameter and 3.75 inch (9.53 cm) height was used for the HB

mixture. Under the given loading condition the corresponding horizontal deformation was measured. The selection of sample size was made considering the nominal maximum aggregate size in the mixture. Also, the test was performed at five temperature levels (32, 50, 68, 86, and 104°F (0, 10, 20, 30, and 40°C)), and the applied vertical load levels were adjusted appropriately based on temperatures and specimen sizes used.

The equation for calculating the resilient modulus from the applied load and the induced horizontal deformation, was based on analytical work conducted by Timoshenko (1951) and Frocht (1957) on an elastic thin disk, with the assumption that the material is linearly elastic and in a plain stress-strain condition. Based on their work, Schmidt (1972) derived the following relationship between the resilient modulus and the induced horizontal deformation of the specimens in the diametral resilient modulus test:

$$M_r = \frac{P(0.2734 + \mu)}{ht} \qquad (5.4)$$

where M_r = resilient modulus,

P = applied vertical load,

μ = Poisson's ratio,

h = recoverable horizontal deformation, and

t = thickness of diametral specimen.

The ASTM standard D 4123-82 suggested Poisson's ratio of 0.35 at 77°F (25°C). However, Poisson's ratio of asphalt concrete varies from about 0.25 to 0.50 depending upon the temperature. For low temperatures the value is minimum, while as the temperature increases the Poisson's ratio increases. Therefore, in this research, the Poisson's ratio of asphalt concrete at different temperatures was adjusted based on research conducted by Nair et al. (1972). The assumed Poisson's ratios are shown in Table 5.8.

5.3.1 Experimental Design for Resilient Modulus Determination

In this part of the study, the mechanical properties of the asphalt paving mixtures were characterized. The experiment was designed to study the effects, of the three different

Table 5.8 Asphalt concrete temperature versus Poisson's ratio.

Temperature (°F)	Poisson's ratio
32	0.25
50	0.32
68	0.39
86	0.45
104	0.47

asphalt mixtures, and, five different temperatures, on resilient modulus. The experimental design is presented in Table 5.9.

Independent (Controlled) Variables

(1) Asphalt Mixture: Three levels of asphalt mixture were used. The three asphalt mixtures were the most commonly used mixture types in pavement construction: Heavy Duty Surface Course (HDS), Heavy Duty Binder Course (HDB), and Asphalt-Stabilized Base Course (HB).

(2) Temperature: Temperature is the most important variable in determining both the elastic and viscoelastic properties of the asphalt paving mixtures. Therefore, the specimens were tested at five temperature levels for estimating both the resilient modulus of the asphalt paving mixtures and temperature susceptibility of these mixtures.

Dependent (Response) Variables

Resilient modulus is defined as the ratio of applied stress to the recoverable strain when a repetitive load is applied. It is used to calculate the structural responses, such as stress, strain, and deflection, of the pavement system under applied loads.

5.3.2 Test Fixture and Measurement

In this research, the Model 643.01 A resilient modulus fixture fabricated and supplied by the MTS corporation was used to measure the resilient modulus of asphalt concrete specimens. This device was designed to determine the resilient modulus of bituminous (asphalt) specimens according to the ASTM standard D 4123-82. The horizontal deformations are measured by extensometer assemblies that are spring-loaded to the specimen. The schematic presentations of this fixture are shown in Figures 5.6 through 5.8. The fixture was installed inside an environmental chamber in which temperature could be maintained within ±1°F (±0.56°C) for extended periods.

Table 5.9 Experimental design for resilient modulus determination.

Temperature	Mix Type		
(°F)	HDS	HDB	HB
32	x	x	x
50	x	x	x
68	x	x	x
86	x	x	x
104	x	x	x

Note: Three replications in each cell.

The diametral device consists of two extensometers with gauge length extenders and two specimen adapter brackets as shown in Figure 5.6. The brackets are machined to the same radius as the specimen and remain in contact with the specimen all along the circumference. This design allows each bracket to measure the maximum deformation, instead of measuring local deformation due to point contact with an LVDT, which is used in some diametral tensile test fixtures.

The device is located on the specimen by guiding pins with the same lengths that extend from the side of the fixture (Figure 5.7). Having the distance between the brackets and the specimen equal, ensures that the centerline of the specimen is parallel to the direction of the upper and lower loading strips when the brackets are pulled away completely. Also, because the brackets are placed at the sides of the specimen and guided by pin screws through the holes in fixed side walls, this fixture gives more precise control over the vertical locations of the brackets.

Once the test starts, the low friction anti-rotate bar in the upper fixture (Figure 5.6) prevents possible rotation of the actuator due to repetitive loading. Another advantage of this fixture is that improper measurements due to "rocking" of the specimen can be minimized by using spring-loaded extensometers. That is, the extraneous deformation due to rigid-body-rotation cannot affect the deformation measurements, since the extensometers rotate with the specimen (see Figure 5.8).

5.3.3 Test Procedure

The diametral resilient modulus test was conducted as follows:

(1) Test specimens were placed in the temperature controlled chamber. The specimens were maintained in the temperature controlled chamber at a specified test temperature for 15 hours prior to testing.

(2) A specimen, selected at random, was placed in the loading apparatus, and the loading strips were positioned in a way that is parallel and centered on the vertical diametral plane. A seating load of 10 lbs. (44.48 N) was applied to hold the specimen in place. The electronic measuring systems were adjusted and balanced as necessary.

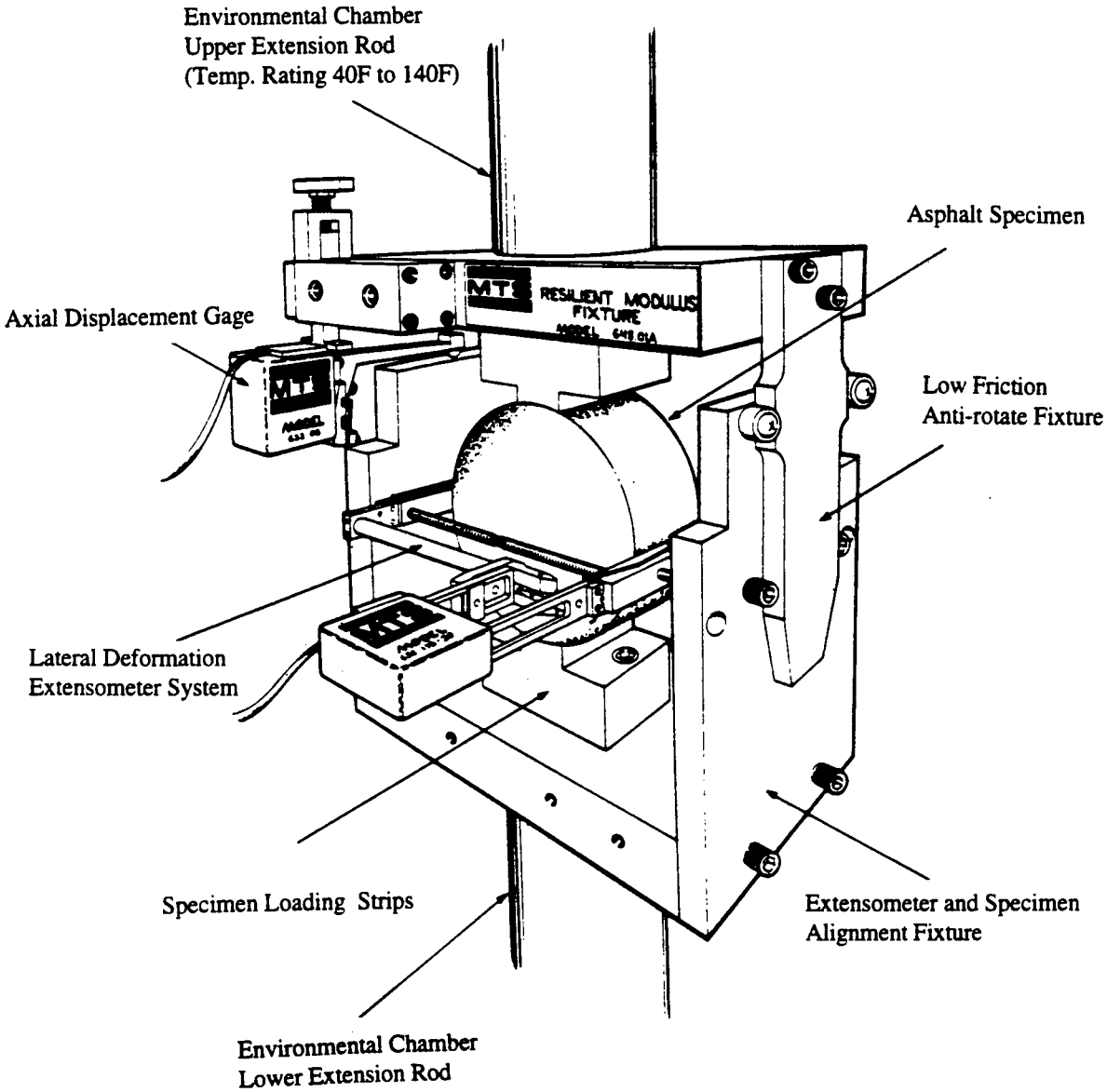

Figure 5.6 Diametral testing fixture and extensometers.

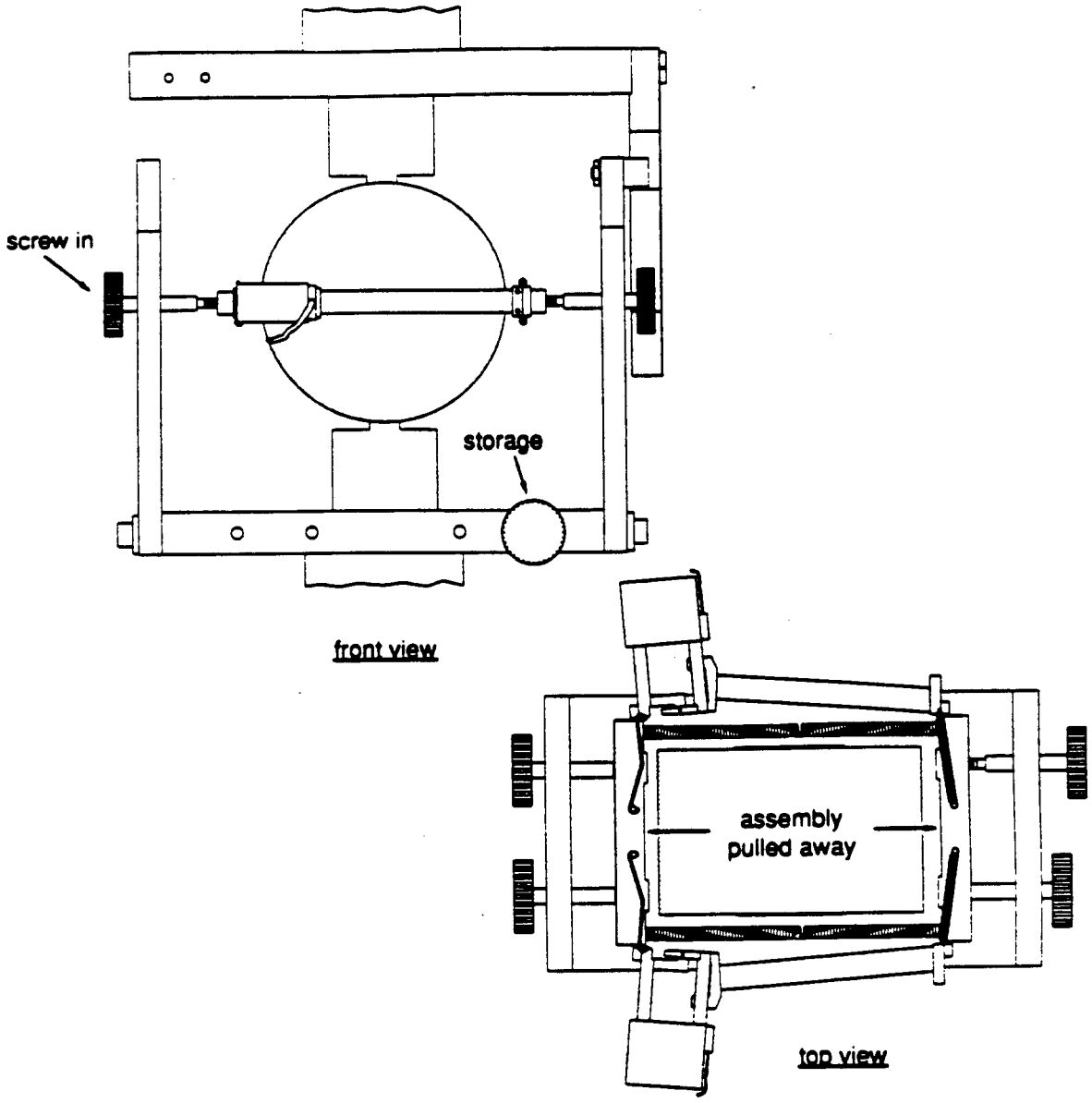

Figure 5.7 Positioning of side brackets using thumbscrews.

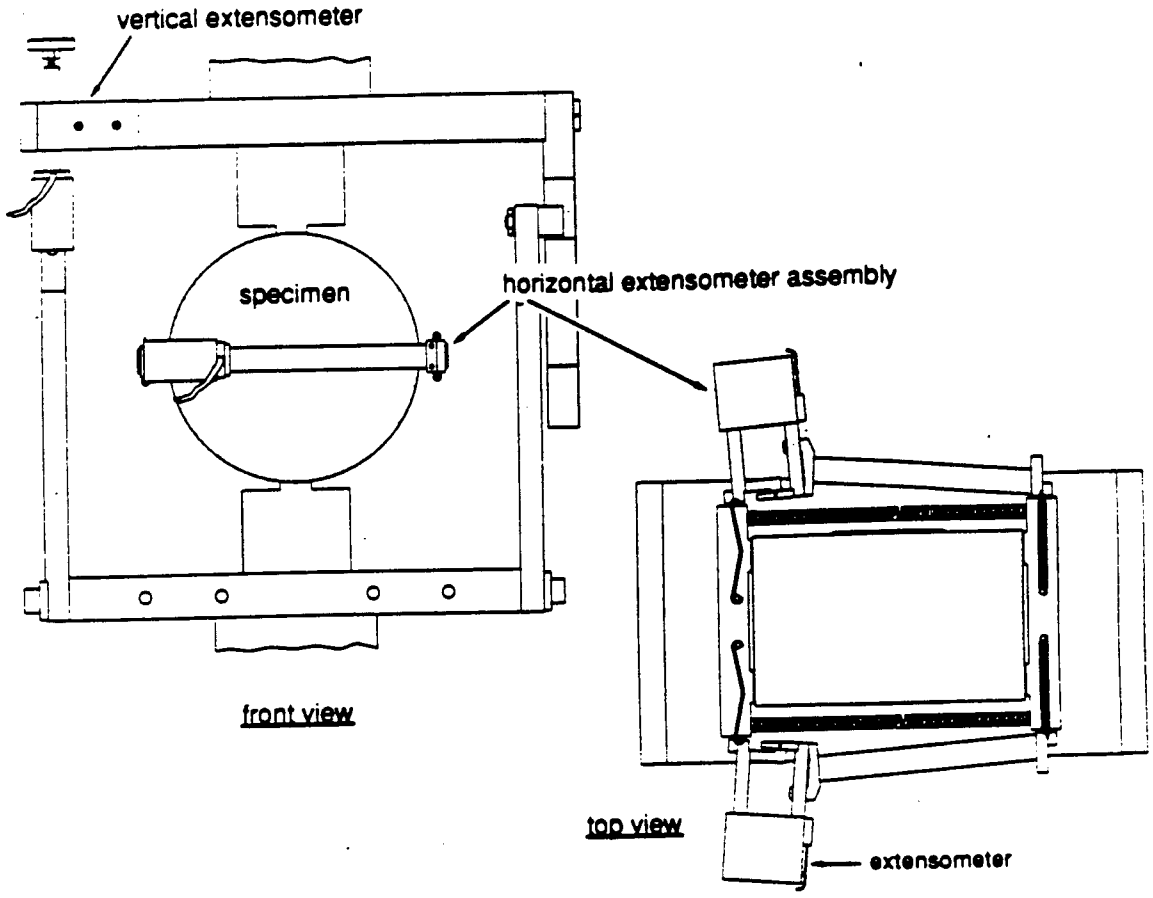

Figure 5.8 Setup ready for testing with spring-loaded extensometers.

(3) A repetitive haversine waveform load with 0.05-second loading time was applied to the specimen. The transient vertical loads and the corresponding horizontal deformations were measured at the point (at 200th cycle) where the resilient (recoverable) deformation began to stabilize.

(4) After the vertical loads and horizontal deformations were measured, the application of the load was stopped, and the specimen was rotated 90 degrees and tested again, using the same procedures as described in steps (2) through (3).

(5) Steps (2) through (4) were repeated using new specimens. Two specimens were selected at random and tested for each mixture.

(6) Steps (1) through (5) were repeated using five different testing temperatures.

5.3.4 Resilient Modulus Test Result

The resilient modulus of an asphalt mixture is greatly affected by the type of mixture and the service temperature. To investigate the effect of temperature on resilient moduli, Marshall size (4"x2.6" (10.16x6.60 cm)) specimens for HDS and HDB mixtures and specimens with dimensions of 6 inch (15.24 cm) diameter and 3.75 inch (9.53 cm) height for HB mixtures, were tested at five different temperatures (32, 50, 68, 86, and 104°F (0, 10, 20, 30, and 40°C)). Two replicates were tested for each mixture at each temperature. The three different mixtures (HDS, HDB, and HB) characterized in this research are considered the most commonly used conventional asphalt paving mixtures in North Carolina.

Figure 5.9 presents the resilient modulus values of the three mixtures as a function of temperature. As expected, the resilient modulus decreased as the temperature increased. The resilient modulus values with HDS mixture showed the lowest values among the three mixtures throughout the testing temperatures, and the resilient modulus values with HDB mixture showed the highest.

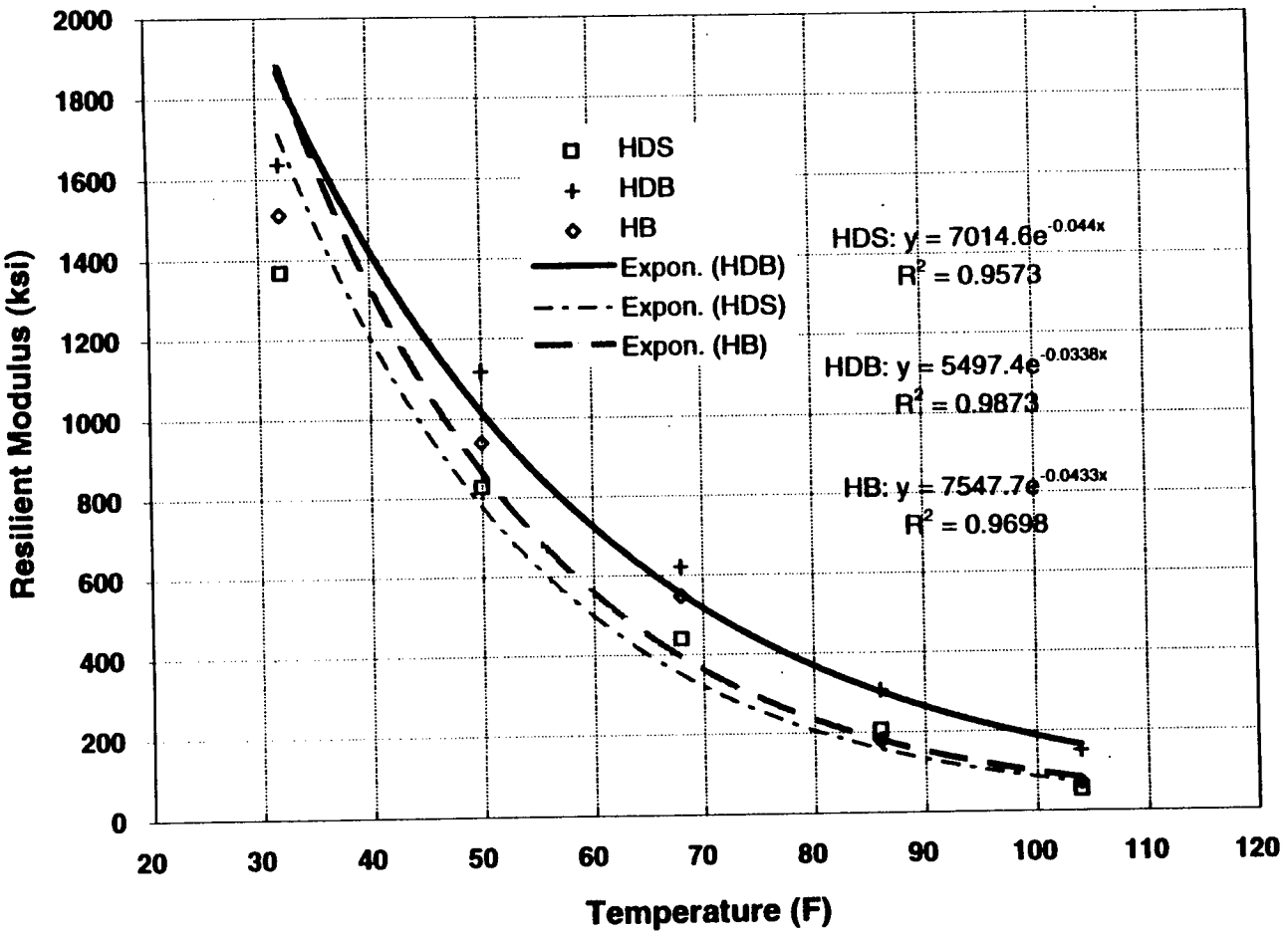

Figure 5.9 Resilient modulus versus temperature for asphalt concrete mixes.

5.4 Resilient Modulus Tests for Subgrade Soils

Soil samples from all the twenty four sections were subjected to the following tests namely:

(1) Tests for Index Properties

(2) Compaction Tests for Determining Optimum Moisture Content.

(3) Resilient Modulus Tests

(1) Tests for Index Properties

Tests to determine the following Index Properties were run on the tests. The properties determined were liquid limit, plasticity index and sieve size analysis. Soils were predominantly in the A-6, A-7, A-7-5 and A-4 categories. Table 5.10 summarizes the basic properties of the soil. The soils have been located on Casagrande's plasticity chart as shown in Figure 5.10

(2) Compaction Tests for Determining Optimum Moisture Content.

The standard proctor test was carried out to determine the maximum dry density and the optimum moisture content. The testing was based on existing AASHTO procedures. Maximum dry densities and optimum water content measurements for the various soils are shown in Table 5.10

(3) Resilient Modulus Tests

Resilient modulus tests were carried out, one at optimum moisture content and the other, at about 3% wet of optimum. The resilient modulus testing procedure involved the following stages:

(a) Sample Preparation

(b) Cyclic Loading of Specimens, and

(c) Processing of Data.

Table 5.10 Basic soil properties.

Sample Number	LL	PI	% Passing			AASHTO Type	w_{opt} (%)	γ_d (kg/m^3)
			#10	#40	#200			
1	49	22	98	89	75	A-7-6	17.5	1682
2	46	20	97	87	77	A-7-6	15	1762
9	47	19	98	94	77	A-7-6	22.5	1538
10	48	20	93	91	81	A-7-6	22	1626
13	50	21	99	93	86	A-7-6	20.5	1563
19	41	18	97	89	78	A-7-6	14.5	1858
20	41	17	94	90	78	A-7-6	16.5	1794
21	44	21	96	83	72	A-7-6	16.5	1746
3	40	16	95	82	69	A-6	18	1698
4	36	11	90	75	65	A-6	15	1858
5	36	13	98	88	71	A-6	15.5	1762
7	38	16	98	87	63	A-6	16	1762
15	39	18	98	89	78	A-6	17	1730
16	39	16	88	76	68	A-6	16	1834
17	34	14	96	84	68	A-6	18	1674
18	35	12	98	91	75	A-6	15	1826
22	37	15	97	92	81	A-6	16	1890
23	37	14	98	89	79	A-6	17	1650
24	39	15	97	90	81	A-6	17	1682
11	52	20	98	94	86	A-7-5	24	1522
12	56	19	99	95	86	A-7-5	22	1634
14	47	15	98	90	77	A-7-5	21	1634
6	25	2	98	89	51	A-4	13	1858

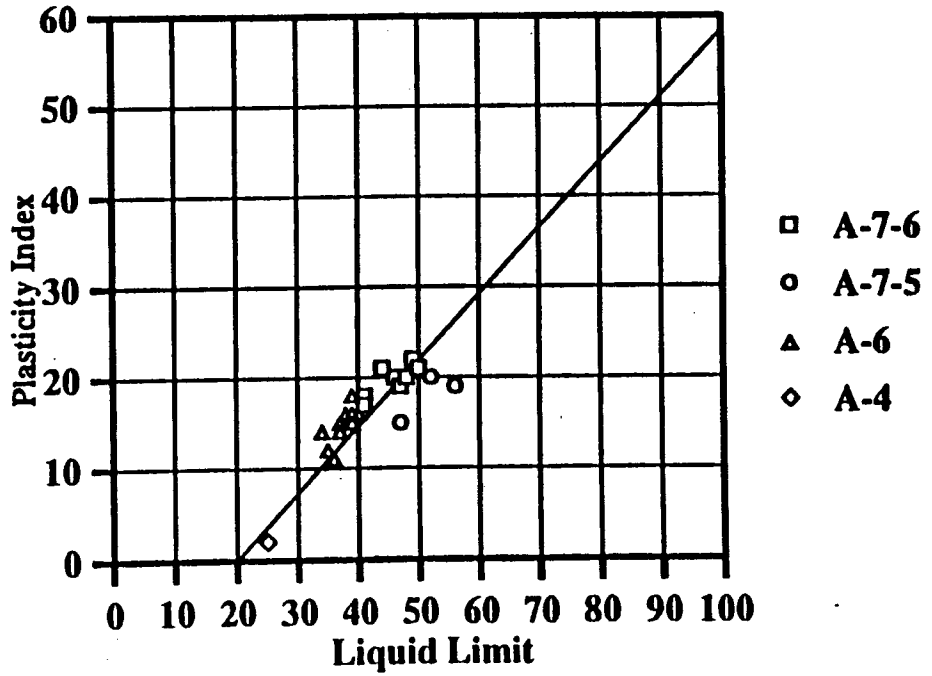

Figure 5.10 Plasticity chart.

(a) **Sample preparation**

About 8 lbs. (35.58 N) of air dried soil passing through No. 4 sieve was mixed thoroughly with tap water corresponding to the target moisture content. This was left to sit for about two hours, covered by a polythene sheet.

The mixed soil was compacted into a cylindrical steel mold of size 8 inches (20.32 cm) long and 4 inches (10.16 cm) in diameter, using a 5.5 pound (24.46 N) hammer, in five layers of equal thickness, applying 26 blows per layer.

The sample was extruded from the mold and was mounted on the triaxial cell with porous stones on both the ends. A rubber membrane was used to separate the sample from the confining fluid. The pore outlet of the triaxial cell was kept open to atmosphere during the test.

(b) **Cyclic Loading of Specimens**

The soil specimen was positioned inside a triaxial cell as shown in Figure 5.11. Two inside LVDTs with a range of +/- 0.1 inches (+/- .254 cm) and an accuracy of 4.88×10^{-4} inches (12.40×10^{-4} cm) were setup to measure the inside deformations. A third LVDT was setup outside the triaxial cell to measure the deformation externally, which had a range of +/- 0.25 inches (.635 cm) and an accuracy of 1.22×10^{-4} inches (3.10×10^{-4} cm).

The loading was applied using a MTS machine with a max. loading capacity of 22 kips (97.86 KN). A load cell having a capacity of 2000 lbs (8.896 KN) was used. The setup could measure a minimum of 0.976 lbs (4.34 N). Air was used as the confining fluid inside the triaxial cell. The loading sequence is as shown in Table 5.11. The cyclic load pulse was a haversine, with a peak corresponding to the deviator stress, σ_d. The duration of the haversine loading was 0.1 seconds. It was followed by 0.9 seconds of rest. The haversine pulse was divided into ten equal time segments and the required vertical load was calculated taking into account the load applications on the sample. The seating load, which corresponds to $0.2\sigma_c$ was applied to the beginning of each confining pressure change. The confining pressure is measured by the pressure transducer connected to the triaxial cell.

To condition the sample (i.e., to get rid of most of the seating errors and thixotropic

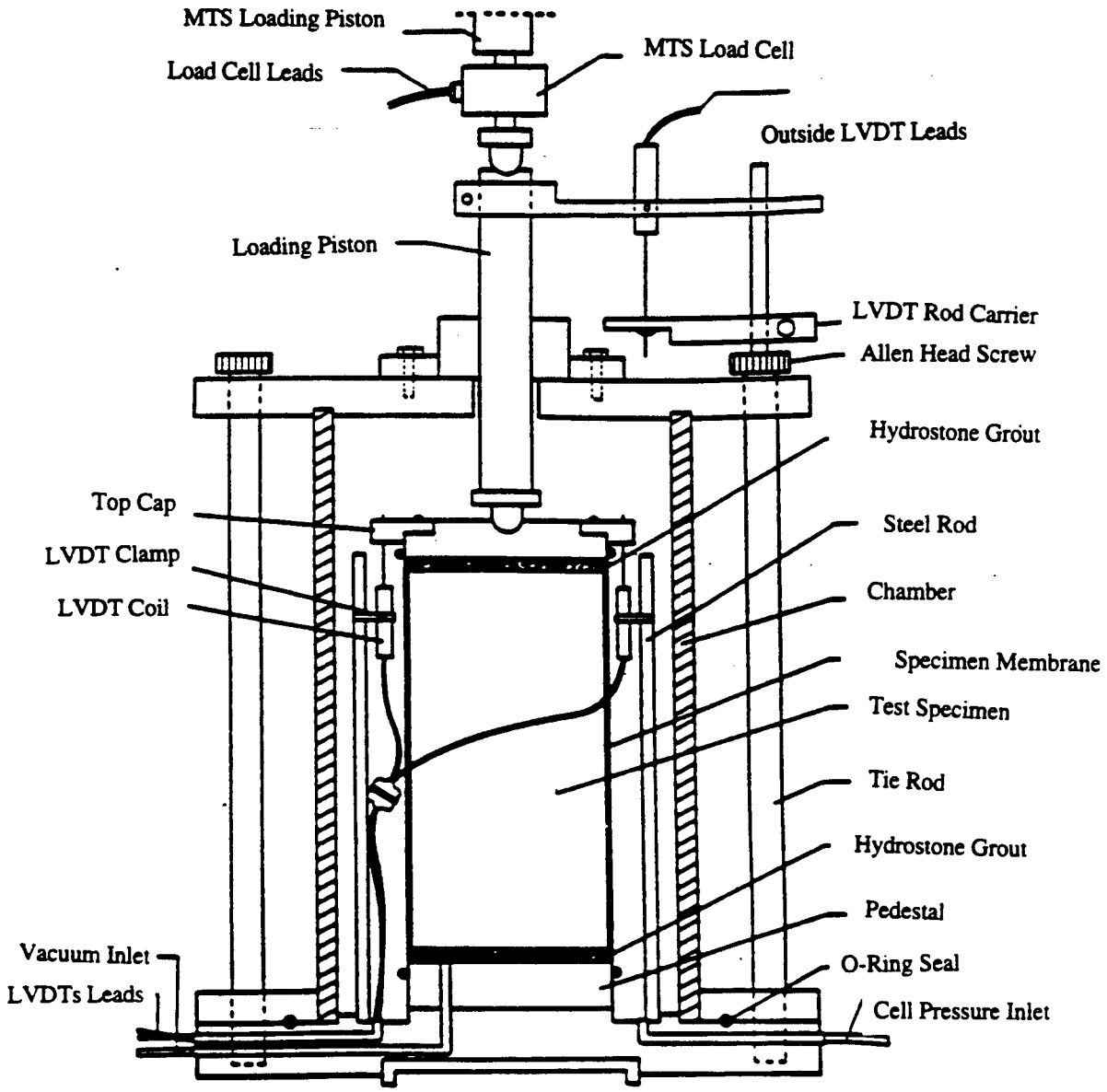

Figure 5.11 Resilient modulus triaxial set-up.

Table 5.11 Loading sequence for roadbed specimens.

Sequence	Confining Pressure (kPa)	Deviator Axial Pressure (kPa)	Contact Stress 0.2 σ_c (kPa)	Load Applications
1	40	55	8	1000
2	30	7	6	100
3	30	15	6	100
4	30	30	6	100
5	30	40	6	100
6	30	55	6	100
7	15	7	3	100
8	15	15	3	100
9	15	30	3	100
10	15	40	3	100
11	15	55	3	100
12	7	7	1.4	100
13	7	15	1.4	100
14	7	30	1.4	100
15	7	40	1.4	100
16	7	55	1.4	100

effects) the sample was subjected to 1000 cycles of load corresponding to σ_d = 8 psi (55.2 KPa) and σ_c = 6 psi (41.4 KPa).

(c) Processing of data.

Every load combination was applied 100 times and the data for the last five cycles were picked up by the data acquisition program. The signals from the load cell and the LVDTs were recorded in binary format. The frequency of data acquisition was 200 data per second. This data was later converted to an ASCII format.

(d) Resilient Modulus Test Results

The resilient moduli at confining pressure(σ_c) of 2 psi and at a deviatoric stress(σ_d) of 4 psi have been reported in Table 5.12. An attempt was made to cast the resilient moduli data at optimum moisture content into the exponential model suggested by Thompson et al. (1979),

$$MR = K\sigma_d^n \qquad (5.5)$$

where,

MR = resilient modulus of the soil

σ_d = deviatoric stress

k,n = constants

The K and n values and the correlation parameters obtained by least square fit are shown in Table 5.13. This model works reasonably well for most of the soils. The range of values for different soils tested are as follows:

SOIL TYPE	K	n
A-6	19500-80000	-0.29 to -0.81
A-7-6	19300-85800	-0.35 to -1.03
A7-5	18900-35700	-0.24 to -0.69

Table 5.12 Test results for US 421 subgrade material.

Section Number	Optimum Moisture			Wet of Optimum		
	Mr (Mpa)	w (%)	γ_d (kg/m^3)	Mr (Mpa)	w (%)	γ_d (kg/m^3)
A-7-6						
1	180	17.4	1682	50	21.3	1666
2	180	15	1762	80	16.4	1778
9	170	22.5	1537	90	24.8	1553
10	100	22.5	1626	30	23.8	1602
13	120	21	1570	80	22	1570
19	150	14.5	1858	70	21	1762
20	90	16.2	1794	10	22	1698
21	200	16.9	1746	140	20.7	1714
A-7-5						
11	100	23.7	1515	80	27.8	1495
12	50	22	1629	30	25.3	1570
14	150	20.7	1631	100	23.1	1618
A-6						
3	80	17.9	1698	30	21.6	1666
4	80	15	1858	20	17.4	1794
5	100	15.2	1826	--	17.6	1794
7	110	16.6	1757	100	20	1682
15	90	17.1	1722	70	21.9	1703
16	70	15.6	1836	30	16.4	1828
17	100	17.6	1674	60	22.3	1655
18	180	14.1	1839	50	17.9	1784
22	110	15.9	1773	20	20.1	1685
23	210	16.8	1645	100	21.9	1612
24	180	17	1687	70	19.7	1677
A-4						
6	130	12.7	1858	230	14.[illegible]	1890

Table 5.13 Model Parameters ($M_r = K\sigma_d^n$)

Section No.	K	n	Corr. Coef.	R^2
A-6				
3	495	-0..49	0.982	0.964
4	423	-0.52	0.964	0.929
5	880	-1.70	0.982	0.963
7	728	-0.51	0.973	0.947
15	513	-0.32	0.918	0.843
16	567	-0.61	0.949	0.90
17	514	-0.29	0.838	0.545
18	798	-0.54	0.807	0.499
22	711	-0.84	0.960	0.921
23	1010	-0.51	0.76	0.578
24	1476	-0.81	0.898	0.806
A-7-6				
1	1495	-0.81	0.945	0.892
2	1191	-0.79	0.942	0.887
9	1287	-0.63	0.937	0.878
10	1000	-1.03	0.887	0.787
13	790	-0.57	0.916	0.839
19	1145	-0.80	0.800	0.640
20	446	-0.35	0.971	0.942
21	1349	-0.74	0.867	0.752
A-7-5				
11	474	-0.24	0.813	0.661
12	423	-0.69	0.979	0.959
14	828	-0.31	0.927	0.859
A-4				
6	1603	-0.91	0.943	0.890

Also by including σ_c as a variable, a model of the following form was obtained.

$$MR = K\sigma_d^n\sigma_c^m \qquad (5.6)$$

MR = resilient modulus of the soil

σ_d = deviatoric stress

σ_v = confining stress

k,n,m = constants

The correlation coefficients were found to have improved considerably. The regression coefficients obtained are given in Table 5.14. The range of values for different soils tested are as follows:

SOIL TYPE	k	n	m
A-6	17310-59770	-0.65 to -2.47	0.12 to 0.62
A-7-6	18000-60500	-0.46 to -2.50	0.078 to -1.285
A-7-5	17130-33530	-0.42 to -0.867	0.16 to -0.31

5.5 Resilient Modulus Test Results for Aggregate Base Course Materials

Resilient modulus tests were performed using a triaxial setup with varying confining and deviatoric stresses. Table 5.15(a) shows the general properties of aggregates used in this study and Table 5.15(b) shows resilient modulus results obtained for the aggregate base courses materials.

Table 5.14 Model Parameters $(M_r = K\sigma_d^n\sigma_c^m)$

Section No.	K	m	n	Corr. Coef.	R^2
A-6					
3	495	0.13	-0.65	0.990	0.981
4	423	0.15	-0.59	0.980	0.960
5	880	0.18	-1.49	0.960	0.913
7	728	0.20	-0.97	0.978	0.956
15	513	0.18	-0.54	0.916	0.840
16	567	0.18	-0.89	0.905	0.819
17	514	0.54	-0.58	0.893	0.800
18	798	0.51	-1.14	0.817	0.667
22	711	0.11	-1.025	0.966	0.934
23	1010	0.62	-1.38	0.908	0.824
24	1476	0.62	-2.48	0.849	0.721
A-7-6					
1	1495	0.74	-2.50	0.965	0.932
2	1191	0.27	-1.68	0.979	0.959
9	1287	0.46	-1.94	0.950	0.906
10	1000	0.68	-2.02	0.866	0.750
13	790	0.63	-1.25	0.944	0.891
19	1145	1.29	-2.20	0.864	0.746
20	446	0.08	-0.46	0.982	0.965
21	1349	0.75	-2.04	0.961	0.924
A-7-5					
11	474	0.31	-0.42	0.930	0.865
12	423	0.16	-0.72	0.970	0.950
14	828	0.24	-0.87	0.970	0.945
A-4					
6	1603	-0.19	-2.51	0.927	0.860

Table 5.15(a) General properties for North Carolina aggregate (base course) types.

	GT-101		GT-102	GT-103
	10F3S1	10F3S2	20F3S2	30F3S2
Max. Aggregate Size (in.)	1.5	1.5	1.5	1.5
Avg. Aggregate Size, D50 (in.)	.25	.25	.25	.25
Coefficient of Uniformity,Cu	33	33	28	40
Dry Unit Weight (pcf.)				
Average	151.1	151.1	149.7	149.7
Lab Result	145.6	148.3	148.5	147.9
Water Content %				
Average	3.5	3.5	5.6	5.6
Lab Result	4.17	6.75	6.7	8.1
% Fines Content	5	5	5	5
% Compaction of T-180	100	100	100	100

General Summary of Properties

Well graded, 1.5 inches maximum size, subangular to angular crushed stone, 5% fines.

Specimen compacted to 100% T-180 density.

Dry density = 151 pcf at 3.5 % water content

Dry density = 149.7 pcf at 5.6% water content

Table 5. 15(b) Resilient Modulus results for aggregate base course materials used in US421 project.

			Resilient modulus (psi) measured from clamps							
Confining Pressure S3(psi)	Deviator Stress Sd (psi)	Bulk Stress Theta(psi)	10F3S1	10F3S1	10F3S2	10F3S2	20F3S2	20F3S2	30F3S2	30F3S2
3	3	12	41833	40143	22726	23671	24314	25003	27568	27065
3	6	15	33171	33318	22304	22348	22152	22057	25830	26125
3	9	18	32978	32549	22922	23135	22816	22669	26958	26768
5	5	20	46911	44989	25307	25576	29917	29790	28400	28385
5	10	25	40708	39662	28188	27893	27097	27589	30011	29904
5	15	30	39259	40833	30158	28964	29676	30454	30963	30710
10	10	40	64399	59528	39882	39649	41382	41334	38944	41060
10	20	50	58416	58492	41891	41771	41482	42633	42266	41200
10	30	60	60858	60654	43443	42983	44722	44852	41666	41796
15	10	55	74483	74127	50846	50844	51443	52748	47454	47574
15	15	60	74554	70764	49926	49471	52189	51765	47952	48101
15	30	75	75559	74988	54006	51461	55614	54970	50882	50590
20	15	75	91727	89995	60481	60662	62691	61298	57423	56807
20	20	80	83724	83277	59303	59009	60279	60217	55398	55612
20	40	100	88875	89459	64325	63220	63516	63647	60226	59831